Doctoral Dissertation

Doctoral Program in Civil and Environmental Engineering (36th Cycle)

Circular economy of Lithium-ion batteries

Material flow, environmental and economic analysis of Lithium-ion batteries in Europe and technical, environmental and economic optimization of recycling processes

Martina Bruno

* * * * * *

Supervisor

Prof. Silvia Fiore, Supervisor

Politecnico di Torino

April 30, 2024

This thesis is licensed under a Creative Commons License, Attribution - Noncommercial - NoDerivative Works 4.0 International: see www.creativecommons.org. The text may be reproduced for non-commercial purposes, provided that credit is given to the original author.

I hereby declare that, the contents and organisation of this dissertation constitute my own original work and does not compromise in any way the rights of third parties, including those relating to the security of personal data.

Martina Bruno

……..

Martina Bruno

Turin, April 30, 2024

Summary

Lithium-ion batteries are crucial for Europe's goals on emissions control, due to their manifold applications as energy storage devices for renewable energy production and electric transport. The widespread use of Lithium-ion batteries leads to the increased demand for raw materials and efficient recycling processes for the recovery of secondary raw materials become essential to ensure the supply chain and limit the environmental impacts and costs associated with the extraction of raw materials. Current recycling methods involve pyrometallurgy and hydrometallurgy, However, the costs entailed by existing technologies are prohibitive to recycle batteries containing lower cobalt content, specifically lithium iron phosphate cathodes.

This Thesis tackles the circular economy perspective for lithium-ion batteries. Initially the environmental and economic implications of material flows associated with end-of-life batteries from electric vehicles in Europe have been analysed, considering the supply chain for primary raw materials and the recycling infrastructure providing secondary raw materials. Findings underline how the existing recycling infrastructure in Europe falls short in meeting the collection and recovery targets set by the European Union for batteries recycling. Furthermore, the prescribed requirements for materials circularity in the battery sector seems unattainable when relying solely on secondary raw materials sourced from European recycling plants.

The environmental implication of mining activities for batteries supply chain often overshadows the environmental benefits of electric transport systems, compared to traditional internal combustion engines. Enhancing the recycling capabilities in Europe is

imperative in fulfilling regulatory mandates and ensuring a stable supply chain for essential raw materials sourced from regions beyond Europe, often entangled in geopolitical complexities and to provide secondary raw materials avoiding the environmental impacts due to mining activities. From an economic perspective, hydrometallurgical processes represent the best cost-benefit solution to address the proven inadequacy of European recycling capacity. Nonetheless, the costs entailed by conventional hydrometallurgy are still prohibitive to recycle low-value batteries such as lithium iron phosphate batteries.

In the experimental section of this Thesis several steps of the lithium-ion batteries recycling process have been studied in order to limit their environmental and economic costs, considering cells electrochemical discharge, cathodes pre-treatments, and hydrometallurgical processes of end-of-life lithium iron phosphate cathodes and their production scraps. The results of the experimental activities conducted in this Thesis, proved the viability of carbonates solutions for the electrochemical discharge of lithium-ion batteries, without corrosion phenomena and the release of harmful gaseous contaminants and carbon dioxide. A physic-mechanical method to detach the active materials from the current collector of end-of-life and production scraps lithium iron phosphate cathodes have been proposed, by optimizing technical parameters and limiting environmental and economic costs. Besides, different hydrometallurgical processes have been tested for the recycling of end-of-life and production scraps lithium iron phosphate cathodes identifying the importance of selective leaching processes and the application of organic acids to ensure economic viability of the overall recycling process.

Acknowledgment

I wish to express my deepest gratitude to all those who have contributed to the completion of this doctoral Thesis. Without their support, encouragement, and guidance, this work would not have been possible.

First and foremost, I would like to thank my supervisor, Prof. Silvia Fiore for her invaluable guidance and support. Over the years, Prof. Silvia Fiore dedicated her expertise and valuable mentorship, which have been crucial to the success of this work. Thank you for believing in me and your never-ending encouragement.

I would like to extend my deepest gratitude to Professor Annukka Santasalo-Aarnio for graciously hosting me during my exchange period at Aalto University. Thank you for providing me with the opportunity to learn and grow in such a stimulating environment.

I would like to thank my Reviewers, Prof. Annukka Santasalo-Aarnio and Prof. Juan Manuel Pérez, for their meticulous revisions and comments, which helped me improve the work presented in this Thesis.

I thank all the members of the Doctoral Committee for their interest and courteous availability.

A special thanks to my colleagues and friends for their daily support and friendship. Thanks to Livia, Ilaria, Stefano, Alice, Heejin, Marco and Vincenzo, and my office mates Anna, Beatrice, Ingrid, Matilde, Laura and Paolo, which shared with me the highs and lows of the

PhD journey. I am greatly thankful for the positive environment we created and shared together.

Thanks to Alice, Alessia, Alessandro M., Alessandro R., Andrea, Flavia, Francesca, Lorenzo, Martina, Michele and Stefano for always being there to listen, to laugh, and to provide much-needed distractions. Thanks for being a source of strength and joy during these years.

A special thanks to my parents, Lucia and Marco, for their unconditional love, emotional support, and constant encouragement. Thank you for showing me the importance of always giving my best effort, while also embracing the lessons from failure. Thank you for the dedication you showed when I was younger in spending a summer and countless nights teaching me math when I struggled with multiplication and division, which in the long run led me to become an engineer and now discuss my PhD. Thank you for always being there for me.

Thanks to all my family and in particular to my *nonne* Elda and Vincenza, which will always be my greatest supporters.

Thanks to Matteo for being always by my side to guide me back when I feel adrift, and to cheer for me with every success.

List of contents

	Introduction and objectives	1
1	State of the art on lithium-ion batteries recycling	4
1.1	Introduction	5
1.2	Methodology for literature review	6
1.3	Lithium-ion batteries recycling	6
1.3.1	Discharge	7
1.3.2	Mechanical treatments	8
1.3.3	Pyrometallurgy	11
1.3.4	Hydrometallurgy	13
1.3.5	Biological treatments	17
1.3.6	Direct recycling	18
1.3.7	Environmental analysis	18
1.3.8	Material flow analysis	19
1.4	Discussion	20
1.5	Conclusions	21
2	Material flow analysis of recycling and supply chains	23
2.1	Introduction	24
2.2	Methodology	25
2.3	Results	26
2.3.1	Material flow analysis of European recycling capacity	27
2.3.2	Material flow analysis of supply chain for European EVs market	30
2.4	Discussion	34
2.5	Conclusions	35
3	Environmental and economic analysis of recycling and supply chain material flows	37
3.1	Introduction	38

3.2 Methodology……39
3.2.1 Environmental analysis.....39
3.2.2 Economic analysis.....40
3.3 Results……..41
3.3.1 Environmental analysis.....41
3.3.2 Economic analysis.....42
3.4 Discussion……45
3.5 Conclusion……45
4 Electrochemical discharge for lithium-ion batteries recycling 47
4.1 Introduction……..48
4.2 Methodology……49
4.3 Results……..50
4.3.1 Reduction of residual voltage.....50
4.3.2 Monitoring of gaseous products release.....52
4.3.3 Trends in pH of discharge solutions.....54
4.4 Discussion……56
4.5 Conclusions……..56
5 Pre-treatment for lithium iron phosphate cathodes recycling……58
5.1 Introduction……..59
5.2 Methodology……60
5.2.1 Experimental procedure.....60
5.2.2 Environmental analysis.....61
5.3 Results……..……...62
5.3.1 Samples' characterization.....62
5.3.2 Ultrasound washing.....63
5.3.3 Mechanical detachment.....64
5.3.4 Thermal treatment and mechanical detachment.....66
5.3.5 Correlation analysis.....68
5.3.6 Environmental analysis.....71

5.4 Discussion…….73
5.5 Conclusions……...73
6 Hydrometallurgical recycling of end-of-life lithium iron phosphate cathodes…...75
6.1 Introduction……...76
6.2 Methodology…….77
6.3 Results……...79
6.3.1 Initial sample characterization.....79
6.3.2 Leaching process.....80
6.3.3 Iron and Phosphorous recovery.....81
6.3.4 Lithium recovery.....84
6.3.5 Regeneration through carbothermal reduction.....85
6.4 Discussions……86
6.5 Conclusions……...87
7 Hydrometallurgical recycling of lithium iron phosphate cathodes production scraps…….89
7.1 Introduction……...90
7.2 Methodology…….91
7.3 Results……...93
7.3.1 Initial sample characterization.....93
7.3.2 Leaching process.....94
7.3.3 Lithium recovery.....97
7.4 Discussion.....98
7.5 Conclusions.....99
8 Economic analysis of lithium iron phosphate cathodes recycling.....101
8.1 Introduction.....102
8.2 Methodology.....103
8.3 Results.....103
8.3.1 Physical mechanical detachment.....103

8.3.2 Hydrometallurgical recycling of end-of-life cathodes.....104
8.3.3 Hydrometallurgical recycling of production scraps.....105
8.4 Discussion……...106
8.5 Conclusions……109
Conclusions.....111
References.....114
Appendix A.....152
Appendix B.....155

List of Tables

Table 1-1 Recycling efficiency of pyrometallurgical treatment 12

Table 1-2 Recycling efficiency of hydrometallurgical treatment 14

Table 2-1 Compositions of the LIBs identified by the different cathodes 25

Table 2-2 Inventory of lithium-ion batteries' recycling plants in Europe in 2020..... 28

Table 2-3 Circularity indicators and recycling efficiency parameters 30

Table 2-4 Inventory of current and forecasted Gigafactories for lithium-ion batteries' production in Europe..... 32

Table 3-1 Environmental impacts of virgin metals' mining 39

Table 3-2 Comparison between of costs, revenues and profit of different LIBs' recycling strategies..... 44

Table 5-1 Pearson's correlation coefficient between operative parameters and KPIs for production scraps samples..... 69

Table 5-2 Pearson's correlation coefficient between operative parameters and KPIs for production scraps samples..... 70

Table 6-1. Leaching conditions (concentration of leaching agent and hydrogen peroxide, temperature, contact time, S/L: solid to liquid ratio) applied in this study 79

Table 7-1 Leaching conditions (concentration of leaching agents and hydrogen peroxide, temperature, contact time, S/L: solid to liquid ratio) 93

Table 8-1 Results of economic analysis from literature overview on LFP recycling 109

List of Figures

Figure 1-1 Categorization of selected references according to year of publication and research topics 6
Figure 2-1 Projection of EVs batteries reaching end-of-life by 2030 in Europe 27
Figure 2-2 Projection of metals from EVs batteries reaching end-of-life by 2030 in Europe 27
Figure 2-3 Projection of recycled metals from EVs batteries reaching end-of-life by 2030 in Europe 29
Figure 2-4 Projection of metals demand for EVs batteries reaching in Europe in 2030 ... 31
Figure 2-5 Projected replacement rate of metals demand for European EVs fleet in 2030 34
Figure 3-1 GHG emissions associated with the recycling of 1 t of LIBs 41
Figure 3-2 GHG emissions associated with the metals mining and avoided by recycling of 1 t of LIBs 42
Figure 3-3 Projected costs of European LIBs recycling infrastructure in 2030 43
Figure 3-4 Potential incomes associated to the market value of the secondary raw materials involved by LIBs' recycling in 2030 (CC: current collector) 44
Figure 4-1 Experimental settings used in electrochemical discharge tests 49
Figure 4-2 Discharge curves during the conventional electrochemical discharge 50
Figure 4-3 Discharge curves during electrochemical discharge with the half-cells set-up with sodium carbonate 51
Figure 4-4 Discharge curves during electrochemical discharge with the half-cells set-up with potassium carbonate 51
Figure 4-5 Trends of H2 release rate (ppm/h) during conventional electrochemical discharge 53
Figure 4-6 Trends of pH during conventional electrochemical discharge 54
Figure 4-7 Trends of pH during electrochemical discharge with the half-cells set-up with sodium carbonate 55
Figure 4-8 Trends of pH during electrochemical discharge with the half-cells set-up with potassium carbonate 55

Figure 5-1 Outline of experimental approach for mechanical detachment of LFP cathodes (production scraps production scraps , and end-of-life end-of-life) from aluminium current collectors 60
Figure 5-2 Elemental composition of LFP cathodes active material 62
Figure 5-3 SEM images of production scraps (on the left) and end-of-life (on the right) 62
Figure 5-4 Separation efficiency through ultrasound washing 63
Figure 5-5 SEM images of (A-C) production scraps cathodes and (D-F) end-of-life cathodes after ultrasound washing for 5, 15 and 30 minutes 64
Figure 5-6 Separation efficiency through ball milling 65
Figure 5-7 SEM images of (A-D) production scraps cathodes and (E-H) end-of-life cathodes after ball milling at 1080 rpm for 8-24 minutes and 840 rpm for 16 minutes.... 66
Figure 5-8 Weight loss rate of production scraps and end-of-life samples after thermal treatment..... 67
Figure 5-9 Separation efficiency through thermal treatment and ball milling 67
Figure 5-10 SEM images of (A-D) production scraps cathodes and (E-H) end-of-life cathodes after thermal treatment at 200-350°C and ball milling 68
Figure 5-11 Energy consumption (kWh/kg_{OUTPUT}) associated to the pre-treatment processes 72
Figure 5-12 Global warming impact (GWP_{100}) associated to the pre-treatment processes 73
Figure 6-1. Outline of the experimental approach with conventional and selective leaching 79
Figure 6-2 XRD spectrum of LFP powder from end-of-life cathodes 80
Figure 6-3. Leaching efficiency of lithium, iron, phosphorous and aluminium with conventional and selective leaching 81
Figure 6-4 XRD spectrum of the recovered powders obtained from sulfuric acid leaching at pH 2 after thermal treatment at 700°C 82
Figure 6-5 XRD spectra of the recovered powders obtained from sulfuric acid leaching at pH 5.5 83
Figure 6-6 XRD spectrum of the recovered powders obtained from citric acid leaching at pH 2 after thermal treatment at 700°C 83

Figure 6-6 XRD spectrum of the recovered powders obtained from citric acid leaching at pH 5.5 83
Figure 6-8 XRD spectra of precipitates obtained at pH 12 from conventional sulfuric acid leachates 85
Figure 6-9 XRD spectra of precipitates obtained at pH 12 from selective 0.25M citric acid and hydrogen peroxide leachates 86
Figure 6-10 XRD spectra of recycled LFP powders deriving from conventional leaching with sulfuric acid 86
Figure 6-11 XRD spectra of recycled LFP powders deriving from selective leaching with citric acid and hydrogen peroxide 87
Figure 7-1 Outline of the experimental approach for selective leaching of production scraps cathodes 93
Figure 7-2 XRD spectrum of LFP cathodes' production scraps 94
Figure 7-3 Leaching efficiency (%) of lithium, iron and phosphorous via selective leaching with sulfuric acid and hydrogen peroxide 95
Figure 7-4 Leaching efficiency (%) of lithium, iron and phosphorous via selective leaching with citric acid and hydrogen peroxide 95
Figure 7-5 XRD spectra of solid residues after leaching with sulfuric acid and hydrogen peroxide 97
Figure 7-6 XRD spectra of solid residues after leaching with citric acid and hydrogen peroxide 97
Figure 7-7 FESEM images of (A) initial LFP powder, (B) residues after sulfuric acid leaching and (C) after citric acid leaching 98
Figure 7-7 XRD spectra of precipitates obtained at pH 12 from selective leaching with sulfuric acid and hydrogen peroxide 99
Figure 8-1 Operative costs of pre-treatments for 1 kg of LFP cathodes 105
Figure 8-3 Operative costs of the considered routes applied to recycling of 1 kg of end-of-life LFP cathodic material 106
Figure 8-4 Operative costs of the considered routes applied to recycling of 1 kg of LFP cathodic material from production scraps 107

List of abbreviations

- DMC: Dimethyl carbonate
- EV: Electric vehicle
- FAA: Flame atomic absorption
- FESEM: Field emission scanning electron microscopy
- GHG: Greenhouse gas
- KPI: Key performance indicator
- LCA: Life cycle assessment
- LCO: Lithium cobalt oxide
- LFP: Lithium iron phosphate
- LIB: Lithium-ion battery
- MFA: Material flow analysis
- NCA: Nickel cobalt aluminium
- NMC: Nickel cobalt and manganese oxide
- SEM-EDS: Scanning electron microscope - energy dispersive x-ray spectrometry
- XRF: X-ray fluorescence

Introduction and objectives

Lithium-ion batteries (LIBs) are fundamental energy storage technologies to achieve Europe's target of reaching zero emissions by 2050. The demand of raw materials for LIBs production is expected to increase dramatically in the near future, and recycling processes for the recovery of secondary raw materials are essential to ensure the supply chain and limit the environmental impacts and costs associated with the extraction of raw materials. State of the art technologies for LIBs recycling rely on pyrometallurgy, to recover the most valuable components (Co, Ni and Mn) in form of metal alloys, and hydrometallurgy, to extract the target metals by acid leaching and recover them via solvent extraction and precipitation. Despite hydrometallurgical LIBs recycling is widely applied at full scale and intensively researched; current technologies are not suited for battery chemistries with lower content of cobalt. Indeed, recycling of Lithium Iron Phosphate (LFP) cathodes result not economically favourable due to operative costs associated with state-of-the-art processes.

This thesis aims to investigate circularity of materials for the LIBs market, to ensure reliable supply chains and limit environmental and economic impacts associated with secondary materials recovery from LIBs recycling. The material flow analysis of LIBs supply chain and recycling, and the main environmental and economic implications of secondary raw materials recovery to supply European materials demands have been studied. Afterwards, several experimental activities have been carried out to limit environmental and economic impacts of LIBs recycling, considering electrochemical discharge, pre-treatments and hydrometallurgical recycling, with a particular focus on the recovery of Lithium Iron Phosphate (LFP) from end-of-life cathodes and production scraps. The contents of this thesis are organized in the following chapters:

Chapter 1 - State-of-the-art on Lithium-ion batteries recycling:

This Chapter serves as a review of the state-of-the-art technologies for LIBs recycling, comparing advantages. technical limitations and critical aspects. The results of this Chapter identify the research gaps addressed in this Thesis.

Chapter 2 - Material flow analysis of recycling and supply chains:

This Chapter presents the results of the material flows associated with LIBs full-scale supply and recycling infrastructure, considering current (2020) and forecasted (2030) demand for EVs market.

Chapter 3 – Environmental and economic analysis of recycling and supply chain material flows:

This Chapter compares environmental impacts, in terms of GHG emissions associated with LIBs recycling and with extraction of virgin minerals for LIBs manufacturing. Eventually different LIBs recycling technologies have been compared to identify the most economically efficient.

Chapter 4 – Electrochemical discharge for lithium-ion batteries recycling:

This Chapter studies the application of non-corrosive solutions (sodium carbonate and potassium carbonate) for electrochemically discharge of end-of-life LIBs. Gaseous emissions and solutions pH were monitored to understand better the discharge mechanism of LIBs in carbonates solutions. In addition, a novel experimental set-up was developed to observe separately the behaviour of the positive and negative half-cells during discharge.

Chapter 5 – Pre-treatment for lithium iron phosphate cathodes recycling:

This Chapter studies the application of chemical-free pre-treatment for the detachment of cathodic active materials from current collectors of LFP end-of-life cathodes and production scraps. Ultrasound washing, ball milling and thermal treatment followed by ball milling have been compared considering separation efficiency and purity of the recovered materials.

Chapter 6 – Hydrometallurgical recycling of end-of-life lithium iron phosphate cathodes:

This Chapter studies hydrometallurgical recycling of end-of-life LFP cathodes via conventional leaching and selective leaching, based on the use of citric acid and hydrogen peroxide. Both for conventional and selective leaching the recycling processes have been completed up to the recovery of mineral precursors for the production of new battery cathodes.

Chapter 7 – Hydrometallurgical recycling of lithium iron phosphate cathodes production scraps:

This Chapter studies hydrometallurgical recycling of LFP cathodes production scraps via selective leaching, based on the use of sulfuric acid or citric acid combined with hydrogen peroxide.

Chapter 8 – Economic analysis of lithium iron phosphate cathodes recycling:

This chapter concludes the experimental activities on the recycling of LFP end-of-life cathodes and production scraps, with the economic analysis of the recycling processes tested in the previous Chapters and the comparison of the results of this Thesis with scientific literature.

Eventually, one final section has been added to draw the conclusions of this work and discuss potential implication and future research developments. The appendix of this Thesis reports the list of academic dissemination activities carried out to present the main results obtained by this Thesis.

Chapter 1

State of the art on lithium-ion batteries recycling

This chapter presents an overview of current state of the art technologies for LIBs recycling. The content of this chapter has been presented in a research articles titled "*Review of Lithium-Ion Batteries' supply-chain in Europe: material flow analysis and environmental assessment*", authored by **Martina Bruno** and Professor Silvia Fiore and published on Journal of Environmental Management (Bruno and Fiore, 2024a) and "*Review of up-stream processes for Li-ion batteries recycling: safety and economic concerns*" authored by **Martina Bruno** and Professor Silvia Fiore (under review).

1.1 Introduction

LIBs are an emerging technology utilized for energy storage that has a wide range of applications, including electric vehicles (EVs) and portable electronic devices such as laptops, smartphones, and tablets. LIBs play a crucial role in the transition to clean energy and the decarbonization of transportation and energy systems. Renewable energy harvesting relies on LIBs, to store the intermittent energy supply provided by sources such as wind and solar energies and providing a reliable alimentation to energy grid applications (Diouf and Pode, 2015).

On the other hand, LIBs application on electric transport systems are being boosted to tackle the greenhouse gas (GHG) emissions associated with transportation based on conventional internal combustion engines (Singh et al., 2024). GHG emissions from transport in Europe in 2023 were above 800 Mt CO_2 eq. (European Environment Agency, 2023). Due to the potential reduction of GHG emissions by electrification of the transport systems, countries worldwide are setting target for EVs diffusion to achieve decarbonification goals: e.g. 35% of newly immatriculated vehicles in Europe (International Energy Agency, 2023) and 50% in the USA (National Academies of Sciences Engineering and Medicine, 2021) should be EVs.

The main components of LIBs are the active materials contained in the electrodes, were redox reactions take place during the charge and discharge phases over use (Xie and Lu, 2020). The electrodes are defined as a positive electrode where reduction reactions occur during discharge and oxidation takes place during charge, here on referred to as "cathode" and negative electrode with opposite behaviour defined as "anode". In LIBs, the cathode contains lithium and transition metal oxides (aluminium, cobalt, iron, manganese, nickel and phosphorous) deposed over an aluminium foil acting as current collector while the anode contains graphite over a copper current collector (Abe et al., 2024). The composition of LIBs includes economically valuable elements and critical raw materials (CRMs), the extraction of which often comes with significant costs and environmental impacts. GHG emissions generated during EVs manufacturing are 30% higher than during manufacturing of conventional vehicles, mostly due to mining and processing of metallic components for LIBs cathodes (Hao et al., 2017a). Besides, the European Commission (EC) recognizes several components of LIBs, such as lithium, cobalt, phosphorous, and graphite, as CRMs (European Commission, 2020b).

Thereby, recycling LIBs is crucial for mitigating the shortage of raw materials and reducing the economic and environmental costs associated with primary extraction and mitigating environmental risks due to improper disposal (Harper et al., 2019). This Chapter provides a literature overview on LIBs recycling presenting state of the art recycling technologies and discussing main advantages and limitations.

1.2 Methodology for literature review

A review of scientific literature on LIBs recycling technologies was conducted on the Scopus database with the following keywords: “lithium-ion battery recycling” AND “waste batteries characterisation”, “thermal treatment”, “pyrometallurgy”, “hydrometallurgy”, “mechanical treatment” in various combinations. The 1.476 research and review papers published between 2013 and 2023 were analysed to filter out the ones less relevant to this review: studies on recycling processes of other waste streams in order to produce LIBs, design for recycling and electrochemical performance were taken out of the database. The resulting 1.238 studies were categorised according to the following topics: review on recycling, discharge, pre-treatment, thermal treatment, chemical treatment, biological treatment, direct recycling, environmental analysis and material flow analysis. To trends in different topics are displayed in Figure 1-1.

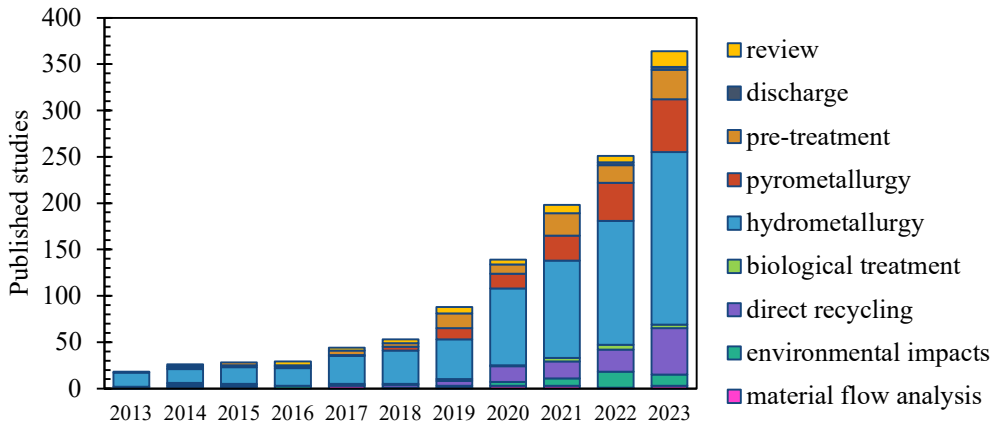


Figure 1-1 Categorization of selected references according to year of publication and research topics

1.3 Lithium-ion batteries recycling

Previous research on LIBs’ recycling has predominantly focused on: hydrometallurgy, pyrometallurgy, pre-treatments (including discharge, disassembly, and physic-mechanical/thermal processes), and general recycling. On the other hand, life cycle assessment (LCA) and material flow analysis (MFA) of virgin raw materials and secondary raw materials for LIBs received less attention. According to the results of this review the most prevalent topic for LIBs recycling consists in hydrometallurgy, accounting for 55% of papers published in the last ten years, followed by pyrometallurgy (13%), direct recycling (10%) and pre-treatments (9%). Pyrometallurgy and hydrometallurgy are well-established technologies for metals processing which are commonly applied in LIBs

recycling as well as other sectors such as manufacturing processes for the energy, aerospace and prosthetic industries. Discharge for LIBs recycling, biological processes, environmental and material flow analysis are less discussed topics, accounting together to 8% of the selected studies. It is worth to notice that while research only recently started to focus on discharge processes, biological treatments and environmental and material flow analysis have always been studied during the last decade. However, while the interest on environmental impacts of LIBs recycling processes appears steadily increasing, material flow analysis and biological treatment are constantly overlooked. In this chapter, the most relevant results of this literature review are presented according to the selected topics, summarizing advantages and challenges presented by different recycling treatments and research gaps in environmental and material flow analyses.

In terms of the specific battery cathodes studied, the majority of the research (50%) evaluated the recycling of lithium nickel cobalt and manganese oxide (NMC) cathodes. The rationale behind the emphasis on the recycling of NMC cathodes in scientific research can be attributed to the dominance of NMC cathodes in the battery market and their content of economically valuable metals, such as cobalt, manganese and nickel. Comparatively, less attention was given to the recycling of lithium iron phosphate (LFP) and lithium cobalt oxide (LCO) cathodes, with 24% and 18% of the studies focusing on these chemistries, respectively. It is worth noting that the scientific community's interest in LIBs' recycling has primarily revolved around the development and optimization of recycling processes, particularly in the context of hydrometallurgy applied to NMC cathodes. On the other hand, topics such as material flow analysis and economic assessment have remained relatively unexplored in the last decade.

1.3.1 Discharge

Residual energy in end-of-life Li-ion batteries may pose safety issues during further recovery treatments, leading often to fire and explosion hazard (Gaines, 2014), thereby discharging is an essential pre-treatment. Discharging can be carried out by water electrolysis in presence of ionic solutions in mildly acidic or alkaline solutions (Shaw-Stewart et al., 2019) to improve discharging performances (Bi et al., 2020; Ojanen et al., 2018; Xiao et al., 2020). The most commonly used salt is NaCl, which, however, leads often to undesirable corrosion phenomena (Rouhi et al., 2021).

In order to limit corrosion during electrochemical discharge process, various technical advancements have been explored by researchers. For instance, a recent study proposed a vertical parallel arrangement of the batteries in the discharge solutions, which serves to decrease the required contact time and prevent corrosion (Torabian et al., 2022). This design configuration, however, is only applicable to pouch cells. Recently, other

researchers have developed an "ex-situ" discharge method (Rouhi et al., 2022), wherein the battery electrodes are connected to platinum wires that are immersed in the discharge solutions. This innovative approach aims to avoid any direct contact between the solution and the batteries. Additionally, an alternative discharge process has been suggested, which involves replacing the discharging solutions with conductive powders made of copper or graphite (Yao et al., 2020). This unique approach has proven to provide a discharge rate comparable to that achieved with NaCl, while completely eliminating the issue of corrosion (Yao et al., 2020). Physical discharge takes advantage of the discharge capacity of iron or graphite powder (Yao et al., 2020). Metal powders guarantee high discharging rates, however, they lead to overheating, and instability during discharge (Yao et al., 2020).

Recently, alternative discharge solutions, such as halogen salts (Cl^-, Br^- and I^-) and $Na_2S_2O_3$ have been proposed (Ojanen et al., 2018; Shaw-Stewart et al., 2019) however they still generate corrosion on battery casing (Shaw-Stewart et al., 2019). Further research studied sulfate-based electrochemical discharge solutions, achieving voltage reductions down to 70% of starting voltage for $ZnSO_4$ (Ojanen et al., 2018), 60% for $NaSO_4$ (Ojanen et al., 2018; H. Wang et al., 2022), 50% for $MnSO_4$ and 40% for $MgSO_4$ (Torabian et al., 2022) that were unsatisfactory when compared to the nearly full discharge achieved by NaCl (Ojanen et al., 2018; Torabian et al., 2022). Nevertheless, they prevented corrosion and release of hazardous substances: for example, the concentration of alkane gasses was 0% during Sodium carbonate discharge and 0.8% during NaCl discharge (H. Wang et al., 2022). As a result, they have been identified as possible "greener" replacements to NaCl for LIBs electrochemical discharge (Yao et al., 2020).

Discharge of residual voltage from end-of-life batteries is essential to guarantee safe handling during down-stream recycling processes and research is dedicating more focus towards these issues. Nonetheless corrosion phenomena and release of gaseous products during discharge deserve follow-up study.

1.3.2 Mechanical treatments

After discharge, LIBs are disassembled into modules and cells. Disassembly is usually performed manually and entails high operative costs. Operative costs of dismantling have been estimated to range from 32 €/kWh, for battery removal from car, to 76 €/kWh, for complete modules disassembly into cells (Rallo et al., 2020). Nonetheless, despite being more time consuming and expensive compared with automatic shredding, manual disassembly provides higher purity in the separated material streams enhancing efficiency and safety of the following recycling steps (Marshall et al., 2020). Thereby, recent studies focused on the optimization of this step. Among the proposed improvements, partial disassembly, compared to complete cells disassembly, has shown great promises for

improving the costs-benefits trade-off (Alfaro-Algaba and Ramirez, 2020). Besides, the use of an hybrid workstation with automatic robotic appliances manually operated by monitoring workers resulted as the most optimised solution in terms of both safety and cost (Tan et al., 2021) and new design solutions have been developed in order to improve both cells configurations for agile disassembly (Wegener et al., 2014) and disassembly lines flexibility and adaptability to different cells configurations (Stief et al., 2019). These initial steps are critical, since they require long time and high costs, due to their inherit complexity, and pose a safety hazard of potential fire or explosions.

Afterwards, the disassembled components undergo a series of pre-treatments involving: comminution, classification or separation and further dissolution or thermal treatments (Kim et al., 2021). The main aim of this steps is to produce concentrated streams of valuable metals from spent batteries is the separation of the active materials (black mass for the cathode and graphite for the anode) from the metallic foils used as current collectors (Al for the cathode and Cu for the anode).

The detachment of electrodes active materials is achieved by removal of organic binders, which is performed by chemical or thermal treatments. Chemical processes based on the use of organic solvents and thermal processes target the degradation of binders and residual electrolyte from the electrodes, to loosen the chemical bond between the active material and the current collectors (Buken et al., 2021; Hanisch et al., 2015; M. Jafari et al., 2020; Vieceli et al., 2021; S. D. Widijatmoko et al., 2020; Xie et al., 2021), by dissolution in organic solvents, such as N-methyl-2-pyrrolidon, dimethylformamide, dimethyl carbonate (DMC) and formamide (N. Zhang et al., 2022) or thermal treatments between 400°C and 550°C (Hanisch et al., 2015; M. Jafari et al., 2020; Liang et al., 2020; S. Widijatmoko et al., 2020a; S. D. Widijatmoko et al., 2020; Xie et al., 2021). Thermal treatments do not usually require previous mechanical processing (Kim et al., 2021), however, beneficial effects of pre-treatment prior to pyrolysis and incineration have been highlighted (Liang et al., 2020). Separation rate of active material from current collectors after thermal pre-treatment ranges between 80% and 85% when pyrolysis is applied (Da Costa et al., 2015; Salces et al., 2022) and 89% and 93% after calcination (Bi et al., 2019; Vanderbruggen et al., 2022).

Mechanical processes instead aim at physically detached the active material, via ultrasound washing or milling, and its comminution to enhance the efficiency of further recycling processes. Common mechanical and physical treatments are: crushing, milling, sieving and separation based on physical properties, such as densiometric splitter, magnetic, eddy current or pneumatic separators (Georgi-Maschler et al., 2012; Granata et al., 2012) and are often implemented in order to facilitate the following materials separation and further acid leaching and solvent extraction steps (Peng et al., 2018; Takahashi et al.,

2020). Several milling machines have been investigated for battery recycling, mainly: ball milling devices (J. Liu et al., 2021), impact crusher and shredding machines (Hanisch et al., 2011; Wuschke et al., 2016; Zhan et al., 2020; G. Zhang et al., 2022). When comparing the effects of different milling principles, ceramics balls mills and hammer crushing did not prove effective compared to knife milling (Takahashi et al., 2020). Besides, lower operative temperature, boost up separation efficiency by milling, due to the induced brittle behaviour at cryogenic temperature (J. Liu et al., 2021). Physical detachment via ball milling can be followed by different separation methods and achieve high separation efficiency of 95% after sieving (Sohn et al., 2015), 97% after pneumatic separation (Zhu et al., 2021) and 99% after eddy current separation (Bi et al., 2019).

Energy requests for comminution range from 99.0 kWh/kg up to 185 kWh/kg, depending on the configuration and the materials of the cells (Wuschke et al., 2019). Recently less energy consuming processes have been developed in order to preserve physical integrity of the separated components, throughout exfoliation of the active electrode components from the current collector foils (Chen et al., 2017b; He et al., 2020, 2019). He et al., 2020 exploited the mechanical effect of gaseous H_2 released by contact of the aluminium of the cathode current collector with H_2O and obtained almost complete separation of the $LiFePO_4$ active material. Otherwise, liquid exfoliating agent can be applied to loosen the chemical bonds between active materials and current collectors (He et al., 2019). In both cases separation efficiency reached almost 100% (He et al., 2020, 2019).

However, concerns arise about safety levels of mechanical treatments (Lewandowski et al., 2020), in particular for the release of harmful volatile components during mechanical comminution (Diaz et al., 2019; Wuschke et al., 2019), thereby off-gas emissions are commonly drawn by vacuum systems and purified though activated carbon adsorption (Stehmann et al., 2017). An innovative solution to tackle fluorine release by polyvinylidene fluoride processing has been implemented using excess $LiOH \cdot H_2O$ to react with the fluorine, removing the binder and lithiating the cathodes (Ross et al., 2020).

Eventually, physical separation of the scraps can be achieved exploiting different properties of the cell's components. Magnetic separation proved to be highly efficient in concentration of Co, since it splits the material into a magnetic fraction, where 90% of the Co gathers, and a tailing fraction containing graphite, Mn, Cu; Al and Li carbonates (J. Li et al., 2016; Vishvakarma and Dhawan, 2019). Similarly, froth floatation has been proposed as a viable separation mechanism to concentrate active materials, upholding electrochemical characteristics in order to be further regenerated via direct recycling (Shin et al., 2020; Zhan et al., 2021).

Besides, mechanochemical processes have been also proposed as effective pre-treatment to combine the mechanical effect of ultrasounds or milling with leaching or reducing reagents (Fan et al., 2018; Li et al., 2021, 2010a; Wang et al., 2016). Physical detachment of cathodes material from current collectors through ultrasound washing has a limited separation efficiency of 46% of active material, which can be improved by adding organic solvents, such as NMP (He et al., 2021), to dissolve the binder, hydrogen peroxide to dissolve the aluminium from current collectors (S. Zhao et al., 2020) or sulfuric acid to enhance leaching of the active material from the cathodes (Chen et al., 2020). Different operative conditions have been studied for ultrasound washing It is worth noting that a significant amount of energy is dissipated as heat during these processes, which can limit the comminution capacity when shredding is carried out at standard rates.

Pre-treatments for LIBs' recycling are based on thermal and physical processes. Nonetheless, most of the studies focused on the optimization of technical parameters and more research is necessary to limit energy consumption of pre-treatments.

1.3.3 Pyrometallurgy

Pyrometallurgy is an high-temperature smelting process aimed at reduction of Co, Ni and Cu as alloys (Mansur et al., 2021). During pyrometallurgical processes the carbon-based components, e.g. plastics, organic solvents, and graphite are lost in the combustion, and the residual elements, such as Li, Al, Si, Ca and Fe in the slug (Assefi et al., 2020). Indeed the main target of pyrometallurgy is reclaiming valuable metals including cobalt, manganese, and nickel (He et al., 2023; Hu et al., 2021b). It is noteworthy to mention that pyrometallurgy transforms the black mass into metal oxides or alloys and that subsequent hydrometallurgy is essential for the extraction of individual metals (Assefi et al., 2020).

Smelting involves subjecting the black mass to temperatures exceeding the melting point of metals (1250-1500 °C), thereby enabling the separation of the reduced components (Makuza et al., 2021). The recovery yields achieved through smelting are as follows: 98% for cobalt and nickel, and 85-92% for manganese (Hu et al., 2021b). It is also worth noting that thermal treatments conducted at lower temperatures (650-1000 °C) manifest in the form of pyrolysis (Makuza et al., 2021; Pindar and Dhawan, 2020a), or incineration, (Lombardo et al., 2021). Pyrolysis has been found to significantly enhance the separation efficiency of electrode active materials in cathodes, resulting in recovery rates ranging from 83% to 99%, and in anodes, with recovery rates ranging from 88% to 97%, (Zhang, 2022). Moreover, the employment of high temperature pyrolysis (>950 °C) has proven to be highly effective in recovering up to 99% nickel from NMC cathodes (Ebin et al., 2019).

Pyrolysis of the black mass yields different outcomes depending on the chemistries of the cathodes: NMC is transformed into oxides such as Co_3O_4, NiO, Mn_3O_4, and Li_2CO_3,

with the release of CO, CO_2, and HF from the binder (Lombardo et al., 2021) LCO is converted into metallic cobalt and lithium carbonate, resulting in the release of the majority of lithium (64-97%) and phosphorous (68%) in the form of gases (Holzer et al., 2022).

Carbothermic reduction induces the volatilization of corrosive gas due to the decomposition of the polypropylene separator and polyvinylidene fluoride binder (Lombardo et al., 2021). Remarkably, the temperature range of 470-599 °C has been associated with the highest rate of material loss, while the release of fluorine decreases with increasing temperature, with no HF being emitted above 470 °C (J. Yu et al., 2020) A limited number of studies have conducted preliminary investigations into the recovery of lithium through carbothermal reduction (Zhang, 2022) or sulphation roasting (Biswas et al., 2023) followed by water leaching, as well as the recovery of lithium and phosphorous from gaseous emissions (Holzer et al., 2022). The energy required for pyrometallurgy amounts to 1.08 kWh/t (Hu et al., 2021a).

Recovery rates resulting from pyrometallurgical processes, see Table 1-1, indicate an average recovery rate of 99% for aluminium, 96% for copper, 86±15% for cobalt, 88±4% for manganese, and 98±1% for nickel. It should be noted that the recovery of iron and lithium is not achieved through these processes. In conclusion, pyrometallurgy represents an efficient means of recovering the metals predominantly found in NMC cathodes, with limited references to the recovery of aluminium and copper from current collectors, while the recovery of lithium and iron remains unattainable. The management of the production of gaseous corrosive and hazardous fractions during thermal processes must be approached with utmost care.

Table 1-1 Recycling efficiency of pyrometallurgical treatment

Al	Co	Mn	Ni	Reference
-	97.90%	91.50%	97.70%	(Hu et al., 2021a)
-	98.20%	85.30%	98.40%	(Hu et al., 2021b)
-	68.00%	-	-	(Pindar and Dhawan, 2020a)
99.34%	-	-	-	(Zhong et al., 2019)
-	81.30%	-	-	(Ruismäki et al., 2020)
-	-	-	99.00%	(Ebin et al., 2019)
	95.6%			(M. Li et al., 2022)
99.34%	86.35% ±15%	88.40% ±4%	98.37% ±1%	average values*

Pyrometallurgical processes are technologically mature and applied in full scale, nonetheless, they present elevated energy demand and emissions generation due to

combustion of plastic components and electrolytes (Y. Wang et al., 2020). Moreover, The materials loss due to limitations of the pyrometallurgical recycling hinders material circularity as promoted by current European legislation, that aims to reach recycling rates of 65% of battery weight by 2025 and 70% by 2030, with specific targets for critical materials recovery of 90% of Co and 35% of Li by 2026 and 95% of Co and 70% of Li by 2030 (European Commission, 2020a).

1.3.4 Hydrometallurgy

Hydrometallurgy is a chemical technique conventional applied in the mining sector to recover metals from mineral ores, throughout leaching in acid solutions, purification of the leaching solution and metals recovery (Free, 2022). Hydrometallurgy relies on the extraction of valuable metals from cathodic active materials in an acidic environment (Larouche et al., 2020). The leaching process typically occurs after either mechanical treatments, (Takahashi et al., 2020) or thermal treatments, (Chen et al., 2020; Fu et al., 2020; Vieceli et al., 2021). Acidic solvents are utilized during leaching at temperatures ranging between 40 °C (Chen et al., 2017b; L. P. He et al., 2017; Y. Jian et al., 2020) and 100 °C, as documented by (Chen et al., 2020, 2018a; Musariri et al., 2019; Wu et al., 2020). Additionally, leaching can also be conducted at ambient temperatures between 20°C and 25°C (Takahashi et al., 2020).

The most commonly employed agent for leaching purposes is sulfuric acid (Chan et al., 2020; Chen et al., 2018a; Diaz et al., 2020; Dutta et al., 2018; L. P. He et al., 2017; Sattar et al., 2019; Urbańska, 2020; Vieceli et al., 2021; Y. Zhao et al., 2020), followed by hydrochloric acid (Guo et al., 2016; Y. Jian et al., 2020; Xu et al., 2020), phosphoric acid (Chen et al., 2020; Meng et al., 2017; Zhuang et al., 2019), and organic acids, predominantly citric (Chabhadiya et al., 2021; Patil et al., 2020; Wu et al., 2020; Xing et al., 2021), alginic (Cai et al., 2022), benzenesulfonic (Fu et al., 2019), formic (Chen et al., 2021; Gao et al., 2017), gluconic (Fan et al., 2020a), and L-tartaric (Ma et al., 2022) acids.

The concentrations of leaching agents typically range from 1-2 M for both organic and inorganic acids, with the exception of sulfuric acid, which occasionally exceeds 5M (Fan et al., 2021; J. Zhao et al., 2020). Compared to inorganic acids, organic acids require higher process temperatures and lower solid/liquid ratios, while the contact time remains similar for all acids, typically ranging from 60-120 minutes. However, citric and ascorbic acids require longer contact times (Nayaka et al., 2018). The reduction of metals valence state favours leaching, and enhances the efficiency of hydrometallurgical recycling, reducing agents are often employed. Hydrogen peroxide is the most commonly used reducing agent, with concentrations of 1.5-2% vol. (Chabhadiya et al., 2021; Musariri et al., 2019) and 4-5% vol. (Chen et al., 2017a; Sattar et al., 2019; Shin et al., 2019). Other

reducing agents that are frequently employed include glucose (Chen et al., 2018a; Meng et al., 2017), starch (Y. Jian et al., 2020), orange peel powder (Wu et al., 2020), ethanol (J. Zhao et al., 2020), citric acid (Zhuang et al., 2019) and glutaric acid (Y. Jian et al., 2020). Furthermore, it has been found that the presence of impurities such as iron and copper in the range of 0.05-0.006 mol/L can improve cobalt leaching efficiencies (Peng et al., 2019).

After leaching, numerous methods have been investigated to recover metals from the leachate. These methods include solvent extraction (Nadimi and Karazmoudeh, 2021; Shin et al., 2023), as well as multi-step processes (Nguyen and Lee, 2021; Yang et al., 2020) and crystallization (Djoudi et al., 2021; Sattar et al., 2019). Prior to metals recovery, hydrometallurgical recycling may require purification of the leachate solutions, which is performed with deep eutectic solvents (Schiavi et al., 2021; Tran et al., 2019; Wang et al., 2019; Zante et al., 2020), supercritical extraction in water and in carbon dioxide (Rothermel et al., 2016) or ionic liquids (Schaeffer et al., 2020; Zante et al., 2020). Similarly, ion-exchange resins have been investigated for their application as chelating and cation-exchange resins (Chiu and Chen, 2017; Virolainen et al., 2021) has been explored by Chiu and Chen (2017). Nonetheless, precipitation (Chu et al., 2020; Peng et al., 2019; Yang et al., 2020; G. Zhang et al., 2020) and co-precipitation (Beak et al., 2021; Guo et al., 2017; Swain, 2018; Jingjing Zhao et al., 2020) remain the simplest and most frequently applied methods to recover metals from leachate solutions.

Lithium and Cobalt recovery is the most studied aspects of LIBs' hydrometallurgical recycling and it has proven to be effective in obtaining materials with purity grades that ensure electrochemical performances comparable to commercially available electrodes (Jo et al., 2018). Finally, the energy consumption associated with hydrometallurgy has been quantified as 1.65 kWh/t (Romare and Dahllöf, 2017). The recycling efficiencies of hydrometallurgical processes obtained by different studies are listed in Table 1-2.

Table 1-2 Recycling efficiency of hydrometallurgical treatment

Al	Co	Fe	Li	Mn	Ni	Reference
			99.4			(Guo et al., 2016)
			97			(Yang et al., 2020)
	97.25		97.72			(Xing et al., 2021)
		95	95			(Liu et al., 2022)
			98			(Ilyas et al., 2023)
	99					(Chen et al., 2017a)
	98		100			(Meng et al., 2017)
		97.67	94.29			(Yang et al., 2020)

91.63		100	92.35	83.1	(Zhuang et al., 2019)
	97.96	93.51			(K. Wang et al., 2022)
	98.24	97.72			(P. Li et al., 2022)
98.9		99.6	97.3	99.1	(Zhou et al., 2023a)
70		99.1			(Jha et al., 2013)
66.2		93.4	50.2	96.3	(Meshram et al., 2020)
74			65	68	(Tanong et al., 2016)
99.7		99.7	99.7	99.7	(L.-P. He et al., 2017)
96		86			(Pagnanelli et al., 2017)
96			94	68	(Tanong et al., 2017)
97		99			(Dutta et al., 2018)
79.4	68.5		91.9	66.2	(Sobianowska-Turek, 2018)
98		96			(Chen et al., 2018b)
93.8		95.7			(Peng et al., 2018)
94.63		98.62			(Jiang et al., 2018)
93.2		80.2	90.3	91.5	(Cheng et al., 2019)
68		92	34.8		(Sattar et al., 2019)
99					(J. Zhao et al., 2020)
99.29		99.78	99.91	98.62	(S. Wang et al., 2020)
98.91		92.67			(Ghassa et al., 2020)
100		100	100	100	(Chan et al., 2021)
92.84			90.18	93.11	(Wang et al., 2018)
23.2		100	18.3	25.6	(Fan et al., 2021)
70		70	70	70	(Vieceli et al., 2021)
99		99			(Aboulaich et al., 2022)

	90	90			(Partinen et al., 2022)
		99.62	98.13		(Chang et al., 2022)
	99	99			(Kong et al., 2022)
	88.6	99.9			(Jiang et al., 2022)
				99.9	(Permatasari et al., 2023)
	97.24	99.79	96.88	99.46	(M. Li et al., 2022)
	95	98	92	95	(Yang Jian et al., 2020)
	98.7	99.9	99.5		(Natarajan et al., 2018)
	91.7	99.6	97.3	99.1	(Zhou et al., 2023a)
94.7	94.61	98.56	97.97	96.39	(Z. Wang et al., 2022)
	90	99			(Prasetyo et al., 2022)
	97.58	98.59			(Cai et al., 2022)
	94.8	98.5			(Li et al., 2012)
	90				(Nayaka et al., 2018)
	99.56	99.69	99.87	99.6	(Chen et al., 2018a)
	96.53	99.58			(Fu et al., 2019)
	95	99	94	97	(Fu et al., 2019)
	96	99			(Gao et al., 2019)
		92			(Golmohammadzadeh et al., 2017)
	95	99			(Chen and Zhou, 2014)
	95	95			(Musariri et al., 2019)
47.24		94.83			(Kumar et al., 2020)
	90	94	98	98	(Pindar and Dhawan, 2020b)
	90	91	89	94	(Meng et al., 2017)
	96	100		96	(Esmaeili et al., 2020)
	96.1	94.1		97.2	(Nakajima et al., 2022)

	95.6	98.3	94.9	90.7	(Choi et al., 2022)
	85	85			(Patil et al., 2020)
	94.3	98.9	96.4	95.1	(Sun et al., 2018)
	90	90			(de Oliveira Demarco et al., 2019)
	97.6	98	97.3	97.8	(Ning et al., 2020)
	98.86	98.13			(Zhou et al., 2021)
	97.1	98.1	97.6	96.2	(Cheng et al., 2022)
	95	95	95	95	(Sidiq et al., 2022)
		99.93			(Zheng et al., 2017)
	95	95	95	95	(Fan et al., 2020b)
	98.5		98.5	98.5	(Ma et al., 2022)
	98	95	98	98	(Fan et al., 2020a)
	97	98			(Zeng et al., 2015)
		98.9			(Rouquette et al., 2023)
	91.8	99.7	89.8	93	(Zhang et al., 2015)
71.0±34 %	91.7±12 %	91.5±13 %	96.2±5 %	88.4±19 %	90.1±15 %	

In conclusion, the average efficiencies of hydrometallurgy, as derived from the literature, are remarkably high when compared to pyrometallurgy (71± 34% for Al, 91.7±12% for Co, 91.5± 13% for Fe, 96.2± 5% for Li,88.4± 19% for Mn and 90.1± 15% for Ni). Additionally, hydrometallurgical processes can recover a greater number of metals, including iron and lithium. However, there are notable challenges associated with this approach, such as the substantial energy requirements, the presence of numerous post-leaching phases, and the use of toxic solvents. Recent literature has focused on addressing these concerns by exploring more environmentally friendly leaching agents and downstream processes. This entails the adoption of lower temperatures and the possible use of milder (potentially organic) acids under safe conditions.

1.3.5 Biological treatments

Biological treatments have been recently proposed to avoid the need of hazardous chemicals for metals recovery from end-of-life LIBs (Roy et al., 2023), as bioleaching to take metals into solution (Roy et al., 2021) and metals recovery from leaching solutions via biosorption and bioaccumulation processes (Nancharaiah et al., 2016). Bioleaching processes rely on redox activity of bacteria, such as mesophiles, Aspergillus niger,

Penicillium simplicissimum, which oxidize sulfur and iron, which enhance metals solubility (Roy et al., 2021). Although bioleaching presents some advantages in terms of energy saving and environmental protection, its lower efficiency and slow microbial cultivation have limited its industrial applications compared to hydrometallurgical recycling (Fan et al., 2020a).

1.3.6 Direct recycling

Direct recycling consists in non-destructive techniques such as mechanical, electrochemical, and cathode regeneration (Harper et al., 2019). Cells components are initially pre-treated using mechanical processes to detach the active materials from current collectors and magnetic separation to concentrate them. Then the residual PVDF binder is dissolved through solvents or thermal treatment (Shi et al., 2018) and the cathodes are regenerated through re-lithiation

Direct recycling offers an alternative low-cost method to recover LIBs components, without altering the materials they contain into new raw materials (H. Wang et al., 2023) by combining re-lithiation processes (T. Yang et al., 2023), mainly employing LiOH (Chan et al., 2023), Li_2CO_3 (G. Jiang et al., 2020), LiCl (J. Wang et al., 2023), $LiNO_3$ (Shi et al., 2019), or Li_2SO_4 (L. Zhang et al., 2020) as lithium supplements and reconstruction of the desired morphological phase via hydrothermal reaction (Chan et al., 2023) electrochemical reaction (L. Zhang et al., 2020). Direct recycling allows to recover end-of-life electrodes or production scraps through non-destructive rejuvenating processes (Shin et al., 2023), reducing costs and mitigating environmental impacts (P. Xu et al., 2023). Nonetheless, direct recycling is strictly dependent on the specific composition and mineralogy of different cathodes chemistries thereby accurate sorting of cathodes chemistries is imperative for direct recycling. The difficulty in achieving accurate sorting of different batteries hinders the application of direct recycling processes at full-scale.

1.3.7 Environmental analysis

Life cycle assessment (LCA) has been extensively utilized in the evaluation of the environmental performances of newly developed technologies in LIBs (Raugei and Winfield, 2019). This method has been employed to compare the lifecycle impacts of LIBs with other energy storage systems, as well as to analyse and contrast different manufacturing or recycling processes associated with LIBs (Charles et al., 2019; Sullivan and Gaines, 2012; Terlouw et al., 2019).

Impacts related to resource consumption and battery production has been estimated to range between 300 and 600 kJ/kg, depending on the cathode chemistry (Swart et al., 2014). Environmental impacts of Li-ion batteries during the manufacturing and use phases

show a strong dependency of environmental performances on the type of energy sources used for electricity production (Burchart-Korol et al., 2020; Peters et al., 2017). Energy demand, internal efficiency and lifetime appear to strongly affect LIBs' environmental impacts during the use stage of their life-cycle (Peters et al., 2017) thus fewer impacts are expected in the future when European countries will rely more on renewable energy sources (Burchart-Korol et al., 2020). Relying to renewable energy (e.g. photovoltaic energy) a 67% emissions drop can be expected (Delgado et al., 2019).

LIBs' manufacturing has been found to be the most impacting phase in the whole life cycle, in terms of global warming potential, photochemical oxidation formation potential, particulate matter formation potential, freshwater eutrophication potential and metal depletion potential (Ahmadi et al., 2017). The initial steps of material extraction, transport and processing have been considered accountable for emissions values ranging from 96-107 kg CO_2/kWh (Hao et al., 2017b), 110 kg CO_2/kWh (Peters et al., 2017) and 150-200 kg CO_2/kWh (Romare and Dahllöf, 2017) up to 157 kg CO_2/kWh (Ellingsen et al., 2016). Compar3ed with conventional internal combustion engines, impacts due to electric vehicles manufacturing are higher (Ellingsen et al., 2016; Qiao et al., 2017), however, they appear to be compensated by a smaller environmental footprint during the use phase of the life cycle (Nealer et al., 2015).

1.3.8 Material flow analysis

Material flow analysis (MFA) is a common tool to model materials and substances supply chains and assessing the potential for recycling critical raw materials across various geographical and temporal scales (C. Zhang et al., 2023). The global perspective reveals growing concerns as the rate of demand expansion surpasses the capacity of material supply, leading to misalignments in the geographical distribution of mining reservoirs, manufacturing sites, and market locations for LIBs (Miao et al., 2023). To address this challenge, previous MFA studies recognizes the essential role of recycling in meeting the growing demand in the LIBs market (Lähdesmäki et al., 2023). Besides, in order to tackle the issue of raw materials shortage several alternatives have been proposed: from the development of batteries with low Li and Co contents to reintroduction of spent LIBs with secondary applications or enhancement of the recycling infrastructure (Greim et al., 2020).

With an anticipated shift in market shares towards LIB chemistries with reduced cobalt content (Tang et al., 2021), the adoption of circular economy approaches is projected to achieve global circularity targets ranging from 60% to 85% for cobalt by 2040 (Dunn et al., 2021), consequently reducing lithium waste disposal from 75-85% to 7-47%, (Lähdesmäki et al., 2023). Furthermore, the recycling of LIBs offers substantial economic advantages through the recovery of secondary materials, with copper, aluminum, and

manganese extracted from recycled batteries estimated to have economic values of 7.9, 4.4, and 3.9 billion US dollars, respectively, (Shafique et al., 2023). Countries such as China and the United States, anticipating LIBs sales to exceed 18 million units by 2030, heavily rely on importing raw materials for battery production and stand to gain from implementing circular resource management strategies (Shafique et al., 2022).

Previous research in the field of MFA for LIBs material predominantly focused on analysing material flows pertaining to the electric vehicles (EVs) market and only a limited number of studies concern batteries designed for stationary energy storage (Vandepaer et al., 2019) or batteries utilized in portable electronic devices (Apalkova et al., 2021; Arain et al., 2022; Nigl et al., 2020). This research gap could potentially be attributed to the current dominance of LIBs for electric transportation (Rajaeifar et al., 2022). One of the main drivers of global demand for cobalt and lithium is electric mobility (Zhang et al., 2021). In order to address the shortage of raw materials, various strategies can be implemented. For instance, reducing the content of CRMs in the next generation of LIBs can help mitigate the shortage (Amici et al., 2022; Bella et al., 2021).

Interestingly, a limited number of studies have undertaken MFA from a global perspective (Dunn et al., 2021; Ziemann et al., 2018). Conversely, the majority of studies concentrates on specific geographical regions, such as China (W. Liu et al., 2021; Rui et al., 2021; Wang and Ge, 2020; Yang et al., 2021; Y. Yu et al., 2020), South Korea (Kim et al., 2018) and Thailand (Arain et al., 2022) within Asia, or The United States of America (Miatto et al., 2020; Shafique et al., 2022) and Brazil (Castro et al., 2021) in the American continent, as well as Austria (Nigl et al., 2020), The Netherlands (Tang et al., 2021), Switzerland (Vandepaer et al., 2019), and the United Kingdom (Kamran et al., 2021) in Europe. Furthermore, certain studies have honed in on specific material flows like lithium (Miatto et al., 2020; Ziemann et al., 2018), cobalt (Baars et al., 2021) or graphite (Rui et al., 2021).

1.4 Discussion

The material composition of current electric vehicles makes them valuable “urban mines” (Iglesias-Émbil et al., 2020) and material recovery through LIBs recycling will play a significant contribution in addressing supply demand driven by increasing LIBs production (Matos et al., 2022; Mayyas et al., 2019) However, research is currently tackling the optimisation of EoL LIBs recycling strategies in order to maximise quantity and quality of recovered materials and reducing environmental and economic impacts of recycling operations (Asadi Dalini et al., 2020; Heelan et al., 2016; Kader et al., 2021).

There are still numerous challenges that are associated with LIBs recycling. To begin with, the complexity of accurately sorting different battery chemistries during the collection process poses a significant limitation to the technological feasibility of materials recovery. Additionally, there are safety concerns that arise from the initial discharge process, as it has the potential to release harmful gases and pose hazards due to voltage rebound. These safety concerns may, in turn, limit the overall safety during the subsequent disassembly step. During the disassembly process, there is also a risk to workers' safety due to the presence of hazardous chemicals in the batteries' electrolytes and binders. Furthermore, the residual voltage can cause ignition risks, further adding to the risk faced by workers.

Following the dismantling and separation of the batteries' casings, the electrodes undergo pre-treatments aimed at concentrating the valuable black mass from other components of lesser value. However, these pre-treatments consume a significant amount of energy and still have limited efficiency. Metallurgical recycling of LIBs is typically carried out through pyrometallurgical processes, which primarily aim to recover metals such as cobalt (Co), nickel (Ni), and manganese (Mn) as metal alloys. However, during these thermal processes, careful management of corrosive gases and hazardous fractions that are released is crucial.

In addition to pyrometallurgy, novel recycling plants also employ hydrometallurgical recycling to expand material recovery to include lithium, which is lost as slag during the pyrometallurgical process. However, the use of hazardous chemicals and the multiple post-leaching phases raise environmental concerns and make waste management a challenging task. To improve safety and environmental sustainability throughout the entire LIBs recycling process, it is crucial for research to focus on achieving this target.

Finally, future research should aim to enhance the environmental sustainability of hydrometallurgical processes by limiting the operative temperature, utilizing milder organic leaching agents, and simplifying materials recovery after leaching. Overall, although there are challenges associated with LIBs recycling, it is imperative to address these issues to ensure the safety of workers and promote environmental sustainability. By focusing on improving various aspects of the recycling process, such as sorting, discharge, disassembly, pre-treatments, and metallurgical and hydrometallurgical processes, we can move towards a more efficient and sustainable approach to LIBs recycling.

1.5 Conclusions

Recycling LIBs is important for several reasons. Firstly, it helps to reduce the environmental impact of LIBs and prevent ecological and social harm. Secondly, recycling allows for the recovery of valuable materials, such as lithium, cobalt, nickel, and aluminum, which can be used as a reliable source of valuable resources. Thirdly, the recycling of LIBs contributes to achieving a sustainable circular economy and helps address the increasing demand for metals set by the growing LIBs market, reducing the demand for primary mineral resources and mitigates environmental pollution caused by improper disposal.

LIBs recycling consists of a series of processes: discharge of batteries, dismantling into modules and cells, pre-treatments to concentrate targets metals and recovery processes. Recovery of metals from end-of-life LIBs can be performed via pyrometallurgy or hydrometallurgy. Although pyrometallurgy is a well-established technique for recovering metal alloys, its primary disadvantages are the high energy need, the production of gaseous pollutants, and the restriction on the recovery of lithium. Alternatively, hydrometallurgy is a chemical process that uses leaching and separation stages to extract specific metals, such as lithium. In order to recover and isolate the metals from end-of-life LIBs, hydrometallurgical recycling often uses inorganic acids, including as sulfuric, chloridic, and nitric acids, together with hydrogen peroxide as a reducing agent. Biological treatments have been recently studied as a low-energy intensive alternative to hydrometallurgy, similarly direct recycling presents a viable solution for electrodes regeneration, however they are not yet ready for full scale implementation.

Chapter 2

Material flow analysis of recycling and supply chains

This chapter presents the results of the material flow analysis of the main metals for LIBs manufacturing based on the material demand set by European regulation and foreseen recycling capacity in Europe. The data collection for material flow analysis is based on the results of the review of scientific literature on LIBs recycling (Chapter 1). The content of this chapter has been presented in two research articles titled "*Review of Lithium-Ion Batteries' supply-chain in Europe: material flow analysis and environmental assessment*" authored by **Martina Bruno** and Professor Silvia Fiore and published on Journal of Environmental Management (Bruno and Fiore, 2024a) and "*Material Flow Analysis of Lithium-Ion Battery Recycling in Europe: Environmental and Economic Implications*" authored by **Martina Bruno** and Professor Silvia Fiore and published on Batteries (Bruno and Fiore, 2023).

2.1 Introduction

LIBs have an extensive range of applications, from energy storage to electric mobility and portable applications. Battery energy storage is a key flexibility option for the success of the energy transition (Kordkheili and Mohammadi, 2017). Thus, they stand as a key technology in the decarbonisation of transportation and energy systems. The European Green Deal deliberated a target reduction of GHG emissions from transportation of 90% from the levels of 1990, by 2050 (European Commission, 2019a) and electric mobility, based on the use of LIBs, is a key strategy to achieve this target. Indeed, current targets regarding electrification of the European transport system entail a market share of electric vehicles amounting to 15% by 2025 and 35% by 2030 (European Commission, 2019a).

Therefore, the demand of raw materials (lithium, cobalt, manganese and nickel) for LIBs manufacturing is expected to expand dramatically over time (International Energy Agency, 2023). Indeed, Electric mobility appears to be the main driver for Co and Li demand worldwide (Pehlken et al., 2017). In Europe, the number of newly registered electric cars (EVs) in the EU-27 climbed from 2% to 11% of all vehicles in circulation between 2018 and 2020 (EEA, 2021). The composition of LIBs includes economically valuable elements and critical raw materials (CRMs), which supply relies on delicate geopolitical equilibria, that may lead to supply risks (Habib et al., 2016), but it also entails several negative effects both on environment and social conditions. The increasing demand of critical raw materials for LIBs production led to growing concern for their supply risk (Zhang et al., 2021), particularly in geopolitical regions like Europe, that almost completely relies on foreign extraction and import. (Reznikova et al., 2019).

At the moment, there hasn't been a dedicated study on the material flows involved in the recycling of full-scale LIBs throughout Europe and the corresponding economic and environmental effects. This chapter presents the material flow analysis regarding end-of-life LIBs in Europe in 2030, considering the European recycling capacity and the potential reintroduction of recycled materials in LIBs supply chain for the European EVs market. The amount of Al, Co, Fe, Li, Mn, and Ni contained in LIBs from the European electric vehicles (EVs) in 2020 and reaching the end-of-life stage by 2030 has been calculated. The amount of potentially recovered metals has then been then compared with the materials demand set by European Gigafactories for LIBs production and materials demand set by recent European regulation for electrification share of the transport sector.

2.2 Methodology

This chapter present the MFA associated with the supply chain of LIBs for electric mobility in Europe. The material flow analysis considered the following metals, applied in LIBs

cathodes: Al, Co, Fe, Li, Mn and Ni. The typical composition of LIBs varies depending on the battery chemistry utilized. The amount of metals contained in different cathodes chemistries has been considered from literature (Gaines et al., 2018), see Table 2-1. The following abbreviation are present in Table 2-1: CC: current collector; DMC: dimethyl carbonate; EC: ethylene carbonate; LFP: lithium iron phosphate; NCA: nickel cobalt aluminium; NMC: nickel manganese cobalt; PVDF: polyvinylidene fluoride; PE: polyethylene; PET: polyethylene terephthalate.

Table 2-1 Compositions of the LIBs identified by the different cathodes

	Battery	LFP	NCA	NMC 111	NMC 622	NMC 811
Composition (%-wt)	PET	0.4%	0.3%	0.3%	0.3%	0.4%
	PE	0.2%	0.3%	0.3%	0.3%	0.3%
	Electrolyte DMC	9.3%	6.3%	6.2%	6.3%	7.2%
	Electrolyte EC	9.4%	6.3%	6.2%	6.3%	7.2%
	Electrolyte LiPF6	3.3%	2.3%	2.2%	2.2%	2.6%
	Al (CC)	7.5%	8.4%	8.2%	8.4%	8.0%
	Cu (CC)	14.5%	16.9%	16.4%	16.8%	15.7%
	Binder PVDF	2.7%	2.9%	2.9%	2.9%	3.6%
	Carbon black	2.2%	2.1%	2.3%	2.1%	1.7%
	Graphite	16.6%	22.0%	19.0%	20.7%	20.6%
	Li	1.4%	2.2%	2.7%	2.5%	2.4%
	Co	-	2.8%	6.9%	3.8%	1.9%
	Ni	-	14.9%	6.9%	11.5%	14.9%
	Mn	-	-	6.4%	3.6%	1.7%
	Al	-	0.4%	-	-	-
	Fe	11.4%	-	-	-	-
	P	6.3%	-	-	-	-
	O	13.1%	10.1%	11.2%	10.4%	10.2%

External casing of cells is conventionally made by Fe-Ni alloy (20-26% wt.) for cylindrical cells and Al (10% wt.) for prismatic cells (Mossali et al., 2020). Plastic compounds such as polypropylene, polyethylene, and polyethylene terephthalate, constitute approximately 2.3-2.5% by weight. The electrolyte, consisting of LiPF6, ethylene carbonate, and dimethyl

carbonate, comprises approximately 14-22% by weight. The binder, which is commonly polyvinylidene fluoride, makes up approximately 2.7-3.6% by weight. The anode, composed of a copper current collector and graphite, represents approximately 29.5-38.9% by weight. Lastly, the cathode, which includes an aluminium current collector, as well as Al, Co, Fe, Li, Mn, Ni, and P, accounts for approximately 39-48% by weight.

This analysis considered the market shares of different cathodes chemistries in 2020 and as expected for 2030. Indeed, while in 2020 the batteries market was as following: 29% NMC, 26% LCO, 10% NCA, 12% LMO and 23% LFP; by 2030 a future forecast scenario of 48% NMC, 16% LCO, 10% NCA, 10% LMO and 16% LFP has been considered (Lebedeva et al., 2017).

The European EVs circulating fleet in 2020 has been taken a starting point for this analysis. Considering a battery lifetime of 10 years, the amount of LIBs, and consequently the amount of metals (Al, Co, Fe, Li, Mn and Ni) that will reach their end-of-life stage by 2030 has been estimated. The current and foreseen European infrastructure for LIBs recycling has been inventoried and the amount of metals that will be processed and recovered as secondary raw materials has been calculated. The efficiency of recycling processes considered in this Chapter corresponds to the average recovery efficiency reported in the literature review in Chapter 1, specifically in Table 1-1 and Table 1-2.

These results have been compared with foreseen materials demand set by the expected size of the European EVs fleet in 2030. European LIBs production capacity has been estimated based on the inventory of current and forecasted LIBs Gigafactories. The average weight of a LIB pack has been considered 318 kg (Iclodean et al., 2017). Since the available data about current and announced EV battery production capacity are expressed as energy (kWh and GWh) the characteristic average energy density of 0.15 MWh/t has been considered to estimate the amount of produced Li-ion batteries (t). Eventually, the efficiency of pyrometallurgical and hydrometallurgical recycling treatments were derived from the literature review described in Chapter 1.

2.3 Results

According to the fleet of European EVs in 2020, focusing on the market shares of various commercially available battery chemistries and their compositions, it is projected that by 2030, there will be an estimated 229 kt of end-of-life LIBs. The following batteries were present in the European EVs market in 2020: nickel cobalt aluminium (NCA), NMC and LFP. Specifically, the forecast includes 103 kt of NMC622, 55 kt of NMC111, 44 kt of NCA, 23 kt of NMC811, and 4 kt of LFP EoL batteries, see Figure 2-1. In particular, 46.9

kt of graphite, 38 kt of copper, 19 kt of aluminium, 5.6 kt of lithium, 9.3 kt of cobalt, 25.5 kt of nickel, 7.6 kt of manganese, 0.5 kt of iron, and 0.3 kt of phosphorous, see Figure 2-2.

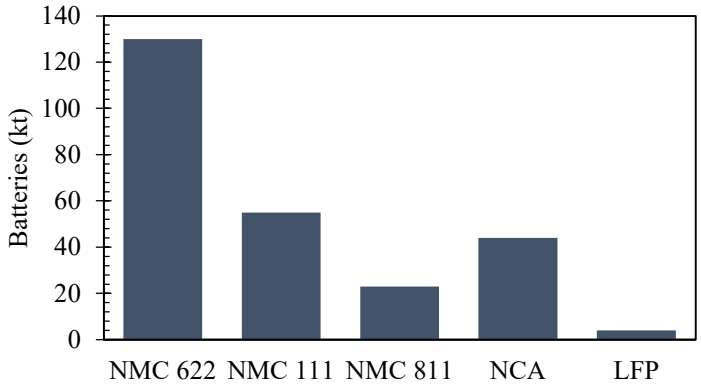


Figure 2-1 Projection of EVs batteries reaching end-of-life by 2030 in Europe

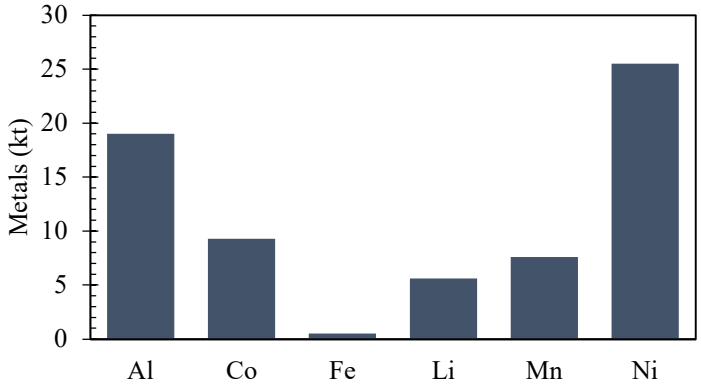


Figure 2-2 Projection of metals from EVs batteries reaching end-of-life by 2030 in Europe

2.3.1 Material flow analysis of European recycling capacity

European LIBs recycling capacity has been estimated according to an inventory of current and forecasted recycling plants in Europe, see Table 2-2. From our inventory of LIBs recycling plants in Europe resulted at a total capacity of 55.810 t/year, considering fourteen plants in Belgium, Finland, France, Germany, Sweden, Switzerland, Norway and United Kingdom. From our inventory results that four countries are currently responsible for 93% of the total European recycling capacity: 13% in Belgium, 37% in France, 30% in Germany and 13% in Norway. The recycling capacity for European LIBs is determined to be 55.8 kt based on the inventory of treatment plants.

Table 2-2 Inventory of LIBs recycling plants in Europe in 2020

Country	Company	Capacity (t/y)	Reference
Belgium	Umicore	7.000	(Danino-Perraud, 2020; Larouche et al., 2020; Winslow et al., 2018)
Finland	Akkuser	4.000	(Danino-Perraud, 2020)
France	SNAM	300	(Danino-Perraud, 2020; Larouche et al., 2020; Winslow et al., 2018)
	Recupyl	110	(Danino-Perraud, 2020; Larouche et al., 2020; Winslow et al., 2018)
	Euro-dieuze	200	(Danino-Perraud, 2020)
	Eramet	20.000	(Danino-Perraud, 2020)
Germany	Accurec GmBH	4.000	(Larouche et al., 2020; Mossali et al., 2020)
	Duesendeld	3.000	(Danino-Perraud, 2020)
	Redux	10.000	(Danino-Perraud, 2020)
	Lithorec	n/a	(Mossali et al., 2020)
Spain	Pilagest	n/a	(Romare and Dahllöf, 2017)
Sweden	uRecycle	n/a	(Danino-Perraud, 2020)
Switzerland	Batrec Industrie AG	200	(Mayyas et al., 2019)
Norway	Glencore	7.000	(Danino-Perraud, 2020)
United Kingdom	AEA Technology	n/a	(Mossali et al., 2020)

Considering the overall European LIBs recycling capacity, 56% of end-of-life LIBs can be treated using pyrometallurgy, 21% using hydrometallurgy, and 23% using a combination of pyrometallurgy and hydrometallurgy. Pre-treatments are also combined with pyrometallurgical and hydrometallurgical processes on site. Indeed, SNAM and Eramet in France, Akkuser in Finland, and Duesendeld in Germany perform pre-treatments followed by pyrometallurgical recycling, while Redux and Lithorec in Germany, Batrec Industries in Switzerland, AEA Technologies in the United Kingdom perform pre-treatments followed by hydrometallurgical recycling. According to this inventory Pilagest in Spain, and uRecycle in Sweden are the only plants in Europe focusing on mechanical processes for LIBs recycling.

The current size of European LIBs recycling infrastructure appears inadequate to treat the projected amount of end-of-life EVs batteries for 2030: which are expected to overcome recycling capacity by almost 3.7 times, resulting in 80% of the metals from end-

of-life batteries to remain untreated. On the other hand, the end-of-life batteries received by recycling plants will be distributed across different facilities and treated according to the processes implemented in the facilities: 56% of input materials will be treated by pyrometallurgy, 21% by hydrometallurgy and 23% by the combination of pyrometallurgy and hydrometallurgy. Pyrometallurgy is the most commonly employed technology in full-scale recycling plants. Consequently, the potentially recoverable secondary raw materials associated with pyrometallurgy are higher (+26%) compared to hydrometallurgy.

The recycling efficiency of full scale treatment plants have been estimated based on the average results of the literature review presented in Chapter 1, see Table 1-1 for efficiency of pyrometallurgical treatment and Table 1-2 for efficiency of hydrometallurgical treatment. Based on the recovery efficiencies of the recycling processes implemented at full scale, the estimated amounts of recovered materials are as follows: 3.5 kt of aluminium (87% of the forecasted recycling input), 7.8 kt of copper (96% of the input), 0.5 kt of lithium (42% of the input), 1.8 kt of cobalt (90% of the input), 5.3 kt of nickel (98% of the input), 1.5 kt of manganese (90% of the input), and 39 t of iron (35% of the input), see Figure 2-3. The majority of the metals that are recovered will come from pyrometallurgical processes, specifically 64% of the recovered aluminium, 56% of copper and nickel, 54% of cobalt, and 55% of manganese. However, the lowest recovery rates are seen for lithium (42% of the potentially recoverable amount) and iron (35%), which are lost in the slags during pyrometallurgy. The majority of treatment plants inventoried performs pyrometallurgical recycling processes, thereby the amount of recovered metals, following the amount of processed metals, results higher from pyrometallurgical facilities.

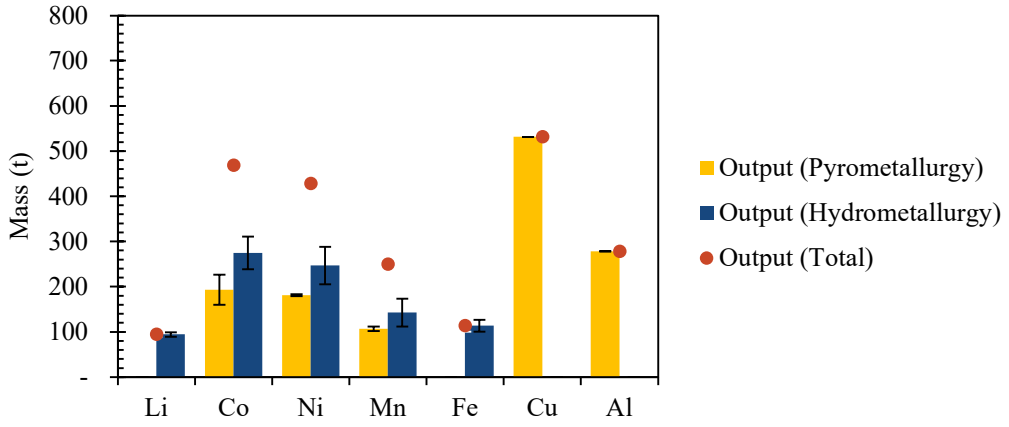


Figure 2-3 Projection of recycled metals from EVs batteries reaching end-of-life by 2030 in Europe

The efficiency of metals recycling has been compared with the potential of materials circularity. Firstly, the amount of recovered materials based on the generated input from

end-of-life EVs batteries has been calculated and compared with the amount of recovered metals based on the treated input from end-of-life EVs batteries. Eventually, the amount of recovered materials based on the input of treated end-of-life EVs batteries, and the reagents used during recycling has been calculated. The results of these circularity indicators are presented in Table 2-3.

Table 2-3 Circularity indicators and recycling efficiency parameters

	Al	Co	Fe	Li	Mn	Ni
R_{TOT}	19%	19%	7%	9%	21%	19%
R_{TREAT}	87%	90%	35%	42%	98%	90%
$\eta_{MATERIALS}$	38%	25%	1%	8%	49%	21%

The values obtained from circularity indicators and recycling efficiency parameters reveal a significant gap in recovery rates when considering the total amount of generated waste (R_{TOT}) compared to the amount of materials entering treatment plants (R_{TREAT}). This is due to the high efficiency of the processes implemented at full scale and the limited capacity of the overall recycling infrastructure. The recovery efficiencies of lithium and iron (both R_{TOT} and R_{TREAT}) are particularly low at 7-9% and 35-42% respectively due to the limited number of facilities using hydrometallurgical processes in Europe. The difference in performance between the recycling infrastructure associated with input materials (R_{TREAT}) and EoL materials (R_{TOT}) clearly indicates that the treatment infrastructure is not suitable for handling EoL LIBs. Additionally, the efficiency in the use of materials ($\eta_{MATERIALS}$) in recycling treatments is particularly low for lithium (8%) and iron (1%), as they are mainly recovered through hydrometallurgy, which requires a larger amount of reagents for leaching and recovery compared to pyrometallurgy.

2.3.2 Material flow analysis of supply chain for European EVs market

Metals demand set by European EVs market in 2030 are based on the projected EVs demand, which is expected to reach 35% of the European vehicles' fleet, in order to meet European target (European Environmental Agency, 2021). Market shares and cathodes compositions have been adjusted to take into consideration the shifts expected between 2020 and 2030. Market shares in 2030 will hold a significant presence of NMC cathodes, while the quota of LCO cathodes is expected to decrease, reducing future demand of cobalt. The following quantities of metals, see Figure 2-4, are required per ton of battery: 2.16 kg of lithium (4,885 tons annually), 4.58 kg of cobalt (10,338 tons annually), 8.64 kg of nickel

(19,509 tons annually), 3.27 kg of manganese (7,393 tons annually), and 1.82 kg of iron (17,986 tons annually).

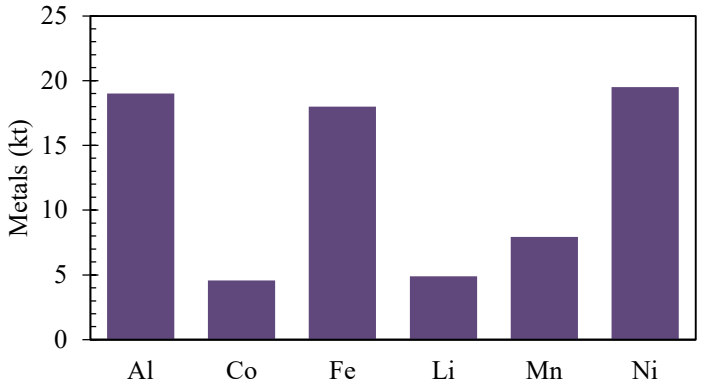


Figure 2-4 Projection of metals demand for EVs batteries reaching in Europe in 2030

The shifts in market share and composition between 2020 and 2030 represent crucial considerations, indicating that LIBs manufactured in 2020 and processed at recycling facilities in 2030 will be capable of supplying metals for a greater number of batteries, highlighting the importance of sustainable resource management in the battery industry. This transition underscores the significance of strategic planning and resource allocation to meet the evolving demands of the electric vehicle market while ensuring the efficient utilization of materials and promoting circular economy principles within the battery supply chain.

European LIBs production capacity has been estimated based on the inventory of current and forecasted LIBS Gigafactories, see Table 2-4. European production facilities, as a whole, demonstrate a production capacity of 2,525,893 t/y, which is deemed sufficient to meet the projected needs of 2,257,800 t/y by the year 2030. LIBs production capacity has undergone significant changes in recent years. In 2016, this capacity was concentrated solely in the United Kingdom, but by 2030, Germany is expected to account for 52.5%, followed by Poland at 20%, Sweden at 12.7%, and Norway at 8.4% as significant contributors. Collectively, these countries are projected to contribute 2,433,333 t/y out of the total European production capacity of 2,525,893 t/y, see Table 2-4. Thereby, the manufacturing capacity of LIBs in Europe is sufficient to supply the demand for LIBs as targeted by European legislation.

Table 2-4 Inventory of current and forecasted Gigafactories for LIBs production in Europe

Country	Company	Capacity (GWh/y)	References:
Austria	Samsung SDI	n.a.	https://samsungsdibs.at/locations/#austria
France	SAFT	0.08	https://www.saftbatteries.com/products-solutions/our-chemistries
Germany	Bitterfeld	10	https://www.argusmedia.com/en/news/1902243-farasis-to-build-german-lithiumion-battery-plant
	CALT	114	https://www.electrive.com/2019/02/04/catl-plans-up-100-gwh-battery-factory-in-germany/
	NorthVolt	40	https://northvolt.com/about
	Svolt	44	https://www.electrive.com/2020/11/17/svolt-to-build-24-gwh-battery-factory-in-german-saarland/
	Willstat	10	https://www.leclanche.com/our-technologies/cell/
Great Britain	Sunderland	25	https://www.leclanche.com/our-technologies/cell/
Hungary	Samsung SDI	3	https://www.power-technology.com/news/lithium-ion-battery-factory-sunderland/
	SK Innovation	8	https://samsungsdibs.at/locations/#austria
Norway	Freyr	32	https://www.freyrbattery.com/
Poland	LG Chem	76	https://www.lgchem.com/company/company-information/global-network/overseas-corporation/europe
Sweden	NorthVolt	48	https://northvolt.com/about

However, the current bottlenecks that are currently being experienced in the European LIBs value-chain are primarily associated with the supply chain. It is worth noting that China, Africa, and Latin America are responsible for providing a significant 74% by weight of all the raw materials needed for the production of these LIBs. Furthermore, when it comes to

the production of the finished LIBs, China alone supplies a staggering 66% of them, highlighting its dominant role in the global LIBs market (European Commission, 2020a).

Among the components of LIBs, lithium, cobalt, nickel, and manganese are identified as posing the highest supply risk in Europe (European Commission, 2019b). While the refining and manufacturing processes predominantly take place in China, the mining activities for these crucial elements are geographically dispersed, with a majority occurring outside of Europe (Sun et al., 2019). The extraction of lithium is primarily carried out in countries such as Australia, Chile, and Argentina, totalling 106,200 tons per year, whereas in Europe, Portugal contributes 800 tons per year (Oliveira et al., 2015). Cobalt supply to Europe is mainly facilitated by Finland with 2,100 tons annually, while the Democratic Republic of Congo leads global production with 130,000 tons per year, followed by Indonesia (10,000 t/y) and Russia (8,900 t/y) (USGS, 2024). Manganese supply is sourced from South Africa, Gabon, Australia, and Ghana, totalling 16,400 tons per year globally, and Europe's contribution includes Ukraine, Hungary, and Romania with a total of 700,200 tons annually (European Commission, 2018). Nickel supply is dominated by Indonesia, Russia, and the Philippines at 2,159,000 tons per year globally, with Europe relying on the United Kingdom, France, Italy, Finland, Poland, and Greece for 228,340 tons annually (European Commission, 2018). China leads the global aluminum production with 40,000 tons out of 69,000 tons annually, while Europe's share stands at 3%, primarily from Norway and Iceland with 2,150 tons per year (USGS, 2024). The major iron reserves are found in Australia, Brazil, China, and India, with an annual production of 196,000 tons globally, while Turkey and Ukraine contribute 57,000 tons per year to Europe's iron mining operations (USGS, 2024). Copper production is predominantly concentrated in countries such as Russia, China, Congo, Peru, and Chile, accounting for 12,500 tons annually globally, with a minor contribution from Europe, primarily Poland with 390 tons per year (USGS, 2024).

In order to address supply concerns to ensure access to raw materials for LIBs manufacturing and to boost materials circularity, the European Commission declared a target amount of recycled metals that new batteries should hold: 12% for cobalt, 4% for lithium and 4% for nickel by 2030 (European Commission, 2015). The plants that produce the highest quantities of recycled metals, such as Eramet in France, Redux in Germany, and Umicore in Belgium, play a crucial role in positioning the host countries as significant players in this industry. These key players are instrumental in driving the circular economy forward by reclaiming valuable metals from end-of-life products. By the year 2030, the recycling capacity within Europe is projected to recover an impressive amount of various metals annually. This includes 278 tonnes of aluminium, 468±69 tonnes of cobalt, 531 tonnes of copper, 114±13 tonnes of iron, 95±5 tonnes of lithium, 250±35 tonnes of

manganese, and 428±43 tonnes of nickel. Despite these promising results, it is important to note that these quantities represent only a fraction of the total metal demand for European electric vehicles in 2030.

The recycled metals sourced from European recycling infrastructure are expected to meet around 2% of the total demand, highlighting the need for further expansion and enhancement of recycling capabilities within the region. The projected replacement rate of metals demand for European EVs fleet in 2030 is provided in Figure 2-5. These results are significantly below the target set by Europe for the minimum quota of recycled cobalt, lithium and nickel for new LIBs.

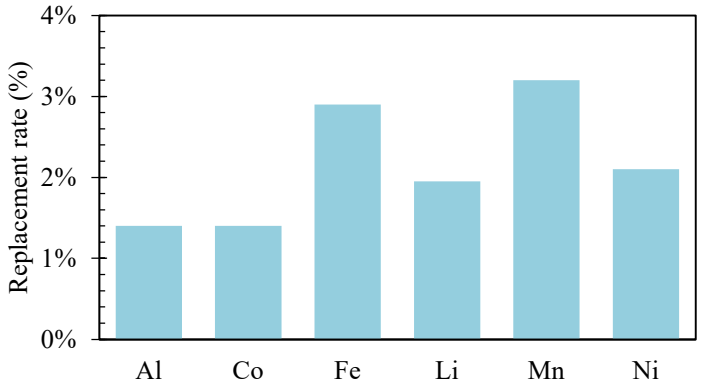


Figure 2-5 Projected replacement rate of metals demand for European EVs fleet in 2030

2.4 Discussion

The European Commission has been actively promoting the electrification of transportation systems to mitigate greenhouse gas emissions, with a specific focus on achieving material circularity in the battery sector. However, our research demonstrates that the existing recycling infrastructure in Europe falls short of meeting the EU's ambitious targets for collection and recovery. Additionally, the mandated minimum levels of recycled content for key metals such as cobalt, lithium, and nickel pose a significant challenge in terms of sourcing secondary raw materials solely from European recycling facilities.

To address these issues and ensure compliance with regulatory standards, it is imperative to increase the recycling capacity across Europe. In recent years, new LIBs recycling plants have been installed across European countries and more have been planned both for black mass processing and further metallurgical processes. Recent projections foreseen European recycling capacity to overcome demand of materials processing (Fraunhofer ISI, 2023). This strategic move will not only help meet the growing demand for recycled metals but also contribute to securing the critical supply chain of raw materials that are predominantly mined outside of the continent. Given the geopolitical complexities

and potential tensions associated with sourcing these materials, bolstering European recycling infrastructure becomes paramount for achieving sustainable resource management and reducing dependencies on external sources.

In terms of their composition, LIBs consist of various metals, such as copper and aluminium, which are used as current collectors in both the anode and cathode. Indeed, LIBs also contain Critical Raw Materials (CRMs), including cobalt (found in cathodes), lithium (found in both cathodes and electrolytes), and graphite (found in anodes). These CRMs present high supply risks in Europe (European Commission, 2020b). Apart from the supply chain concerns, the LIBs' supply chain also raises concerns due to geopolitical uncertainties (Habib et al., 2016). Moreover, the high environmental impacts associated with mining activities further contribute to these concerns (Azadi et al., 2020).

The efficiency reached by state-of-the-art recycling processes for LIBs has proven to be quite effective in recycling metals such as lithium, cobalt, manganese, nickel, aluminium, iron, and copper. It has the potential to recover over 85% of cobalt, nickel, manganese, aluminium, and copper, and approximately 40% of lithium from the input materials. However, these recovery rates significantly decrease when considering the amount of materials discarded as waste, rather than just the inputs to the treatment facilities. Since the recycling infrastructure can only treat around 20% of EoL LIBs, the effective recovery rates are much lower: 21% of nickel, 20% of copper, 19% of cobalt and manganese, 18% of aluminium, and less than 10% of lithium. The bottleneck in LIBs recycling is not the efficiency of material recovery, as the literature review shows recovery rates above 80% for the aforementioned metals. Rather, the lack of hydrometallurgical plants that can recover lithium and iron poses a significant limitation to achieving full material circularity in the battery sector.

2.5 Conclusions

The findings of the MFA presented in this Chapter identified the current deficit in the European recycling infrastructure. This deficit arises from the substantial surplus (approximately 80% of the forecasted EoL LIBs) that cannot be effectively processed in the existing recycling plants. It is estimated that the recovery rate for treated materials will exceed 85% for aluminium, copper, cobalt, manganese, and nickel. However, for iron and lithium, the recovery rates are projected to range between 35% and 42%. Despite the high efficiency achieved by modern recycling technologies, the recovery of critical and secondary raw materials continues to face challenges due to the widespread reliance on pyrometallurgy. This method is employed in over 56% of European recycling plants, but it is unable to recover lithium.

Overall, European recycling capacity according to state-of-the-art recycling efficiencies would allow to recover 354 t of Co, 305 t of Ni, 180 t of Mn, 110 t of Fe, 821 t of Cu and 418 t of Al. We estimated a recovery of 65 t of Li, due to the fact that in 35% of the analysed recycling plants a pyrometallurgical process is implemented without a following hydrometallurgical treatment of the residues slag and this causes loss of Li in the slag phase.

LIBs manufacturing infrastructure in 2030 is expected to be adequate to provide the required amount of LIBs for the amount of electric vehicles (35% of vehicles' fleet) required by European regulations. However, European recycling infrastructure proved to be unable to collect the expected amount of end-of-life LIBs, coming from EVs immatriculated in 2020. Besides, the recovery efficiency of current recycling infrastructure will not be able to meet the required minimum quota of recycled cobalt, lithium and nickel in new batteries. Thereby, the size of European recycling infrastructure is representing a bottleneck in achieving circularity target in the batteries sector and should be incentivised in order to address this issue.

Chapter 3

Environmental and economic analysis of recycling and supply chain material flows

This chapter regards the study of the environmental and economic implications of the material flow analyses of the main metals for LIBs manufacturing based on the material demand set by European regulation and foreseen recycling capacity in Europe. The results presented are based on the results of the review of scientific literature on LIBs recycling (Chapter 1) and the material flow analysis for the European context (Chapter 2). The content of this chapter has been presented at with an oral presentation titled "*Material flows and economic analysis of full scale Lithium-ion batteries recycling processes in Europe*" at CORFU2022 9th International Conference on Sustainable Solid Waste Management Corfu, Greece; and in two research papers titled "*Review of Lithium-Ion Batteries' supply-chain in Europe: material flow analysis and environmental assessment*" authored by **Martina Bruno** and Professor Silvia Fiore and published on Journal of Environmental Management (Bruno and Fiore, 2024a) and "*Material Flow Analysis of Lithium-Ion Battery Recycling in Europe: Environmental and Economic Implications*" authored by **Martina Bruno** and Professor Silvia Fiore and published on Batteries (Bruno and Fiore, 2023).

3.1 Introduction

LIBs application has been boosted by their potential role in reducing environmental impacts associated with energy and transport sectors. Europe aims to reach a 90% reduction in GHG emissions due to transportation by 2050, thereby, since 71,7% of GHG emissions is due to road transportation (European Commission, 2020c), implementing the use of EVs is a key strategy to meet the goal of emissions reduction set by current legislation. Post 2020, European targets for EVs sales set the following sales benchmarks: 15% by 2025 and 35% by 2030 (European Commission, 2019a). Moreover, more stringent climate targets have been set by the recent legislation updates (European Commission, 2020d) and the share of fully electrical vehicles sold by 2030 must increase from 35% to 55%.

Materials supply for batteries production does not only hold concerns due to minerals reservoir shortage and geopolitical uncertainties, as discussed in Chapter 2, but also for the high environmental impacts generated by mining activities, which are in general accountable for 10% of the total energy-related GHG emissions worldwide (Azadi et al., 2020). Increasing LIBs demand is leading to depletion of mineral resources and detrimental environmental effects, such as groundwater pollution and emissions of greenhouse gasses (Agusdinata et al., 2018).

Recent studies analysed different strategies to reduce the environmental footprint of batteries manufacturing, leading to mixed conclusions. While some authors attribute to batteries recycling lower environmental impacts when compared to manufacturing from virgin metals, such as a reduction of CO_2 emissions up to 34% (Hao et al., 2017b) and more than 51% saving of natural resources consumptions (Dewulf et al., 2011), on the other hand, different studies showed greater impacts both in terms of energy demand and air emissions (Golroudbary et al., 2019), possibly due to different recycling strategies which can entail radical effects on impacts mitigation (Modaresi et al., 2014). Previous studies emphasized the need to integrate material flow analysis for circularity evaluation with LCA to conduct a comprehensive investigation into the environmental implications of circular economy strategies concerning LIBs management (Picatoste et al., 2022).

This Chapter presents the environmental and economic implications of the MFA presented in Chapter 2. The environmental analysis was considered as the net GHG emissions between the emissions generated by full scale recycling processes and the emissions avoided by recovery of secondary raw materials. Similarly, the economic analysis was considered as the net balance between costs of full-scale recycling processes and the potential revenues from the recovery of secondary raw materials.

3.2 Methodology

3.2.1 Environmental analysis

The environmental analysis of LIBs recycling and supply chain in Europe has been estimated based on the net GHG emissions (kg CO_2 eq) due to emissions generated during recycling processes and avoided emissions generated during mining activities.

The avoided GHGs emissions due to mining have been calculated considering metals demand for EVs batteries in Europe in 2030, and they were limited to the steps of mining and metals refining. The impacts of mining activities were considered from literature data, see Table 3-1.

Table 3-1 Environmental impacts of virgin metals' mining

Metals	Mining source/process	GWP impact kg CO2 eq/kg	Reference
Al	Bayer - Hall Heroult	22.4	(Norgate et al., 2007)
Co	-	11.7	(Farjana et al., 2019)
Fe	-	0.013	(Ferreira and Leite, 2015)
Li	Rock	16	(S. Jiang et al., 2020)
	Brines	0.33	(S. Jiang et al., 2020)
Mn	-	4.52	(Farjana et al., 2019)
Ni	Sherritt-Gordon	11.4	(Norgate et al., 2007)
	Pressure acid leaching	16.1	(Norgate et al., 2007)

The GHG emissions generated by full scale recycling facilities have been calculated with a bottom-up approach considering European recycling capacity and EVs batteries market shares in Europe in 2020. The impacts of recycling processes were considered from literature data presented in Chapter 1. The energy demand of different recycling processes is: 4.50 kWh/t for mechanical pre-treatment (Wuschke et al., 2019), 1.08 kWh/t for pyrometallurgy (Hu et al., 2021a), and 1.65 kWh/t for hydrometallurgy (Romare and Dahllöf, 2017). These energy demands have been converted in GHG emissions based on

the energy production specific impact of the country where the recycling facilities are sited: 0.207 kg CO_2/kWh for Belgium, 0.111 kg CO_2/kWh for Finland, 0.054 kg CO_2/kWh for France, 0.406 kg CO_2/kWh for Germany, 0.013 kg CO_2/kWh for Sweden and 0.250 kg CO_2/kWh for United Kingdom (European Environmental Agency, 2021). Data about the energy production specific impact for Norway and Switzerland were not available, thus the average European value of 0.275 kg CO_2/kWh (European Environmental Agency, 2021) has been considered instead. Besides, for pyrometallurgical facilities an additional emissions of 1.65 t CO_2/t has been considered, due to incineration of residual battery components (Hu et al., 2021a).

The results based on data from literature have been compared with emissions factors from Ecoinvent database v. 3.9.1 (Ecoinvent, 2023) applying the LCIA method ReCiPe 2016 v1.03, midpoint (H).

3.2.2 Economic analysis

The economic analysis of LIBs recycling in Europe has been estimated based on the net profit due to costs of recycling processes and the revenues from the recycled metals. The cost due to reagents consumption and waste disposal have been considered according to the description of full-scale recycling processes provided by the Ecoinvent databse. Pyrometallurgical facilities require 50%wt. solutions of sodium hydroxide and water and generate plastic mix and non-ferrous metals as residual waste, while hydrometallurgical facilities require sulfuric acid, sodium carbonate and water, and generate plastic mix, non-ferrous metals and gypsum as residual waste.

The costs of recycling processes accounted for energy demand, chemicals used during recycling and landfill fees for the disposed waste. This economic analysis is intended as a comparison between different recycling techniques (pyrometallurgy, hydrometallurgy and the combination of the twos), thus the costs due to cells preparation for recycling, labour costs and equipment maintenance, which can be assumed equivalent between recycling techniques, were excluded. Operative costs have been considered as following: 0.086 €/kWh for energy (Eurostat, 2023) and 22.0 €/t for landfill disposal (Statista, 2017). Costs of reagents (water, sulphuric acid, sodium hydroxide and lime) were considered according to Ecoinvent database (Ecoinvent, 2023)

The potential revenues are based on the market value of recycled metals (Ecoinvent, 2023). Eventually, the net profit of different recycling techniques has been normalized by the amount of treated materials to identify the most convenient recycling route.

3.3 Results

3.3.1 Environmental analysis

The GHG emissions associated with full scale LIBs recycling facility in Europe amounted to 3.7 Mt CO_2 eq. Pyrometallurgical facilities have an overall energy demand of 21.84 GWh and an environmental impact of 2.4 Mt CO_2 eq., thus they represent the main contributors to GHGs emissions across European LIBs recycling infrastructure. Indeed, they are the most commonly applied recycling technology in Europe. However, despite the fact that almost the same quantity of materials will undergo treatment through hydrometallurgy as well as combined pyrometallurgy and hydrometallurgy, it should be noted that the associated greenhouse gas (GHG) emissions would be higher for the combined processes compared to hydrometallurgy alone. Specifically, the combined processes would result in emissions of 10.34 GWh, whereas hydrometallurgy would only contribute to emissions of 1.46 GWh.

These energy demands would consequently lead to approximately 3.7 Mt of CO_2 eq, with pyrometallurgy accounting for 2.4 Mt of CO_2 eq, hydrometallurgy contributing 0.2 Mt of CO_2 eq, and the combination of pyrometallurgy and hydrometallurgy responsible for 1.1 Mt of CO_2 eq.. In terms of carbon efficiency values, it is evident that hydrometallurgy is less emission-intensive, as it is responsible for 16 kg of CO_2 eq./t. On the other hand, pyrometallurgy and the combination of pyrometallurgy followed by hydrometallurgy account for 88 kg CO_2 eq. per ton and 103 kg CO_2 eq. per ton of treated material, respectively.

The environmental impact of LIBs recycling by full scale recycling facilities in Europe has been normalized considering 1 t of treated LIBs and it amounts to 1.05 t of CO_2 eq./t, see Figure 3-1. A similar result has been obtained considering emissions data from the Ecoinvent database, amounting to 1.14 t of CO_2 eq./t.

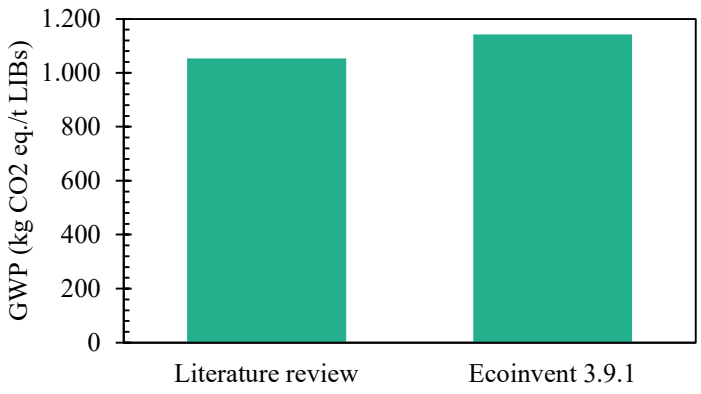


Figure 3-1 GHG emissions associated with the recycling of 1 t of LIBs

The introduction of secondary raw materials in LIBs supply chain through recycling of end-of-life LIBs avoids the necessity of mining primary minerals. Thus, the emissions associated with minerals mining are avoided and are considered as a negative contribution in the emissions balance of this environmental analysis. Specifically, the emissions avoided by LIBs recycling amount to 0.3 t of CO_2 eq./t according to data from literature (Table 3-1) and 0.26 t of CO_2 eq./t according to data from Ecoinvent database, see Figure 3-2. The most influential factors are represented by the recovery of Ni and Co, due to the amount of these metals available for recycling and their high recycling rates.

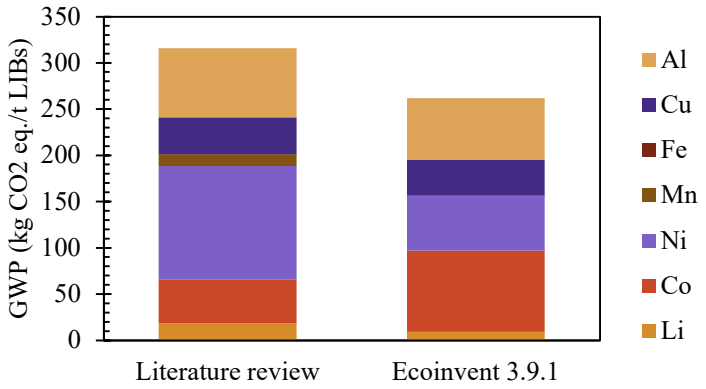


Figure 3-2 GHG emissions associated with the metals mining and avoided by recycling of 1 t of LIBs

Recycling of end-of-life LIBs represents a significant environmental impact, associated with the elevated energy demands of pyrometallurgical and hydrometallurgical processes. Nonetheless, a significant contribution to reduce the environmental impact associated with recycling is posed by the recovery of secondary raw materials, which cuts emissions by 28% by providing an additional supply to LIBs supply chains.

3.3.2 Economic analysis

The economic analysis considered the net profit between the costs entailed by recycling processes and potential revenues from sales of recovered metals. The European LIBs recycling infrastructure present an overall cost of 7.55 mln €, which is mainly due to the use of reagents (53% of overall costs) and energy demand (38% of overall cost) and only partly to disposal of residual waste (9% of overall costs), see Figure 3-3.

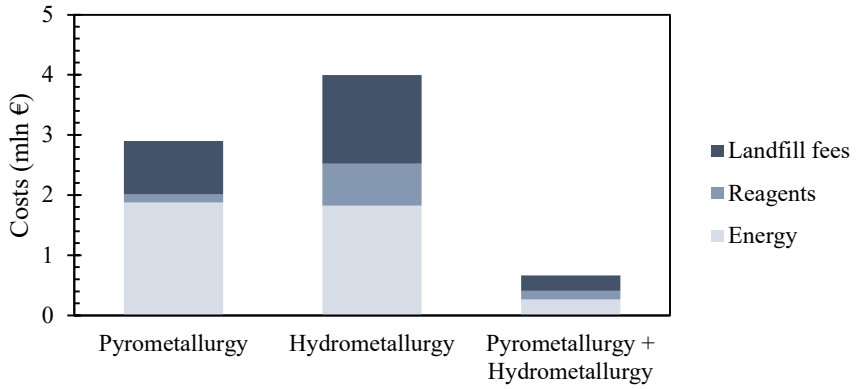


Figure 3-3 Projected costs of European LIBs recycling infrastructure in 2030

Pyrometallurgical plants, which belong to the most common category of recycling facilities in Europe, represent the highest contributor to recycling costs, accounting for 53% of overall costs. Although the quantity of materials treated by hydrometallurgy (21%) or the combination of pyrometallurgy and hydrometallurgy (23%) does not differ significantly, the associated costs is considerably higher for the latter, accounting for approximately 35% of the overall 7.55 mln €.

Costs resulting from the energy demand of the full-scale treatment processes amount to 2.89 M€. This cost is primarily attributed to the significant proportion of end-of-life LIBs (65%) that are treated in facilities employing pyrometallurgy. Costs due to reagent consumption and waste generation are mainly due to pyrometallurgical facilities (46% of reagents costs and 40% of waste disposal costs) and hybrid pyrometallurgical and hydrometallurgical facilities (37% of reagents costs and 39% of waste disposal costs). Costs due to reagents consumption are mainly driven by the amount of sodium hydroxide consumed, which represent 64% of costs due to reagents and 34% of the overall recycling costs.

A total of 22.6 kt of metals recovered through LIBs' recycling would correspond to a sum of 53.6 million €, see Figure 3-4. The majority of these revenues are attributed to cobalt (18.8 M€), copper (27.7 M€), lithium (3.4 M€), and aluminium (2.9 M€). It is worth noting the significant role that critical raw materials (CRMs) such as cobalt and lithium play in the economic analysis. Despite representing only approximately 9% of the total output based on the material flow analysis (MFA), cobalt contributes to 35% of the revenues due to its criticality and subsequent market price. Conversely, lithium, accounting for around 5% of the weight of the recovered materials, only holds a share of the revenues amounting to 6% due to its limited market value despite the criticality of Li supply in Europe.

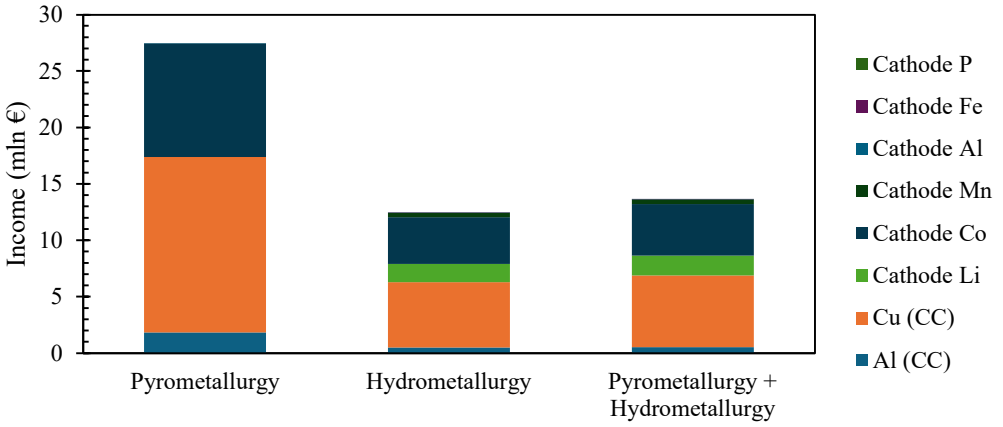


Figure 3-4 Potential incomes associated to the market value of the secondary raw materials involved by LIBs' recycling in 2030 (CC: current collector)

Recycling costs and potential revenues from recovered metals were normalized considering 1 t of recycled LIBs in order to compare the net profit of the three recycling routes (pyrometallurgy, hydrometallurgy and the hybrid process combining pyrometallurgy and hydrometallurgy), see Table 3-2.

Table 3-2 Comparison between of costs, revenues and profit of different LIBs' recycling strategies

Recycling process	Costs (€/t)	Revenues (€/t)	Profit (€/t)
Pyrometallurgy	145.33	1,006.07	860.74
Hydrometallurgy	92.64	1,199.47	1,106.83
Pyrometallurgy and hydrometallurgy	229.085	1,242.05	1,012.97

Facilities that implement a combination of pyrometallurgy and hydrometallurgy processes are associated with the highest revenues amounting to 1242 €/t. However, it is important to note that this specific treatment also incurs the greatest operational costs of 230 €/t. When analysing the trade-off between operational costs and potential revenues of individual treatments, it is evident that pyrometallurgical procedures, despite necessitating high operational costs of 145 €/t, result in limited revenues of 1006 €/t. This is primarily attributed to the loss of materials in the slag phase. On the other hand, hydrometallurgical treatments yield substantial revenues amounting to 1200 €/t, while maintaining the lowest operational costs of 92 €/t.

3.4 Discussion

The environmental benefits of electric cars, when compared to traditional internal combustion engines, are typically eclipsed by the environmental problems connected with mineral mining to extract the key raw materials for LIB production. Recovery of secondary raw materials from LIB recycling will increase GHG emissions over the whole life cycle. Nonetheless, recycling procedures minimize the extraction of basic raw materials, which, in the context of Europe, reduces supply concerns for raw materials necessary for future LIB production.

Furthermore, it is important to consider other potential detrimental environmental consequences that may arise from improper management of untreated end-of-life LIBs that exceed the recycling capacity in Europe. These batteries contain components that pose several pollution hazards, primarily due to the potential release of inflammable or corrosive substances, as well as potentially toxic metals.

Environmental impacts entailed by full scale LIBs recycling processes are significantly high, due to the elevated demand of energy entailed by pyrometallurgical and hydrometallurgical processes. However, the recovery of secondary raw materials from end-of-life batteries will curb the environmental emissions by 28%. This result indicates the essential role of recycling processes, not only to provide security to the LIBs materials supply chain but also reducing their environmental impacts.

Similarly, in light of the inadequacy of the current recycling infrastructure highlighted in the MFA presented in Chapter 2, it is imperative to establish a more extensive system for the collection and treatment of waste LIBs. Furthermore, an assessment of the performance of existing recycling strategies including recovery efficiencies, energy requirements leading to emissions generation, and cost-benefit analysis reveals that hydrometallurgy emerges as the most favourable strategy.

3.5 Conclusion

This Chapter presented the environmental and economic implications of the MFA for LIBs in Europe, In 2030, the entire LIBs recycling infrastructure is expected to result in the emission of 3.7 million metric tons of carbon dioxide equivalent (CO_2 eq.) and require an energy demand of 33.6 gigawatt-hours (GWh). Specifically, pyrometallurgical plants will account for 21.86 GWh of the energy demand, hydrometallurgical facilities will require 1.46 GWh, and plants combining both pyrometallurgy and hydrometallurgy will consume 10.3 GWh.

When considering economic income, which is the net difference between potential revenues and operational costs, the most favourable performance is observed in

hydrometallurgical plants. Despite the potential revenues associated with the combination of pyrometallurgical and hydrometallurgical treatments in series being the highest, the operational costs involved in LIBs recycling processes favour hydrometallurgy as the most economically beneficial solution. Consequently, given the recognized inadequacy of the current European recycling infrastructure, hydrometallurgy, which is already well-established and cost-effective at full-scale, emerges as a strategic recycling route for the design of future recycling facilities.

Chapter 4

Electrochemical discharge for lithium-ion batteries recycling

This chapter regards the study of electrochemical discharge LIBs with non-corrosive solutions and the investigation of gaseous products generated during the initial step of the recycling process. The experimental activity described in this chapter has been completed during a mobility period at Aalto University, Finland. The content of this chapter has been presented in a research article titled "*Gas products detection and accurate pH monitoring for electrochemical discharge of Lithium-ion batteries*" authored by **Martina Bruno**, Professor Annukka Santasalo-Aarnio and Professor Silvia Fiore (under review).

4.1 Introduction

Recycling of end-of-life LIBs requires the removal of residual voltage from batteries cells, to ensure their safe handling during downstream recycling processes (Garg et al., 2019; Kim et al., 2021; Mishra et al., 2022). The discharge process is of utmost importance as it ensures the safe handling of batteries during recycling, minimizing the risk of short-circuits, fire hazards, and potential explosions (Langner et al., 2021). Currently, there are no specific regulations in place regarding the residual battery voltage that should be achieved by discharge processes (H. Rouhi et al., 2021). However, in order to guarantee safety, it is recommended that the difference of potential between the positive and negative poles of a battery cell does not exceed 2 V (Kwade et al., 2018) while it is also crucial to avoid complete discharge of the battery cell to 0 V, as this could lead to cell enlargement and ultimately result in an explosion (Lee et al., 2023).

Discharge of end-of-life LIBs is typically conducted through electrochemical discharge in saline solutions (Kim et al., 2021; Shaw-Stewart et al., 2019; Xiao et al., 2020) or by connecting the batteries to a controlled resistance (Langner et al., 2021). Among the saline solutions commonly used for electrochemical discharge, NaCl is the most frequently applied (Punt et al., 2022; Shaw-Stewart et al., 2019; Yao et al., 2020). By subjecting LIBs to electrochemical discharge in NaCl solutions, the residual voltage can be reduced to below 1 V within a span of 5 hours (Yao et al., 2020). Additionally, after 24 hours, the voltage can be nearly diminished to 0 V (Shaw-Stewart et al., 2019), and this time can be further reduced to 1.5 hours when ultrasonication is combined with the discharge process (Torabian et al., 2022). However, it is important to note that the use of NaCl solutions for electrochemical discharge has negative repercussions, including the corrosion of the battery casing and the release of chlorine and alkane gases (H. Wang et al., 2022). These gasses are recognized as harmful contaminants and pose potential risks to the environment and human health (Liu and Gao, 2021).

Previous studies proposed alternative non-corrosive saline solutions, such as sodium carbonate and potassium carbonate (Hassan Rouhi et al., 2021; Shaw-Stewart et al., 2019), in order to avoid damage to the LIB casing and inhibits chlorine gas leakage since there are no chlorite ions present. However, water splitting reactions keep taking place in the form of oxygen and hydrogen gas posing a significant explosive threat if not adequately managed (Dagdougui et al., 2018). Water electrolysis in alkaline solutions, on the other hand, has been presented as a possible approach for releasing hydrogen provided that contact is avoided between hydrogen and oxygen gasses (Chen et al., 2016). Therefore, the formation of gaseous products during electrochemical discharge with non-corrosive solutions is an area that warrants additional exploration to address both safety concerns and possible economic benefits.

Gas chromatography can be applied to detect total gaseous emission during discharge (Jia Li et al., 2016; Yao et al., 2020) but did not examine the patterns of gaseous products. Thereby, accurate gas detection from non-corrosive discharge solutions has not yet been fully studied. This Chapter presents the results of research activity on electrochemical discharge of LIBs comparing two non-corrosive solutions (Sodium carbonate and potassium carbonate) based on discharge effectiveness and the trends of gaseous products release during discharge. Besides, a novel configuration for the study of electrochemical discharge has been proposed and the monitoring of pH trend in the discharge solutions has been proposed as a proxy indicator of hydrogen release rate and discharge curves.

4.2 Methodology

Cameron Sino CS- NCR18650 Panasonic batteries (3400 mAh, volumetric energy density 676 Wh/L, gravimetric energy density 243 Wh/kg) were used to for the electrochemical discharge tests described in this Chapter. Each battery weighed 47.5 g, measured 18.50 mm in diameter and 69 mm in length, and had a starting voltage of 3.8±0.03 V. Electrochemical discharge in sodium carbonate and potassium carbonate solutions was compared, using 5%-wt. sodium carbonate (99.9% purity, CAS: 497-19-8 VWR Chemical BDH), and 5%-wt. potassium carbonate (99% purity, CAS: 20,961-9 Sigma-Aldrich) in Millipore deionized water. The choices of the salts in the discharge solutions and their concentrations were based on previous studies (H. Rouhi et al., 2021).

The experimental set-up, see Figure 4-1, compared two configurations, in the following defined "conventional" and "half-cells". According to previous studies (Fang et al., 2022; Ojanen et al., 2018; Rouhi et al., 2022; H. Wang et al., 2022) the conventional set-up involved completely immersing a battery in the discharge solution. Whereas the novel "half-cells" configuration has been designed by connecting the electrodes of two cells with a platinum wire and immersing the free electrodes in two separated discharging solutions, connected only by a salt bridge.

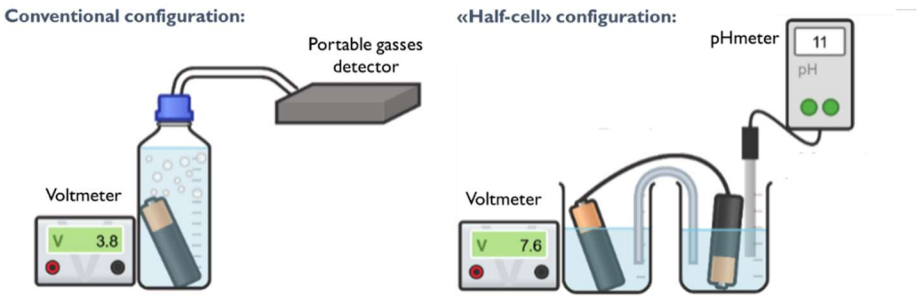


Figure 4-1 Experimental settings used in electrochemical discharge tests

Electrochemical discharge tests were conducted for a total of 120 hours each, during which gaseous products (CO_2, O_2 and H_2) were continuously monitored with a G7c BlackLine Safety portable emissions detector. The pH in the discharge solution was measured hourly with a 1030VWR tester. Alongside pH measurements, the cells were taken out of the discharging solution to measure residual voltage with an 87V IMSK Fluke multimeter.

4.3 Results

4.3.1 Reduction of residual voltage

The trend of residual voltage reduction is presented in the discharge curves in Figure 4-2. The discharge curves of the sodium carbonate and potassium carbonate solutions exhibited a downward trend in the initial 60 hours, subsequently stabilizing at approximately 45±1% of the initial voltage for sodium carbonate and 50±1% for potassium carbonate solutions. In the sodium carbonate solution, the rate of reduction in residual voltage was -0.007±0.003 V/h during the first 48 hours, which then doubled to - 0.015±0.003 V/h before nearly coming to a halt. Conversely, the potassium carbonate solution displayed an initial discharge rate of -0.008±0.003 V/h in the initial 24 hours, escalating to -0.012±0.004 V/h and subsequently decreasing to -0.006±0.001 V/h within the final 24 hours before reaching a plateau.

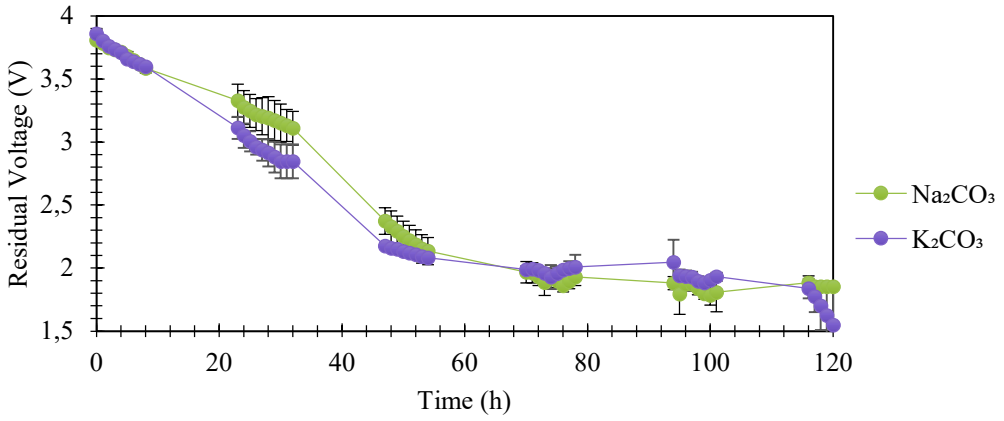


Figure 4-2 Discharge curves during the conventional electrochemical discharge

The discharge efficiency of the sodium carbonate and potassium carbonate solutions aligned with previous findings (H. Rouhi et al., 2021) which indicated that the initial voltage of LIBs immersed in sodium and potassium carbonate solutions dropped to almost 50% after 70 hours. Throughout the discharge tests, no evidence of corrosion or contamination in the discharge solutions was observed within the samples.

The decrease in residual voltage in the half-cells set-up was measured on an hourly basis for the overall system, which encompassed two LIBs connected by a platinum wire and the LIBs immersed from the cathode side ("positive half-cell") and the anode side ("negative half-cell"). The discharge curves of the half-cells systems are presented in Figure 4-3 and Figure 4-4.

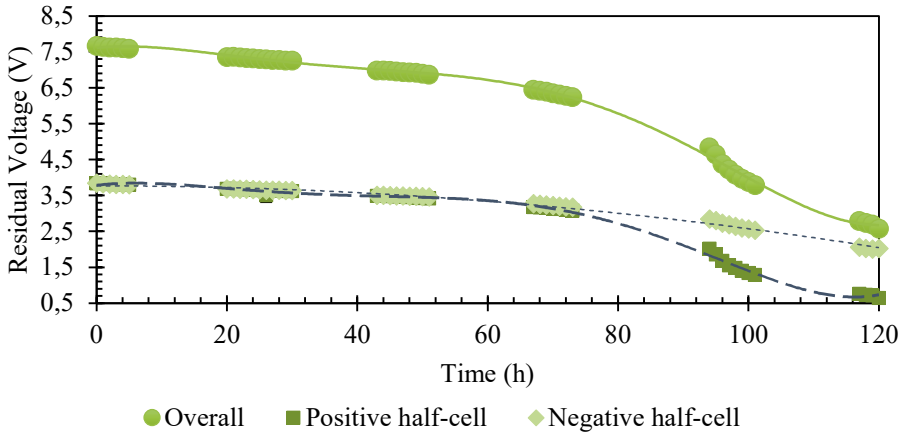


Figure 4-3 Discharge curves during electrochemical discharge with the half-cells set-up with sodium carbonate

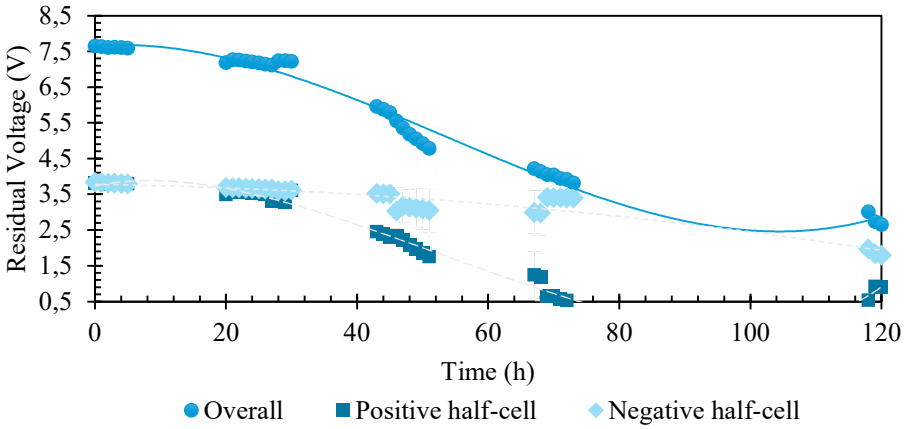


Figure 4-4 Discharge curves during electrochemical discharge with the half-cells set-up with potassium carbonate

Since the two LIBs were connected in parallel, the initial voltage of this set-up stood at 7.6±0.02 v. following 120 hours, the overall residual voltage reached 34±1% of the initial values for sodium carbonate and 35±2.7% for potassium carbonate solutions, indicating a lower level of residual voltage compared to the 45±1% achieved in the traditional set-up employing sodium carbonate and the 50±1% with potassium carbonate. Initially, the rate of residual voltage reduction in the half-cells corresponded to -0.002±0.0008 V/h for sodium carbonate and -0.001±0.00001 V/h for potassium carbonate, which was slower than that observed in the conventional set-up (-0.008±0.002 V/h for sodium carbonate and -

0.009±0.003 V/h for potassium carbonate). However, the rate accelerated after 70 hours in the potassium carbonate solution and after 100 hours in the sodium carbonate solution. In a manner analogous to the conventional configuration, the discharge rate of LIBs using potassium carbonate was faster than that of sodium carbonate, although the discharge efficiency of sodium carbonate surpassed that of potassium carbonate.

Contrary to expectations, the positive and negative half-cells did not discharge at the same rate. The positive half-cell discharged more rapidly than the negative half-cell in both the sodium carbonate and potassium carbonate solutions. Specifically, the residual voltage of the positive half-cells after 120 hours amounted to 17±2% of the initial value in the sodium carbonate solution and 14±1% in the potassium carbonate solution. in contrast, the residual voltage of the negative half-cell was 53±1% in the sodium carbonate solution and 47±1% in the potassium carbonate solution. Initially, during the first 70 hours, the positive and negative half-cells discharged in a similar manner with sodium carbonate, but thereafter, their discharge curves diverged. conversely, the discharge curves of the positive and negative half-cells in potassium carbonate exhibited discrepancies after the initial 24 hours.

4.3.2 Monitoring of gaseous products release

The continuous monitoring of gaseous emissions released during electrochemical discharge has been carried out using a portable device to monitor the concentrations of CO_2 in parts per million (ppm), O_2 in percentage volume (%vol.), and H_2 in ppm. In the headspace, the initial composition consisted of 20.6%vol. O_2, 450 ppm CO_2, and 0 ppm H_2. The device employed CO_2 and O_2 sensors with a sensibility of ±50 ppm and ±0.1%vol., respectively. It is worth noting that no variations in CO_2 concentration were observed in any of the conducted tests. During one of the tests involving sodium carbonate discharge, a slight increase in O_2 concentration was observed, although this finding was not confirmed by the other two replicates. To determine the average emission rate, the measurements of H_2 concentration in the gaseous emissions were normalized over sampling time, see Figure 4-5

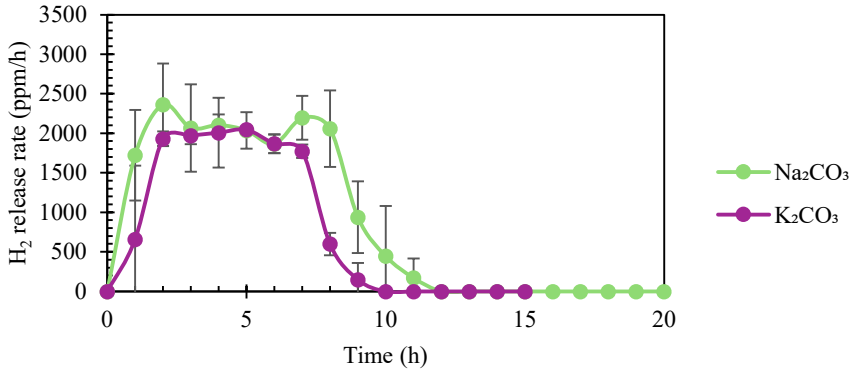


Figure 4-5 Trends of H2 release rate (ppm/h) during conventional electrochemical discharge

Both discharging solutions of sodium carbonate and potassium carbonate exhibited a release of H_2 that was predominantly concentrated in the early hours of discharge, specifically 11 hours for sodium carbonate and 9 hours for potassium carbonate. On average, the hourly H_2 release rate for sodium carbonate amounted to 1722±400 ppm/h, whereas for potassium carbonate, it was 1519±670 ppm/h. Nonetheless, there were distinct differences between the two trends. The H_2 release rate from the sodium carbonate solution experienced a more rapid increase initially, reaching 1722±527 ppm/h in the first hour, followed by a peak at 2363±520 ppm/h in the second hour. Subsequently, it remained relatively constant around 2105±166 ppm/h for the following 6 hours before gradually decreasing. On the other hand, the H_2 release rate from the potassium carbonate solution exhibited a slower initial increase, peaking at 2045±7 ppm/h after 5 hours. It is interesting to note that once the H_2 release ceased, the reduction of residual voltage amounted to 94±1% of the initial value for both sodium carbonate and potassium carbonate.

Sodium carbonate and potassium carbonate solutions did not exhibit significant variations in the concentrations of O_2, CO_2, and H_2 in the headspace above the half-cells. However, it is important to note that these results are limited by the accuracy of the detectors used to monitor gaseous products during electrochemical discharge due to configuration issues with the half-cells system. Therefore, future research needed to optimize the configuration of the half-cells system and allow for accurate and reliable monitoring of gaseous products during electrochemical discharge of the positive and negative electrodes.

4.3.3 Trends in pH of discharge solutions

The initial pH values of the sodium carbonate and potassium carbonate solutions were found to be 11.63±0.01 and 11.55±0.01, respectively. These values remained relatively

stable over the course of the study, with average pH values of 11.59±0.23 for sodium carbonate and 11.60±0.15 for potassium carbonate. However, it is important to note that these values did exhibit some fluctuations, ranging from a minimum of 11.27±0.02 to a maximum of 12.5±0.48 for Sodium carbonate, and from 11.26±0.02 to 12.06±0.06 for potassium carbonate, see Figure 4-6.

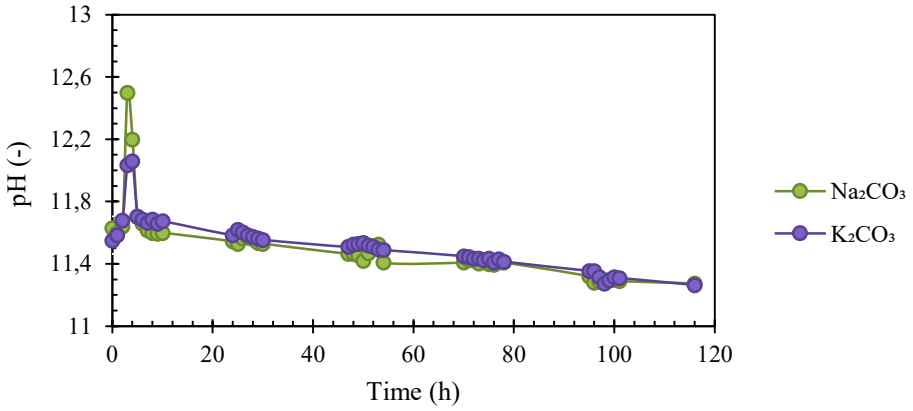


Figure 4-6 Trends of pH during conventional electrochemical discharge

Interestingly, the pH trends observed in the two discharge solutions behaved similarly, with both solutions exhibiting a peak in pH within the first 5 hours of discharge. Specifically, the sodium carbonate solution reached its highest pH value of 12.5±0.48 after 3 hours of discharge, while the potassium carbonate solution reached its peak pH value of 12.06±0.06 after 4 hours of discharge. Following these initial peaks, the pH of both solutions displayed a slight daily decrease. For the sodium carbonate solution, the daily average pH values measured after the first 24 hours were 11.55±0.02, 11.46±0.04, 11.4±0.01, 11.29±0.01, and 11.27±0.02. Similarly, for the potassium carbonate solution, the daily average pH values were found to be 11.58±0.02, 11.52±0.02, 11.44±0.01, 11.35±0.04, and 11.26±0.02. It is worth noting that the drop in pH observed in both solutions was linearly associated with a decrease in residual voltage, as evidenced by the Pearson coefficient values of 0.72 for sodium carbonate and 0.82 for potassium carbonate.

The pH of the solutions in the half cells system followed a different trend, see Figure 4-7 and Figure 4-8. The pH of the solutions in contact with the negative half-cells increased to 12.9±0.05 for sodium carbonate and 12.6±0.18 for potassium carbonate after 5 hours. Simultaneously, the pH of the solutions in contact with the positive half-cells decreased to 10.5±0.03 for sodium carbonate and 10.9±0.05 for potassium carbonate.

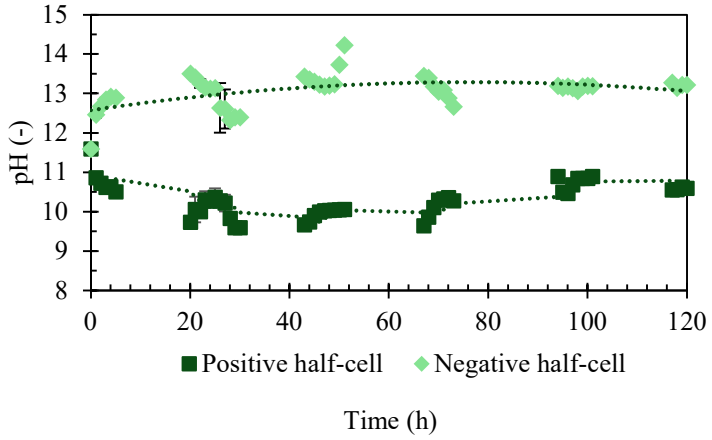


Figure 4-7 Trends of pH during electrochemical discharge with the half-cells set-up with sodium carbonate

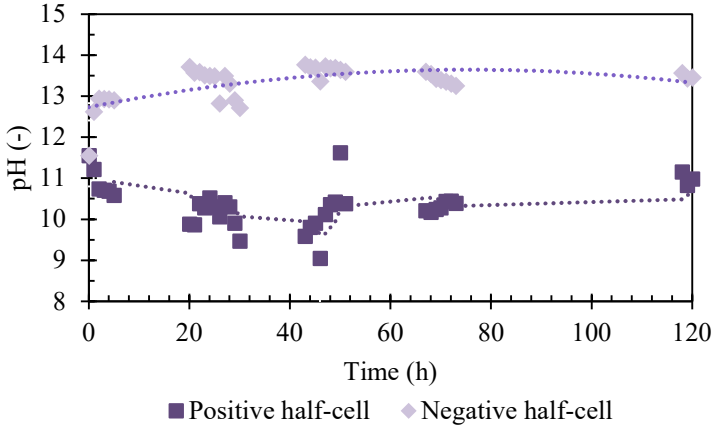


Figure 4-8 Trends of pH during electrochemical discharge with the half-cells set-up with potassium carbonate

Overall, it can be confirmed in the half-cell that the pH changes for the individual electrodes are more pronounced at the beginning of the experiments and tend to stabilize towards the later part of the experiment when the gas formation is less intense. This corresponds well with the findings in the large cell where the pH undergoes greater changes initially but reaches a steady level over time.

4.4 Discussion

Sodium and potassium carbonate solutions proved to be effective in discharging LIBs below safety threshold, according to previous studies (H. Rouhi et al., 2021). The presence of carbonate salts in the discharge solution did not cause release of CO_2 gas, hence confirming the lower environmental impact associated with this alternative.

Monitoring of pH in the discharge solution demonstrated to be correlated both with discharge rate and the emissions of H_2 gas. Despite the initial peaks of pH observed in both sodium and potassium carbonates solutions do not appear to have a direct relationship with the discharge curve, they align with the peaks of H_2 release that were measured in the conventional configuration. This finding suggests that there may be a connection between the release of H_2 and the rise in pH observed in the solutions.

In the half cells configuration pH decreased over time in the positive half-cell and increased in the other one. This outcome is consistent with the observations made in the conventional configuration and the pH behavior that the poles would exhibit in the water splitting reaction in an alkaline solution (equations 1 and 2):

$$4\,H_2O + 4\,e^- \rightarrow 2\,H_2 + 4\,OH^- \quad (1)$$

$$4\,OH^- \rightarrow 4\,e^- + O_2 + 2\,H_2O \quad (2)$$

The hydrogen evolution reaction at the positive half-cell oxidizes water molecules, transforming them into gaseous H_2 and hydroxyl anions, thereby reducing the pH, as explained in reactions 1.

Although the "half-cells" setup did not allow for the direct monitoring of gas production, the findings from both setups were combined in order to confirm the hypothesis of water electrolysis in alkaline conditions as the reaction responsible for the consumption of electrons from the battery in the carbonate solution. Interestingly, it was observed that the pH levels peaked at 12.6-12.9 in the negative half-cell within the first 5 hours, while in the positive half-cell, the pH levels dropped to 10.5-10.9. These observations are consistent with the formation and conversion of hydroxyl ions in each of the half-cells. These findings provide valuable insights into the various reactions occurring during the electrochemical discharge process in carbonate solutions.

4.5 Conclusions

This Chapter presented the study of LIBs electrochemical discharge with a voltage of 3.8 V in non-corrosive carbonate solutions and the release of gaseous products during the discharge process. Two different setups were utilized. The first setup followed the conventional approach as described in the literature, while the second setup utilized a novel "half-cells" configuration that allowed for the individual examination of the behavior of both the positive and negative electrodes. Both configurations were tested with two discharging solutions: sodium carbonate and potassium carbonate. The comparison between discharging solutions were based on discharge curves, gaseous product trends (O_2,

H_2, and CO_2), and discharge solutions' pH. In both configurations, there was no sign of corrosion, and the residual voltage fell to the safety level of 2 V in 70 hours.

In the traditional setup, H_2 generation occurred in the first 9-11 hours (1500-1700 ppm/h), with a maximum emission rate of 2000-2300 ppm/h after 3-4 hours, which corresponded to pH peaks in the saline solutions at around 12. Moreover, it was determined that the experiments did not result in the formation of significant quantities of CO_2 gas.

Simultaneously, the study also involved the continuous monitoring of the pH levels of the solution. This monitoring allowed for a comprehensive understanding of the formation of hydroxyl groups and the subsequent increase in the pH of the negative electrode. These observations are directly related to the evolution of hydrogen gas and the subsequent decrease in voltage of the battery. It is worth mentioning that with further optimization, this non-invasive approach could potentially be used to assess the residual voltage of LIBs and determine their safety for operation.

Chapter 5

Pre-treatment for lithium iron phosphate cathodes recycling

This chapter regards the optimization of pre-treatments to recycle LFP cathodes. The content of this chapter has been presented with a presentation titled "*Pre-treatments of lithium iron phosphate cathodes for lithium-ion batteries recycling*" at SUM2022 6th Symposium on Circular Economy and Urban Mining and with a presentation titled "*Physic-mechanical pre-treatments to recycle lithium iron phosphate cathodes"* at Waste Management Europe at Bergamo, Italy; and in a research article titled "*Low-cost and environmentally friendly physic-mechanical pre-treatments to recycle lithium iron phosphate cathodes*" authored by **Martina Bruno** and Professor Silvia Fiore and published by Journal of Environmental Chemical Engineering (Bruno and Fiore, 2024b).

5.1 Introduction

LIBs market is projected to achieve a capacity of 2,000 GWh by the year 2030 (International Energy Agency, 2023), primarily driven by the electrification of transportation systems (Neidhardt et al., 2022). According with the results presented in Chapters 2 and 3, recycling of batteries materials plays a pivotal role in meeting the anticipated demand of raw materials for LIBs supply chain and it significantly contributes to reducing the environmental impacts throughout the LIBs life cycle. This is achieved by preventing improper end-of-life management practices (Kader et al., 2021) and reducing the energy consumption and environmental consequences associated with the mining of primary materials (Aichberger and Jungmeier, 2020).

Within LIBs, various types of cathodes can be found, with NMC cathodes being the most prevalent (International Energy Agency, 2023), accounting for 29% of the market in 2020. On the other hand, the market for LFP chemistry is anticipated to experience global growth, with its value expected to rise from 0.4 billion USD in 2017 to 15.24 billion USD by 2027 (Neidhardt et al., 2022). LFP batteries are projected to consistently maintain the position as the second most common battery chemistry worldwide, following NMC, in terms of global production capacity up to the year 2030 (Neidhardt et al., 2022). These batteries offer advantages such as rapid charging rates, extended lifespan, and high stability (Li and Ma, 2019). Besides, the absence of cobalt, nickel, and manganese in LFP batteries helps in reducing the production costs associated with them, making them an attractive option in the market. However, the low economic value of LFP components is detrimental form a recycling perspective since it may not be able to sustain the costs of current recycling processes, as discussed in Chapter 3. Thereby, recycling targeting this particular cathode should be optimized to achieve technical and economic viability of the processes.

Technical and economic performance of LIBs' recycling technologies are significantly influenced by the effectiveness of pre-treatments (Latini et al., 2022) since material loss and contamination due to the presence of materials from other components of the batteries, due to ineffective pre-treatments, can compromise the overall recycling efficiency and economic feasibility (Sommerville et al., 2020; Takahashi et al., 2020). Thereby, the liberation of electrode active materials from the current collector, binder, and electrolyte is a critical phase in the recycling process (Sultana et al., 2022). Previous studies reported the liberation of electrodes active materials from current collectors by chemical, mechanical and thermal processes, often combined (Kader et al., 2021; Mossali et al., 2020; Sommerville et al., 2020).

As discussed in Chapter 1, physical detachment of cathodes active material from current collectors can be performed with different methods, which provide elevated separation efficiency. However, they contribute significantly to energy demand and

operative costs entailed by LIBs recycling processes. Reducing operative costs is particularly crucial for recycling of LFP cathodes, which recycling is not economically feasible since they hold lower economic value compared with other cathode chemistries (Mahandra and Ghahreman, 2021).

In this Chapter different physical detachment processes have been compared to separate cathodes active materials from LFP cathodes, both from end-of-life batteries and production scraps. Physic-mechanical treatments (ultrasound washing, ball milling and thermal treatment) have been compared to avoid the need of chemical solvents and reduce energy consumption.

5.2 Methodology

5.2.1 Experimental procedure

The work presented in this Chapter is based on detachment of LFP powders from current collectors of end-of-life cathodes and production scraps. End-of-life cathodes were provided already dismantled from lithium-ion battery cells. The outline of operative conditions compared is provided in Figure 5-1

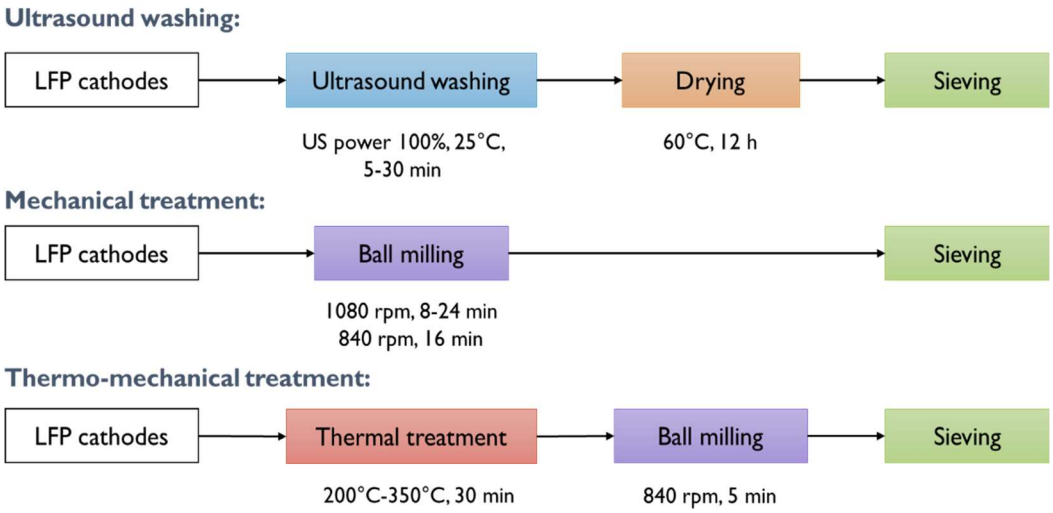


Figure 5-1 Outline of experimental approach for mechanical detachment of LFP cathodes (production scraps, and end-of-life cathodes) from aluminium current collectors

The equipment used were a Bandelin SONOREX DIGIPLUS DL 514 BH ultrasonic bath and an ARGO LAB TCN 30 oven for ultrasound washing, a Retsch MM200 ball mill and a ZE muffle furnace for thermal treatment.

Ultrasound washing was tested at room temperature, specifically at 25°C, by applying a frequency of 35 kHz for varying durations of 5, 15, and 30 minutes. In order to

explore the effects of ball milling, experiments were conducted at 1080 rpm for 8, 16, and 24 minutes, as well as at 840 rpm for 16 minutes. Furthermore, thermal treatment was examined at different temperatures of 200°C, 250°C, 300°C, and 350°C for a constant duration of 30 minutes under air atmosphere, followed by ball milling at 840 rpm for an additional 5 minutes. The thermal treatment temperatures were deliberately kept below 350°C to minimize any potential oxidation of the iron (Fe) present in the cathode materials, as per the recommendations of previous research (Bertrand et al., 2010). To ensure accuracy, each test was replicated three times, utilizing 1.5 grams of the sample in each trial.

The characterization of the samples has been performed with a Rigaku NEX-DE X-ray fluorescence (XRF) spectrometer to analyze aluminium, iron and phosphorous and a GFA-EX7 Schimadzu Flame Atomic Absorption (FAA) Spectrometer to analyze lithium. Prior to FAA spectrometry the solid samples were digested in a solution of nitric acid and chloridic acid in a MILESTONE ETHOS UP microwave system. The characterization of the morphological structure of the samples has been performed with a Phenom XL scanning electron microscopy and energy dispersive spectrometer (SEM-EDS), using an acceleration voltage of 15 keV and a secondary electron detector.

To evaluate the various pre-treatments, a comparison was made based on several Key Performance Indicators (KPIs). These included the recovery rates of lithium, iron, and phosphorus in the cathode powder, the percentage of impurities by weight in the cathode powders following the pre-treatments, as well as the material loss percentage by weight.

5.2.2 Environmental analysis

The environmental impacts associated with the proposed pre-treatment strategies has been calculated based on primary data (energy and water demand) collected during the experimental activity. The energy demand entailed by different processes has been measured with a PM10 Maxcio power meter.

All results have been normalized considering 1 kg of LFP cathodes, both for end-of-life cathodes and production scraps and the processing capacity of the equipment used has been taken into consideration: 1.8 kg of samples (corresponding to 18 l of water) for the ultrasound bath, 50 g of samples for the muffle furnace and 5 g for the ball mill.

The environmental impacts have been calculated according to coefficients retrieved from Ecoinvent 3.9.1 database (Ecoinvent, 2023), applying the impact method Recipe 2016 v1.03 midpoint (H) method.

5.3 Results

5.3.1 Samples' characterization

The composition of the initial production scraps and end-of-life samples and their morphology have been reported in Figure 5-2 and Figure 5-3.

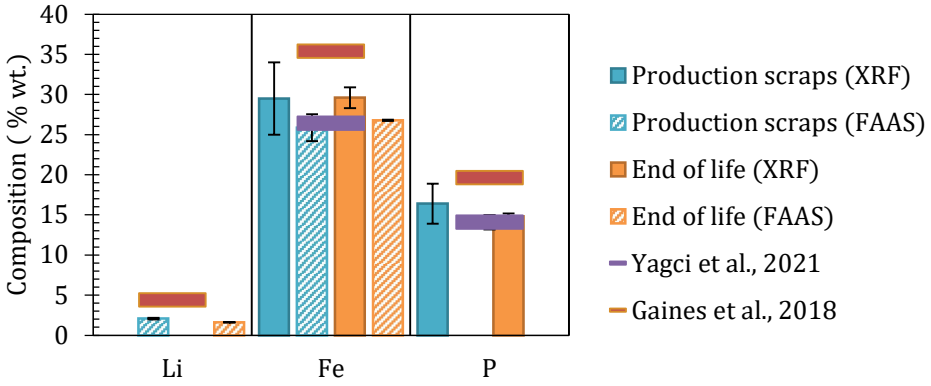


Figure 5-2 Elemental composition of LFP cathodes active material

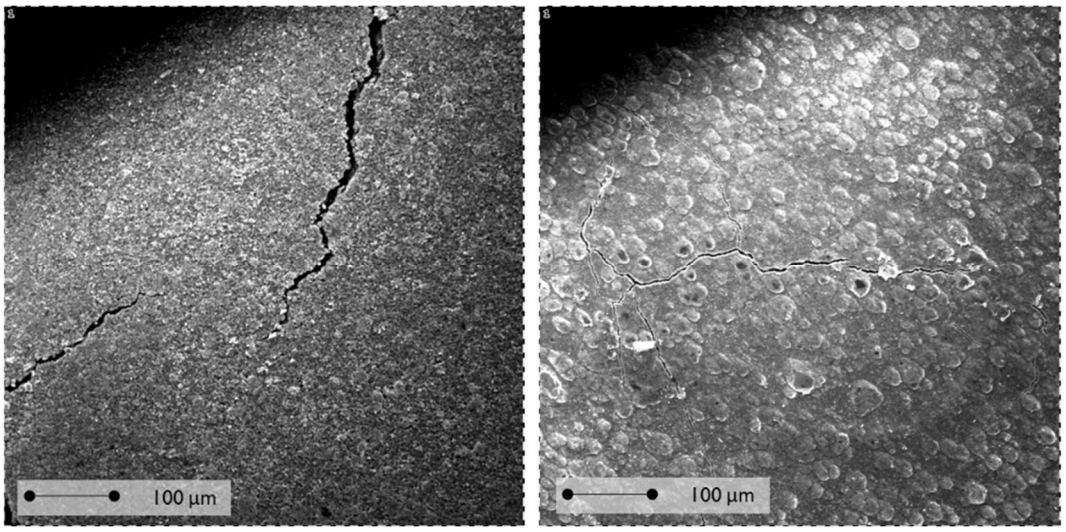


Figure 5-3 SEM images of production scraps (on the left) and end-of-life (on the right)

Production scraps samples consisted of 16% weight of current collectors and 80% weight of powders, which included the cathode active material, residual binder, and electrolyte. On the other hand, the end-of-life samples contained 13% weight of current collectors and 79% weight of powders, in accordance with the findings documented in literature (Bizot et al., 2021; Gaines et al., 2018). The detached cathodic powders in production scraps consisted of 2.1±0.1% weight of lithium, 29.5±4.5% weight of iron, and 16.4±2.5% weight of phosphorous. Similarly, in end-of-life, the percentage of lithium was 1.6±0.001% weight, iron was 29.6±1.3% weight, and phosphorous was 14.8±0.4% weight. These

findings align with the composition of LFP cathodes' active materials, which include 29.4±5.2% weight of iron, 15.9±3.2% weight of phosphorous, and 4% weight of lithium, as reported in the literature (Gaines et al., 2018; Yagci et al., 2021).

5.3.2 Ultrasound washing

The separation efficiency reached through ultrasound washing has been reported in Figure 5-4. The efficacy of ultrasound washing in detaching cathode materials from production scraps electrodes was found to be insufficient, resulting in minimal alteration of the samples. However, when applied to end-of-life samples, ultrasound washing with deionized water successfully detached the materials. Nevertheless, the rates of separation achieved through ultrasound washing were limited to 50±6% for Li, 76±14% for Fe, and 69±12% for P when the process was conducted over a duration of 30 minutes.

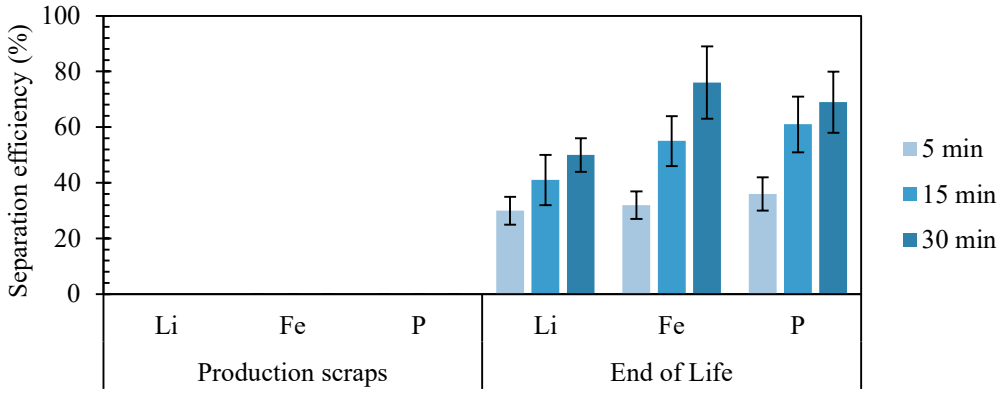


Figure 5-4 Separation efficiency through ultrasound washing

During the ultrasound washing, a significant amount of material loss occurred, amounting to 66±8% after 5 minutes, 53±7% after 15 minutes, and 46±9% after 30 minutes. This material loss cannot be attributed to binder decomposition, as the binder is insoluble in water (S. Zhao et al., 2020). Furthermore, the presence of aluminum contamination in the cathode material after ultrasound washing was minimal, with concentrations of 0.14±0.02% after 5 minutes, 0.13±0.01% after 15 minutes, and 0.24±0.01% after 30 minutes. As expected, the longest duration of ultrasound washing resulted in the highest level of aluminium contamination in the samples.

In terms of the superficial morphology of the production scraps samples, it was observed that ultrasound washing did not bring about significant alterations, see Figure 5-5. Although the force exerted by the ultrasound increased the dimensions of existing cracks on the production scraps cathode surface, it did not succeed in separating the active material from the current collectors. Conversely, when ultrasound washing was applied to end-of-

life samples, plates of active material with dimensions over 1 mm were successfully detached. Moreover, the surface of these detached plates exhibited a smoother texture compared to the initial end-of-life samples. Notably, the concentration of aluminum was below the detection limits for SEM/EDS analyses.

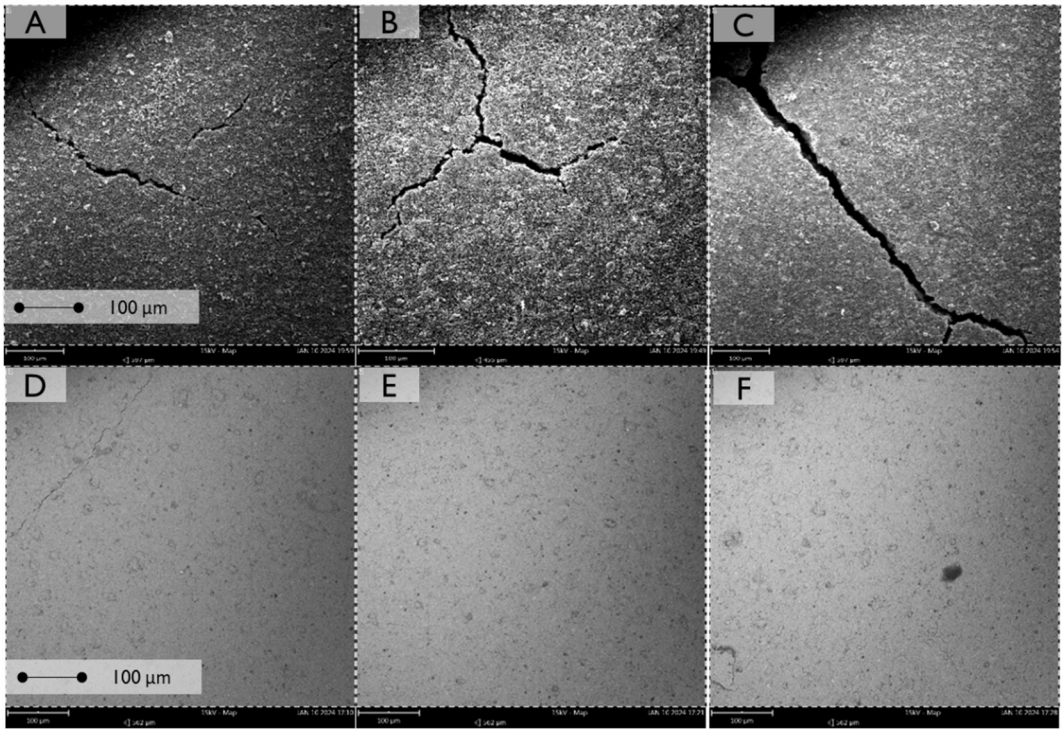


Figure 5-5 SEM images of (A-C) production scraps cathodes and (D-F) end-of-life cathodes after ultrasound washing for 5, 15 and 30 minutes

5.3.3 Mechanical detachment

Ball milling yielded higher separation efficiencies for end-of-life samples compared to production scraps samples, similarly to ultrasound washing. The detachment efficiency reached through ball milling have been reported in Figure 5-6.

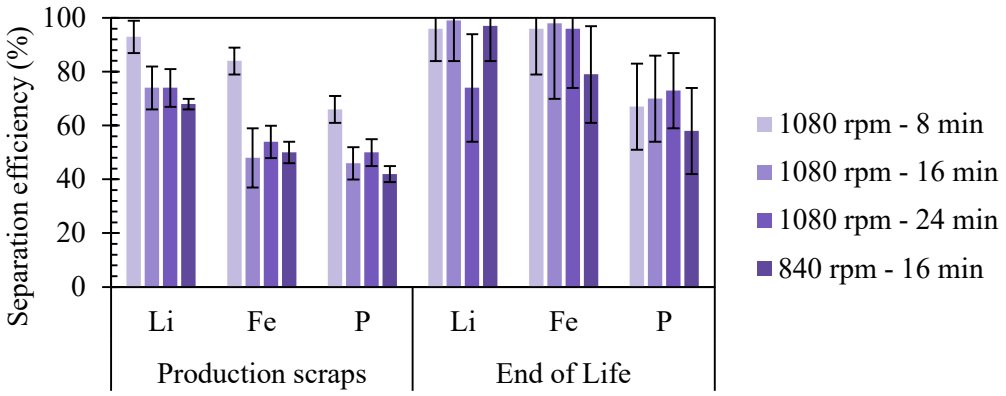


Figure 5-6 Separation efficiency through ball milling

For production scraps samples ball milled at 1080 rpm, the separation rates were as follows: 93±6% for Li, 84±5% for Fe, and 66±5% for P after 8 minutes; 74±8% for Li, 48±11% for Fe, and 46±6% for P after 16 minutes; and 74±7% for Li, 54±6% for Fe, and 50±5% for P after 24 minutes. When the milling frequency was reduced to 840 rpm, the separation rates for production scraps samples remained relatively unchanged: 68±2% for Li, 50±4% for Fe, and 42±3% for P. Conversely, for end-of-life samples ball milled at 1080 rpm, the separation rates were: 96±12% for Li, 96±17% for Fe, and 67±16% for P after 8 minutes; 99±15% for Li, 98±28% for Fe, and 70±16% for P after 16 minutes; and 74±20% for Li, 96±22% for Fe, and 73±14% for P after 24 minutes. In the case of end-of-life samples, ball milling at 840 rpm for 16 minutes resulted in separation rates of 97±13% for Li, 79±18% for Fe, and 58±16% for P.

Notably, an increase in the milling frequency for both production scraps and end-of-life samples corresponded to an increase in the separation rate. However, while the rate of separation appeared to be linearly dependent on the duration of the milling process in the end-of-life samples, this particular tendency did not manifest itself in the production scraps samples. In addition to this, it must be noted that the duration of the milling process has a direct impact on the amount of material lost during milling. Specifically, the production scraps samples experienced a material loss of 16±4% and the end-of-life samples experienced a material loss of 17±6% after 8 minutes at 1080 rpm. However, as the milling process was extended to 24 minutes at the same frequency, the material loss increased to 43±11% for production scraps samples and 37±9% for end-of-life samples. Furthermore, it is important to highlight that the longer the ball milling process, the higher the concentration of aluminum in the cathode powder after separation. Additionally, it should be noted that different milling frequencies utilized for the same duration of 16 minutes yielded similar amounts of aluminum impurities. Specifically, the production scraps samples exhibited aluminum impurities of 0.27±0.74% at 1080 rpm and 0.25±0.21%

at 840 rpm, while the end-of-life samples showed aluminum impurities of 0.32±0.21% at 1080 rpm and 0.28±0.29% at 840 rpm.

The granulometry of the active material that was separated after the ball milling process varies depending on the specific milling settings and also between the production scraps and end-of-life samples, see Figure 5-7. The images acquired through SEM-EDS microscopy have been reported in It can be observed that the grains of active material in the end-of-life samples appear coarser in comparison to those in the production scraps samples. Additionally, it is worth noting that the granulometry of the detached active material following the milling process at 840 rpm is more uniform when compared to samples milled at higher frequencies.

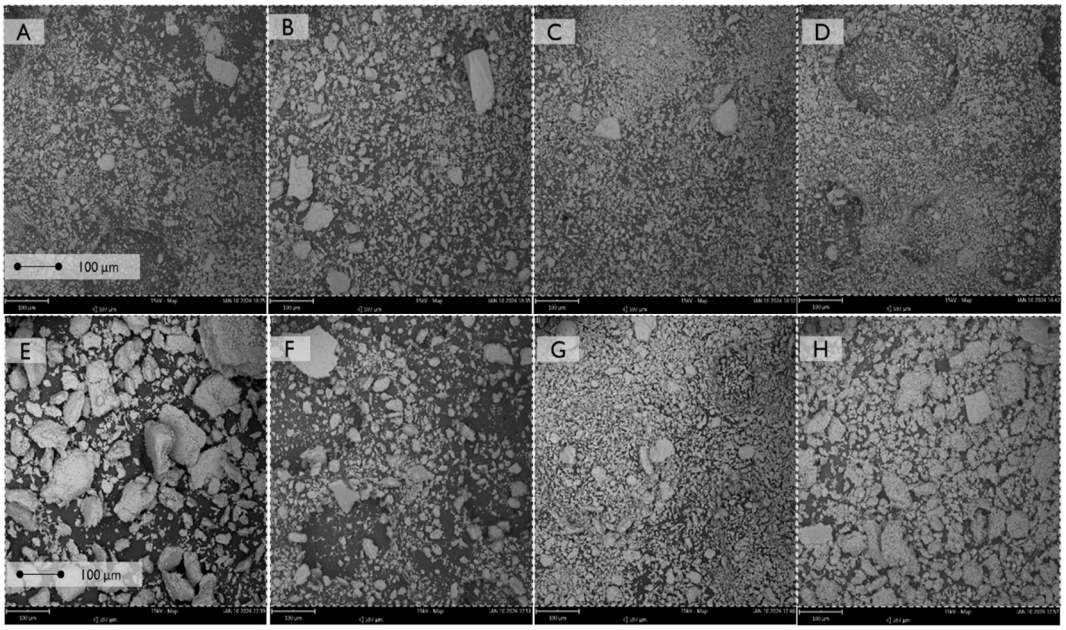


Figure 5-7 SEM images of (A-D) production scraps cathodes and (E-H) end-of-life cathodes after ball milling at 1080 rpm for 8-24 minutes and 840 rpm for 16 minutes

5.3.4 Thermal treatment and mechanical detachment

Thermal treatments carried out at temperatures below 350°C did not result in any noticeable changes in the samples, regardless of whether they were production scraps or end-of-life samples. However, upon closer examination, it is evident that there is a similar correlation between the process temperature and the amount of material lost after the thermal treatment, see Figure 5-8.

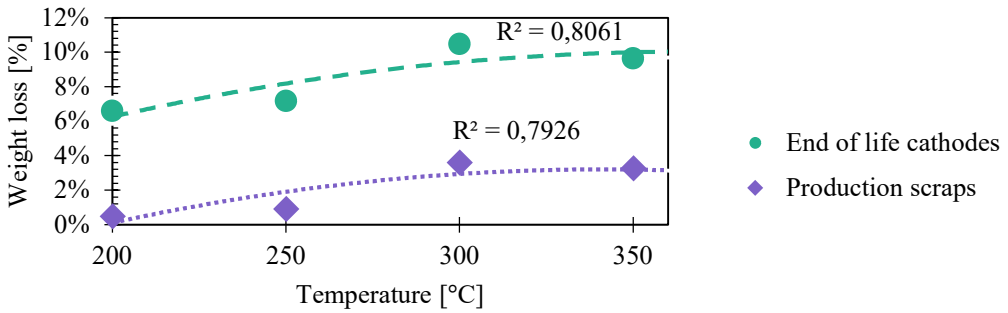


Figure 5-8 Weight loss rate of production scraps and end-of-life samples after thermal treatment

The weight difference resulting from the thermal treatment is directly proportional to the process temperature, with the end-of-life samples exhibiting a greater weight difference in comparison to the production scraps samples. This observation aligns with previous studies that have reported the beneficial effect of thermal treatment in removing residual electrolyte from end-of-life cathodes (Takahashi et al., 2020; S. Widijatmoko et al., 2020b).

Following the thermal treatment, the production scraps and end-of-life samples were subjected to ball milling at 840 rpm for a duration of 5 minutes. The separation rate achieved by this combination of thermal and mechanical treatment is shown in Figure 5-9.

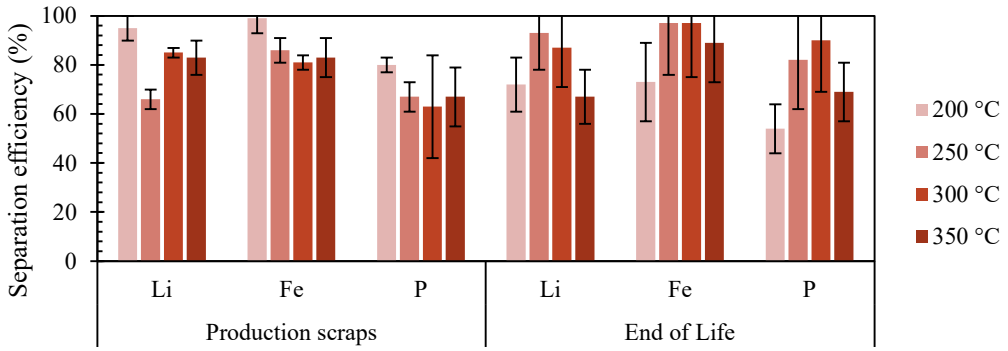


Figure 5-9 Separation efficiency through thermal treatment and ball milling

The separation rates observed in the production scraps samples were as follows: 95±5% for Li, 99±6% for Fe, and 80±3% for P when the temperature of the thermal treatment was 200°C; 66±4% for Li, 86±5% for Fe, and 67±6% for P when the temperature of the thermal treatment was 250°C; 85±2% for Li, 81±3% for Fe, and 63±3% for P when the temperature of the thermal treatment was 300°C; and 91±7% for Li, 83±8% for Fe, and 67±12% for P when the temperature of the thermal treatment was 350°C. On the other hand, the separation rates of the end-of-life samples were: 72±11% for Li, 73±17% for Fe, and 54±10% for P when the temperature of the thermal treatment was 200°C; 93±15% for Li, 97±21% for Fe,

and 82±20% for P when the temperature of the thermal treatment was 250°C; 87±16% for Li, 97±22% for Fe, and 90±21% for P when the temperature of the thermal treatment was 300°C; and 67±11% for Li, 89±16% for Fe, and 69±12% for P when the temperature of the thermal treatment was 350°C. The separation rate of end-of-life samples exhibited varying values depending on the temperature of the thermal treatment. Specifically, when the temperature was set at 200°C, the separation rates were found to be 72±11% for Li, 73±17% for Fe, and 54±10% for P. Increasing the temperature to 250°C resulted in higher separation rates, with values of 93±15% for Li, 97±21% for Fe, and 82±20% for P. Further increasing the temperature to 300°C led to separation rates of 87±16% for Li, 97±22% for Fe, and 90±21% for P. Lastly, when the temperature was set at 350°C, the separation rates were 67±11% for Li, 89±16% for Fe, and 69±12% for P. It is noteworthy that the temperature of the thermal treatment did not have any discernible impact on the material losses observed during the thermal treatment followed by ball milling. Similarly to the separation efficiency, the aluminum content in the end-of-life samples decreased as the temperature of the thermal treatment increased. For instance, the aluminum content declined from 0.13% in samples treated at 250°C to 0.06% in those treated at 350°C. The granulometry of the milled active material after the thermal treatment displayed a coarser nature when the temperature of the thermal treatment was below 250°C, both for production scraps and end-of-life samples. However, it is important to note that the active material detached from the production scraps samples exhibited finer particles compared to the end-of-life samples, irrespective of the temperature of the initial thermal treatment, see Figure 5-10. Among the end-of-life samples, only the sample subjected to thermal treatment at 200°C and subsequent ball milling displayed aluminium concentration above the detection limit of SEM/EDS analyses, reaching a value of 0.51 at%.

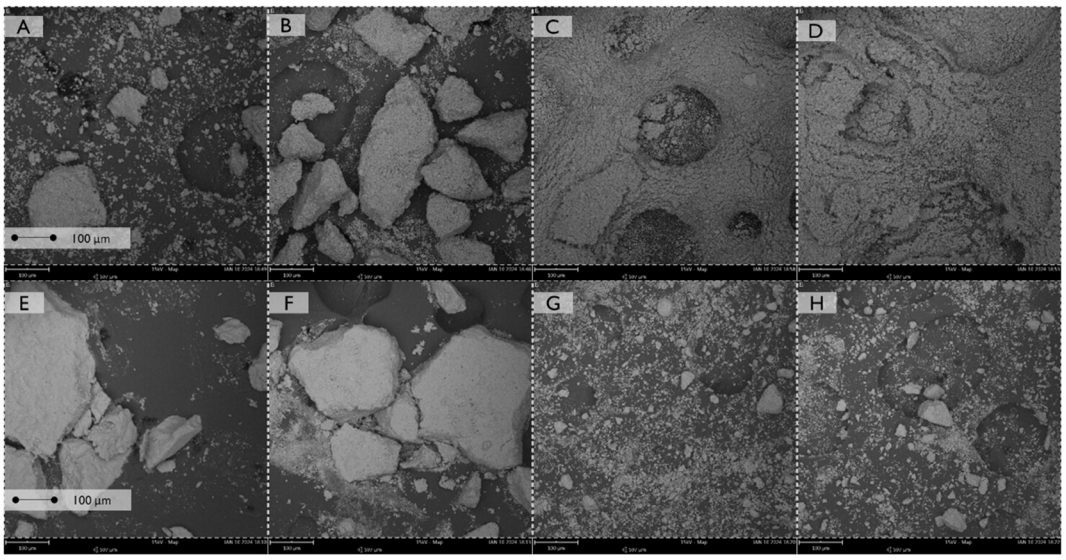


Figure 5-10 SEM images of (A-D) production scraps cathodes and (E-H) end-of-life cathodes after thermal treatment at 200-350°C and ball milling

5.3.5 Correlation analysis

A comprehensive correlation analysis was conducted to examine the relationship between the KPIs describing the effectiveness of the pre-treatment processes and the operational parameters for both the production scraps and end-of-life samples, see
Table 5-1 and

Table 5-2. The following colors scale has been applied: blue = positive correlation; red = negative correlation; white = no correlation. The correlation analysis revealed a strong relationship between the separation efficiency of the cathode powder's main components in both the production scraps and end-of-life samples.

Table 5-1 Pearson's correlation coefficient between operative parameters and KPIs for production scraps samples

	Separation rate Li (%)	Separation rate Fe (%)	Separation rate P (%)	Material loss (%)	Al impurities (%)
Ultrasound washing: time (min)	-78%	-72%	-76%	-70%	-51%
Thermal treatment: temperature (°C)	50%	66%	62%	28%	4%
Ball milling: frequency (Hz)	94%	82%	88%	82%	69%
Ball milling: time (min)	51%	26%	36%	76%	86%
Separation rate Li (%)		94%	97%	72%	49%
Separation rate Fe (%)			99%	69%	41%
Separation rate P (%)				63%	32%
Material loss (%)					74%

Table 5-2 Pearson's correlation coefficient between operative parameters and KPIs for production scraps samples

	Separation rate Li (%)	Separation rate Fe (%)	Separation rate P (%)	Material loss (%)	Al impurities (%)
Ultrasound washing: time (min)	-60%	-38%	-11%	42%	-3%
Thermal treatment: temperature (°C)	17%	35%	46%	-24%	-29%
Ball milling: frequency (Hz)	88%	82%	48%	-76%	23%
Ball milling: time (min)	61%	54%	23%	-40%	76%
Separation rate Li (%)		84%	57%	-89%	11%
Separation rate Fe (%)			85%	-90%	24%
Separation rate P (%)				-78%	21%
Material loss (%)					2%

For the production scraps samples, the correlation coefficients (r^2) were found to be 94% between Li and Fe, 97% between Li and P, and 99% between Fe and P. Similarly, for the end-of-life samples, the correlation coefficients were 84% between Li and Fe, 57% between Li and P, and 85% between Fe and P. Although the patterns observed in both sample types were similar, the key difference lay in the efficiency of ultrasound washing: longer ultrasound washing times resulted in increased material loss in the end-of-life samples (r^2=42%), but this did not have a significant impact on the purity of the separated material (r^2=-3%).

The temperature of thermal treatment had a limited positive effect on the separation efficiency of the cathode material. This effect was more pronounced in the production scraps samples, with correlation coefficients of 50% for Li, 66% for Fe, and 62% for P. In

contrast, the end-of-life samples exhibited lower correlation coefficients of 17% for Li, 35% for Fe, and 46% for P. The time and intensity of ball milling were found to have the greatest influence on the performance of the detachment methods. Higher milling frequencies led to increased separation of the cathode materials in both the production scraps samples (r^2=94% for Li, 82% for Fe, and 88% for P) and the end-of-life samples (r2=88% for Li, 82% for Fe, and 48% for P). On the other hand, longer durations of the milling process had a greater impact on the content of aluminium impurities in the separated materials. This was observed in both the production scraps samples (r^2=86%) and the end-of-life samples (r^2=76%), with a modest effect on the separation rate of the cathode's main components. Specifically, the correlation coefficients for the separation rate were 51% for Li, 26% for Fe, and 36% for P in the production scraps samples, and 61% for Li, 54% for Fe, and 23% for P in the end-of-life samples.

Another significant difference between the production scraps and end-of-life samples was the correlation between material loss and the separation rate of Li, Fe, and P. In the production scraps samples, the physical connection between the cathode powder and the current collectors was stronger due to the binder not yet being deteriorated. Consequently, during the mechanical detachment process, a portion of the cathode powder remained attached to the current collectors, thereby limiting the separation rate. However, this did not result in any changes to the material loss during the processes. On the other hand, the main limitation to the separation efficiency in the end-of-life samples was the loss of fine materials during detachment. The higher the material loss, the lower the recovery rate, as evidenced by the negative correlation coefficients of -89% for Li, -90% for Fe, and -78% for P.

5.3.6 Environmental analysis

During pre-treatments for mechanical detachment of cathodic materials from current collectors the consume of energy and water has been measured and normalized considering 1 kg of treated cathodes and considering the maximum capacity of equipment (ultrasound bath, milling chamber and muffle). Ultrasound washing is the only treatment requiring water and a consumption of 20 kg of water for each kg of treated cathodes has been considered, according to the solid/liquid ratio applied. The energy consumption of the ultrasound bath amounted to 0.117 kWh after 5 minutes, 0.123 kWh after 15 minutes and 0.125 kWh after 30 minutes. The muffle furnace consumed 1.15 kWh after 30 minutes, without significant differences between 200°C and 350°C. Ball milling consumed 0.004 kWh for 5 minutes at 840 rpm, 0.009 kWh for 8 minutes at 1080 rpm, 0.016 for 16 minutes at 1080 rpm, 0.028 for 24 minutes at 1080 rpm and 0.013 for 16 minutes at 840 rpm. These measurements have been normalized as following: 0.59 and 0.63 kWh/kg of input material

for ultrasound washing, between 2.25 and 7.00 kWh/kg of input material for ball milling and 6.75 kWh/kg of input material for thermal treatment followed by ball milling, see Figure 5-11.

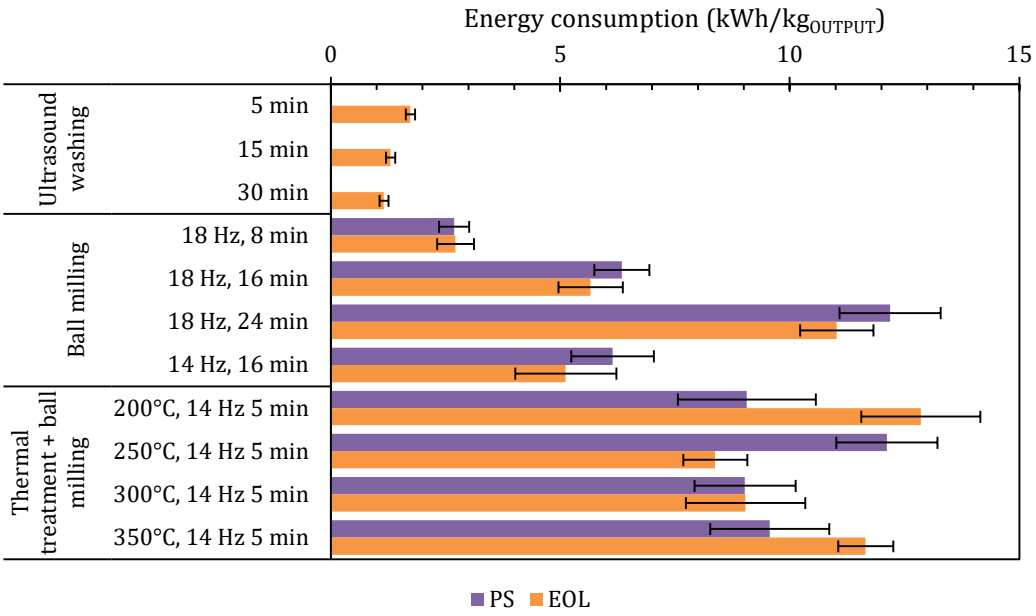


Figure 5-11 Energy consumption (kWh/kg$_{OUTPUT}$) associated to the pre-treatment processes

Ultrasound washing on production scraps cathodes did not have any effect on detaching active material from current collectors, thereby the energy demand associated with these treatments are reported as null. On the other hand, ultrasound washing on end-of-life cathodes presented higher separation rates with longer process durations. Thereby whilst the energy demand increased with longer process durations, the energy demand normalized by the amount of recovered material decreased from 1.73±0.2 kWh/kg of detached cathode material after 5 minutes to 1.16±0.2 kWh/kg after 30 minutes. Water consumption normalized by the amount of recovered material was: 59.2 kg$_{water}$/kg after 5 minutes, 42.3 kg$_{water}$/kg after 15 minutes and 37.0 kg$_{water}$/kg after 30 minutes.

The GWP associated with energy and water consumption of pre-treatments is shown in Figure 5-12. From a technical point of view, the best performing treatment to detach cathodes material from current collectors consists in thermal treatment (at 200°C for production scraps and at 250°C for end-of-life cathodes) followed by ball milling. These processes amounted to a GWP impact of 3.33±0.55 kg CO_2 eq. /kg of detached cathode material for production scraps and 3.08±0.25 kg CO_2 eq. /kg of detached cathode material for end-of-life cathodes.

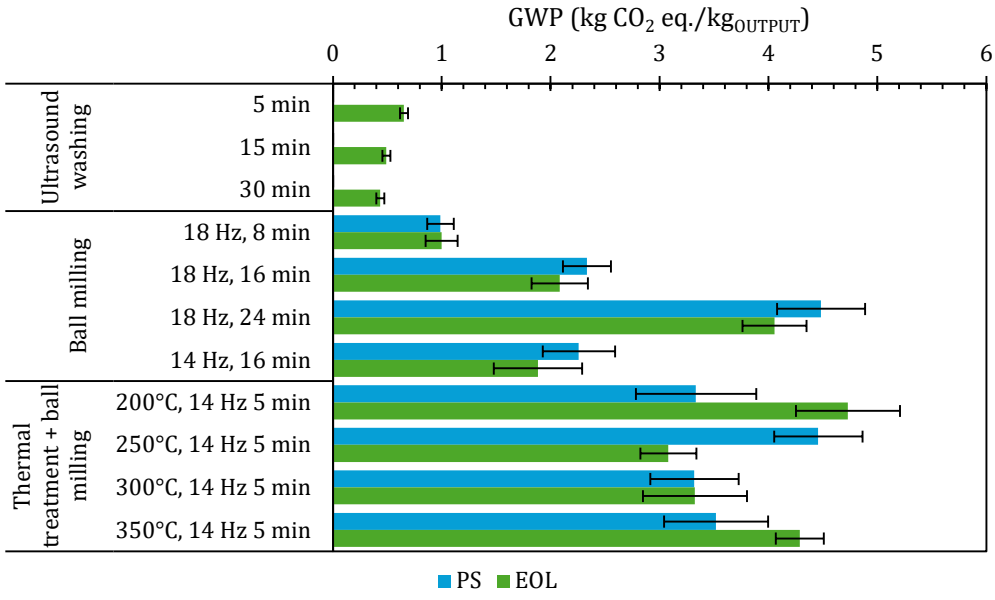


Figure 5-12 Global warming impact (GWP_{100}) associated to the pre-treatment processes

As a comparison, the GWP associated with conventional detachment methods has been calculated. According to the results of the literature review on LIBs recycling, in Chapter 1, conventional removal of binder to detach cathodes material from current collectors is performed with organic solvents, such as acetone, acetonitrile, and DMC, with a ratio of 10 kg of solvents per 1 kg of cathodes (Haas et al., 2018). GWP associated with the production of these solvents were retrieved by Ecoinvent database, resulting in an environmental impact of 26.22 kg CO_2 eq/kg of cathodes for acetone; 50.31 kg CO_2 eq/kg of cathodes for acetonitrile: and 22.69 kg CO_2 eq/kg of cathodes for DMC. The environmental impact entailed by physic-mechanical detachment proposed in work are one order of magnitude lower than conventional methods based on solvents extraction.

5.4 Discussion

All detachment techniques eventually yielded superior results for end-of-life samples. For the production scraps and end-of-life samples, thermal treatment and ball milling yielded the greatest results. A significant difference between production scraps and end-of-life samples is imputed to the degradation of the binder. production scraps cathodes have never been cycled and the bond between cathode material and current collector is stronger, thus some Li, Fe and P remain as coating of the current collectors after detachment. End-of-life samples instead underwent deterioration of the binder during the battery lifetime: during detachment, separation of the cathode material is easier and material loss is due to the fine fraction generated by ball milling.

Particularly, operative parameters of ball milling had a significant effect on the efficiency of the recovery rate of active materials and their grade. Higher milling frequency increased separation rate, as expected, but also the amount of Al impurities in the active material. On the contrary, longer duration of milling increased the concentration of Al impurities without significantly improving recovery rate of active materials. Thus, it is essential to limit the duration of mechanical processes.

Thermal treatment proved essential for the effectiveness of physical separation of LFP powder from current collectors. The greatest separation rates for production scraps samples were 95±5% for Li, 99±6% for Fe, and 80±3% for P after heat treatment at 200°C and ball milling. The results of ball milling and thermal treatment at 250°C for end-of-life samples are 93.15% for Li, 97.21% for Fe, and 82.10% for P, with a 0.13% aluminum content and a 3% material loss. Similar separation efficiencies of 90–97% of cathode material were reported in earlier experiments (Milad Jafari et al., 2020; Xie et al., 2021), with thermal treatment at temperatures as high as 500°C.

The effect of thermal treatment could be mostly attributed to the degradation of the organic binder that provides adhesion of cathodes active materials to current collectors. Novel Libs technologies are applying water soluble binders, which are less hazardous and simplify detachment for recycling. The application of water-soluble binders could alter the results presented in this Chapter, identifying ultrasound washing as a viable option.

5.5 Conclusions

This Chapter presented a comparison between pre-treatment processes aimed at mechanically detaching the active cathode material from the current collector. The focus was on production scraps and end-of-life cathodes from LFP batteries, and the evaluation was based on technical performance, environmental impact, and economic cost. It was observed that all the processes performed better on end-of-life samples compared to production scraps samples in terms of separation rate and material loss. Specifically, ultrasound washing proved to be unsuccessful in detaching the cathode material from production scraps samples. However, both production scraps and end-of-life samples showed the best results with thermal treatment and ball milling.

The highest separation efficiencies were achieved with low-intensity (840 rpm) ball milling for a short duration of 5 minutes, preceded by thermal treatment for 30 minutes at 200°C for production scraps samples and 250°C for end-of-life samples. These conditions led to the recovery of 95±5% of Li, 99±6% of Fe, and 80±3% of P from production scraps samples, and 93±15% of Li, 97±21% of Fe, and 82±20% of P from end-

of-life samples. Moreover, the presence of Al impurities was limited to 0.05% for production scraps samples and 0.13% for end-of-life samples.

In conclusion, it is possible to achieve effective detachment of LFP cathode material from current collectors through methods that have low energy demand and are free of solvents. Thermal pre-treatment is recommended to improve overall process efficiencies, while extended milling times should be avoided to minimize the presence of Al impurities and reduce energy consumption, environmental impacts, and operational costs.

Chapter 6

Hydrometallurgical recycling of end-of-life lithium iron phosphate cathodes

This chapter regards hydrometallurgical recycling of end-of-life lithium iron phosphate cathodes. The content of this chapter has been presented at the 10th International Conference on Sustainable Solid Waste Management CHANIA2023, with a presentation titled "*Preliminary tests aimed at the recycling of Lithium Iron Phosphate (LFP) cathodes*" and in a research paper "*Closed-loop recycling of Lithium Iron Phosphate cathodic powders via citric acid leaching*" authored by **Martina Bruno**, Professor Carlotta Francia and Professor Silvia Fiore and published in Environmental Science and Pollution Research (Bruno et al., 2024).

6.1 Introduction

Batteries based on LFP chemistries are taking an important place in the automotive sector. Indeed Tesla, one of the largest EVs manufacturer worldwide, adopted LFP batteries into Model 3 and Model Y since 2021 (Gong et al., 2022). Similarly, other automotive manufacturing companies, such as Volkswagen, Daimler and Ford are using LFP batteries in their electric vehicles (Kumawat et al., 2023). The main advantages posed by LFP cathodes are the fast charging and discharging rate, the long life-span and the safety of use increased by stability at extreme temperatures (Balakrishnan et al., 2021). Besides LFP cathodes are often preferred due to their lower price, compared with other battery chemistries (International Energy Agency, 2023). This economic aspect boost applications of LFP batteries, but hinders the attention given to the recycling of this specific cathode chemistry (Bi et al., 2019).

As discussed in Chapter 3, the most promising strategy to limit economic cost of recycling consists in hydrometallurgy. Conventional hydrometallurgical recycling involves the use of inorganic acids to achieve high leaching efficiency of target metals (Gerold et al., 2023; Li et al., 2022; Wang et al., 2023). Specifically, leaching efficiencies ranging from 97% to 99.9% for lithium and 98% to 99% for iron have been reported with the use of sulfuric acid (Vieceli et al., 2021,Yang et al., 2023, Song et al., 2021; Wang et al., 2022a). However, the high costs entailed by conventional hydrometallurgy pose an economic bottleneck on the recycling of LFP cathodes, which do not contain highly valuable elements, such as cobalt, nickel and manganese (Mahandra and Ghahreman, 2021).

On the other hand, selective leaching has emerged as a promising hydrometallurgical alternative method for LIBs recycling (Kumar et al., 2022) by targeting the extraction of specific elements, such as Lithium, from the black mass of the batteries. Indeed, selective lithium leaching efficiencies can exceed 97% , while other elements are subsequently extracted in subsequent steps (Jin et al., 2023; Wu et al., 2023). The selective leaching process typically utilizes mild organic acids, such as citric acid (Kumar et al., 2020), formic acid (Mahandra and Ghahreman, 2021), methyl sulfonic acid, and p-toluene sulfonic acid (Yadav et al., 2020). Additionally, during selective leaching, an oxidizing agent, such as hydrogen peroxide (Chen et al., 2018a; Li et al., 2017; Tao et al., 2019; Zhou et al., 2023a) or sodium hypochlorite (K. Liu et al., 2023; Liu et al., 2022; Tang et al., 2020), is often used in combination with the organic acids. Recent studies have proposed innovative selective leaching processes that involve the use of sodium citrate solution (Q. Zhang et al., 2023a) or monosodium phosphate (Zhou et al., 2023a). However, despite the increasing use of organic acids for leaching metals from Nickel Manganese Cobalt (NMC)

and Lithium Cobalt Oxide (LCO) cathodes, citric acid has been rarely applied to the recycling of LFP cathodes (Li et al., 2023,Wang et al., 2022b).

This chapter investigates the comparison of conventional and selective hydrometallurgical processes as closed-loop recycling routes for end-of-life (EoL) LFP cathodes. These routes consist of conventional leaching with sulfuric acid or citric acid, and, as an alternative, selective leaching with citric acid mixed with hydrogen peroxide at a temperature of 25°C. Both routes are completed by recovery through chemical precipitation of the mineral precursors and solid-state synthesis of the recycled LFP material.

6.2 Methodology

6.2.1 Experimental procedure

LFP cathodes were sourced from a recycling company from Italy, already dismantled from EoL cells. Prior to their utilization, the LFP cathodes' powders underwent a series of pre-treatments as outlined in Chapter 5. These pre-treatments involved subjecting the powders to a thermal treatment at 250°C for a duration of 30 minutes in a muffle furnace. Subsequently, the powders were ball milled for 5 minutes at 840 rpm in 50 mL Zirconia jars, incorporating two Zirconia beads with a diameter of 10 mm. Finally, the powders were manually sieved in order to eliminate any particles exceeding the dimensions of 1 mm.

The obtained LFP powder was treated by leaching and chemical precipitation to recover solid samples that were regenerated through calcination. Conventional leaching was performed with sulfuric acid and with citric acid in order to compare the performance of the two leaching solutions with the conventional route. The conventional leaching route required leaching of iron, lithium and phosphorous, chemical precipitation of iron and phosphorous by adjusting the pH with 10M NaOH, precipitation of lithium as carbonate with the addition of 10 M Na_2CO_3, and finally carbothermal reduction of LFP material at a temperature of 700°C. On the other hand, the selective leaching pathway required selective leaching of lithium and its recovery via chemical precipitation with 10 M sodium carbonate, and carbothermal reduction of LFP powders at a temperature of 700°C. All processes were conducted in triplicates, ensuring the reliability and accuracy of the obtained results. During selective leaching, different concentration values of citric acid have been tested. The experimental conditions implemented in this study, as outlined in Table 6-1, were based on previous research studies (Kumar et al., 2022; Qin et al., 2019; Sattar et al., 2019; Takahashi et al., 2020; Vieceli et al., 2021; Yue et al., 2018).

Table 6-1. Leaching conditions (concentration of leaching agent and hydrogen peroxide, temperature, contact time, S/L: solid to liquid ratio) applied in this study

Leaching agent	Concentration	Concentration H_2O_2	Temperature	Time	S/L ratio
sulfuric acid	1 M	0 %vv	40 °C	2 h	50 g/L
citric acid	1 M	0 %vv	25°C	1 h	70 g/L
citric acid	1 M	6 %vv	25°C	1 h	70 g/L
citric acid	0.5 M	6 %vv	25°C	1 h	70 g/L
citric acid	0.25 M	6 %vv	25°C	1 h	70 g/L

Moreover, the leachates obtained from the process underwent filtration using syringe filters with a pore size of 0.45µm and were subsequently analyzed using FAA spectroscopy. Chemical precipitation occurred when the pH of the leachates was adjusted by adding 10M NaOH. These precipitates were then recovered through centrifugation. In order to recover lithium as phosphate, 10M NaOH has been added to the leachate solution until it reached a pH of 11. Subsequently, 10 M Na_2CO_3 was added, and the mixture was heated to 95°C for 2 hours to obtain Li_2CO_3. The recovered powders, with a stoichiometric ratio of Li:Fe:P=1:1:1, were combined and supplemented with 20%wt. D(+)glucose as a carbon source. To ensure homogeneity, the powders were subjected to ball milling using a planetary mill for a duration of 3 hours at a frequency of 20 Hz. Finally, the powders were subjected to thermal treatment at a temperature of 700°C for a duration of 4 hours in a tubular furnace under an argon atmosphere, resulting in the formation of recycled LFP.

Furthermore, the solid samples were recovered using a centrifuge, rinsed with deionized water, followed by drying at a temperature of 70°C in an oven and eventually characterized with XRF and XRD spectroscopy. The experimental activity described in this chapter is shown in Figure 6-1.

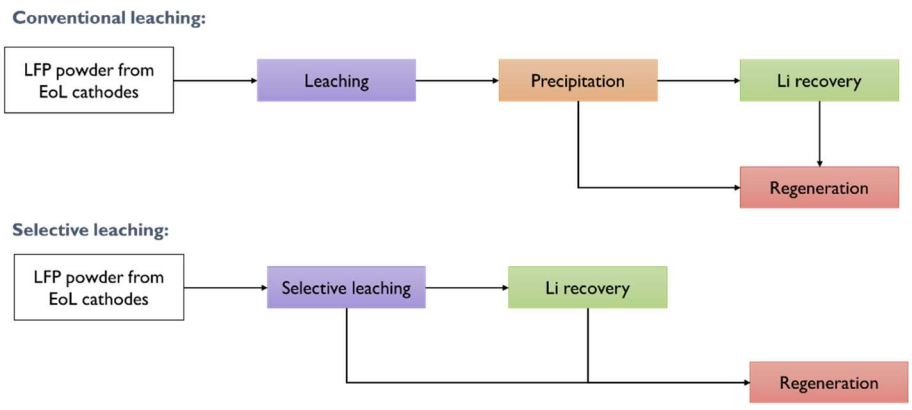


Figure 6-1. Outline of the experimental approach with conventional and selective leaching

The following reagents were used: sulfuric acid (CAS: 7664-93-9, >96% purity, Carlo Erba Reagents); citric acid (CAS: 77-92-9, >99.5% purity, Sigma Aldrich); hydrogen peroxide (CAS: 7722-84-1, 30%v.v., Carlo Erba Reagents); sodium hydroxide (CAS: 1310-73-2, >98% purity, Honeywell/Fluka); sodium carbonate (CAS: 497-19-8, >99.8% purity, Sharlab); D(+)Glucose anhydrous (CAS: 50-99-7, >97.5% purity, Carlo Erba Reagents).

Additionally, The equipment used were: AREX-6DIGITAL PRO heating magnetic stirrer and VTF EVO digital thermoregulatory, both from VELP Scientifica, for leaching and precipitation processes, a Hermle Labor Technik Z 206 A centrifuge for separation of the liquid solution, an ARGO LAB TCN 30 oven to dry the sample before characterization, a Retsch MM400 mill and a Carbolite MTF 12/38/400 tubular furnace for regeneration of the precursor material. Eventually, the samples were characterized with a Rigaku, NEX-DE XRF spectrometer, a PANanalytical X'Pert X-ray Diffraction (XRD) spectrometer and a GFA-EX7 FAA spectrometer.

6.3 Results

6.3.1 Initial sample characterization

The initial samples have been obtained through the thermo-mechanical pre-treatment described in Chapter 5. The crystalline structure of the initial sample has been identified as LiFePO4 with XRD spectrometry, see Figure 6-2.

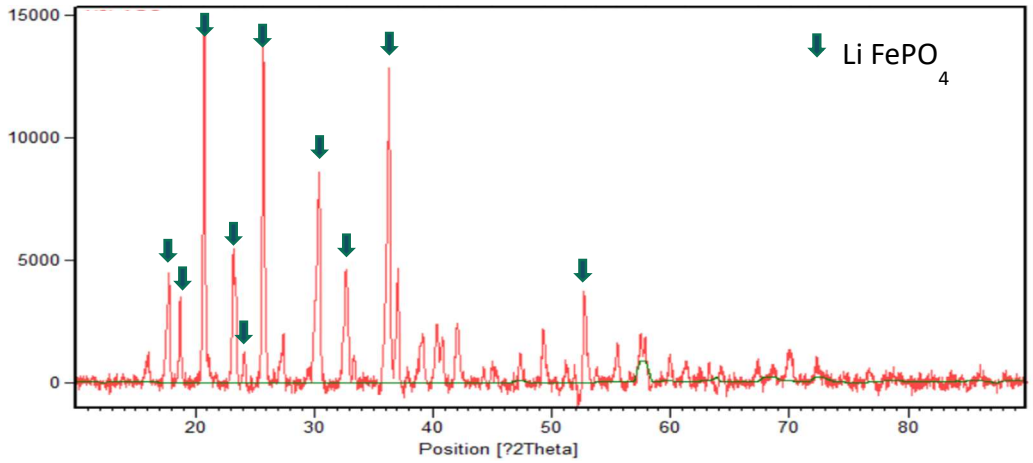


Figure 6-2 XRD spectrum of LFP powder from end-of-life cathodes

The chemical composition of these powders was found to be approximately 1.6±0.01%wt. Li, 29.64±1.32%wt. Fe, and 14.80±0.4%wt. P, which is consistent with the findings reported in literature (Gaines et al., 2018; Yagci et al., 2021; Yang et al., 2018; L. Zhang et al., 2022). Additionally, the presence of aluminum impurities originating from the

current collector was measured to be approximately 0.092±0.06%wt., indicating the effectiveness of the detachment process.

6.3.2 Leaching process

The different leaching conditions compared in these tests have been named: S_0= sulfuric acid 1M, C_0= citric acid 1M, C_1= citric acid 1M+6%v.v. H_2O_2, C_2= citric acid 0.5M+6% v.v. H_2O_2, C_3= citric acid 0.25M+6% v.v. H_2O_2: according to the operative conditions applied. The efficiency of lithium, iron, phosphorous and aluminium leaching have been reported in Figure 6-3.

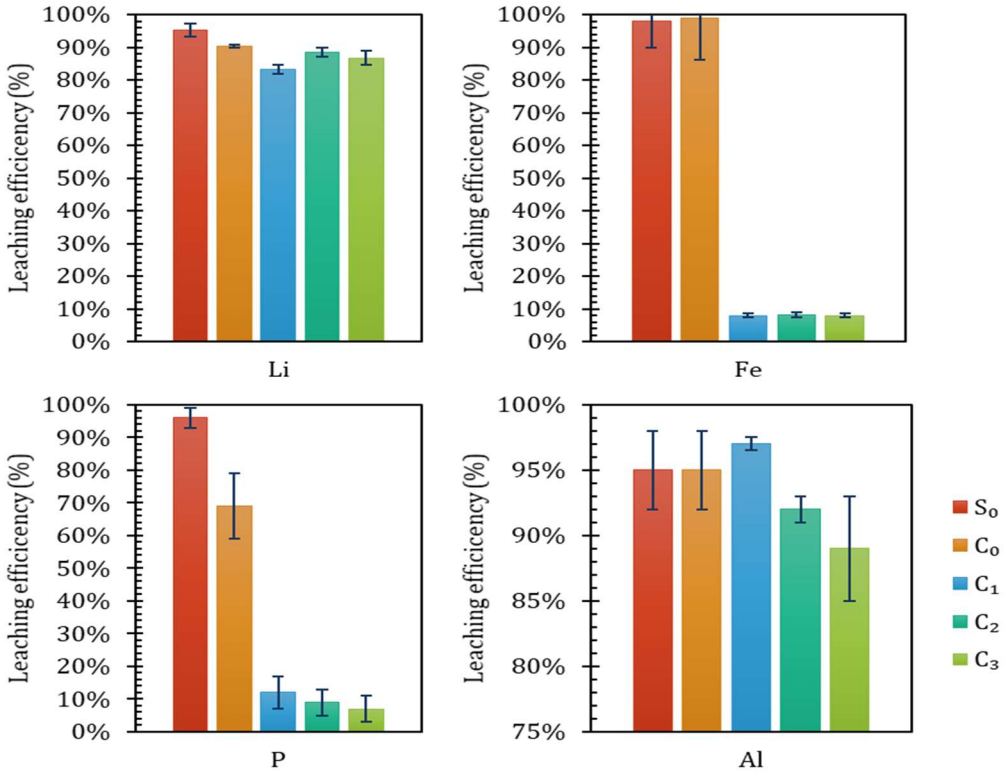


Figure 6-3. Leaching efficiency of lithium, iron, phosphorous and aluminium with conventional and selective leaching

The chemical composition of these powders was found to be approximately 1.6±0.01%wt. Li, 29.64±1.32%wt. Fe, and 14.80±0.4%wt. P, which is consistent with the findings reported in literature (Gaines et al., 2018; Yagci et al., 2021; Yang et al., 2018; L. Zhang et al., 2022). Additionally, the presence of aluminum impurities originating from the current collector was measured to be approximately 0.092±0.06%wt., indicating the effectiveness of the detachment process.

Sulfuric acid exhibited the highest degree of effectiveness as a leaching agent, enabling the extraction of approximately 95±2% of Li, 98±8% of Fe, and 96±3% of P. However, it is important to note that the leaching efficiency of citric acid was comparable, with values of 90±0.6% for Li, 99±13% for Fe, and 69±10% for P. On the other hand, selective leaching with citric acid and hydrogen peroxide allowed to recover lithium into the leaching solution, with limited iron and phosphorous impurities. Besides, the concentration of citric acid did not significantly decrease lithium leaching efficiency. Indeed, 83±0.8% Li, 8±1% Fe, and 12±5% P were leached with 1 M citric acid; 88±1% Li, 8±1% Fe, and 9±4% P with 0.5 M citric acid; and 87±2% Li, 8±1% Fe, and 7±4% P with 0.25 M citric acid.

6.3.3 Iron and Phosphorous recovery

Conventional leaching requires the recovery of iron and phosphorous from the leachate, which has been performed by chemical precipitation. A solution of 10M NaOH has been added at room temperature to the leachates in order to adjust their pH to target levels. Iron phosphate precipitates formed at pH 2 in form of $FePO_4$ and pH 5.5 in form of vivianite $FePO_4 \cdot H_2O$. The overall recovery efficiency was 69±15% Fe and 70±18% P from sulfuric acid leachate and 82±6% for Fe and 74±8% for P from citric acid leachate. The crystalline structure of the precipitates were characterised with XRD spectrometry, see Figure 6-4 and Figure 6-5 for precipitates obtained from sulfuric acid leachate and Figure 6-4 and Figure 6-5 for precipitates obtained from citric acid leachate. It is worth noting that the $FePO_4$ precipitated at pH 2 did not exhibit a crystalline structure and thus required treatment at 700°C for 3 hours.

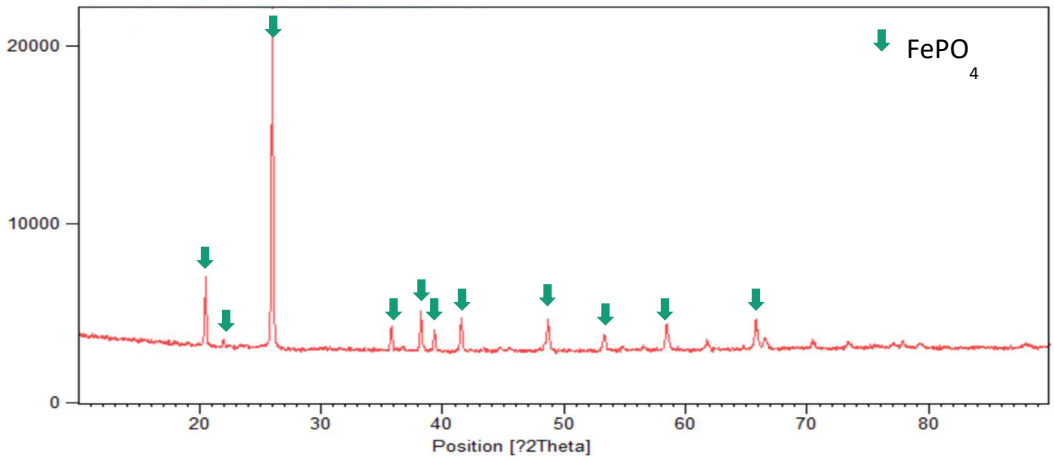


Figure 6-4 XRD spectrum of the recovered powders obtained from sulfuric acid leaching at pH 2 after thermal treatment at 700°C

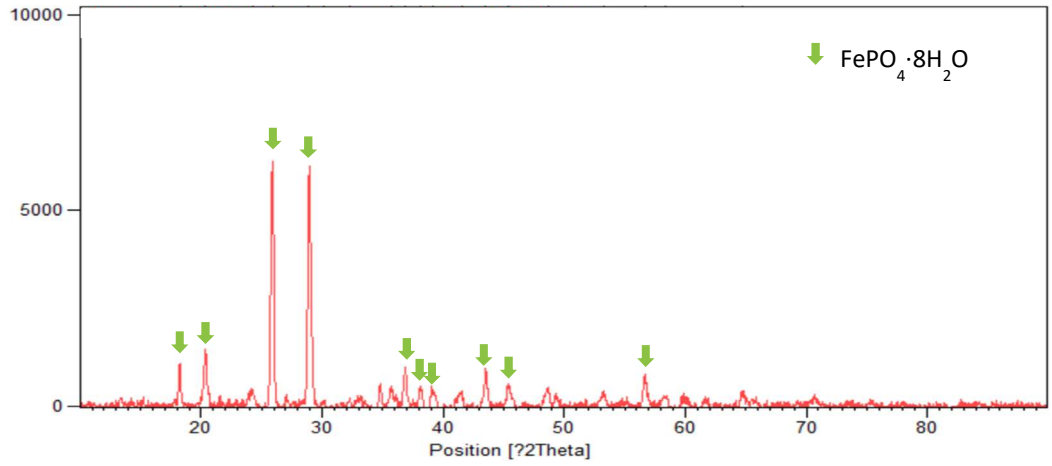


Figure 6-5 XRD spectra of the recovered powders obtained from sulfuric acid leaching at pH 5.5

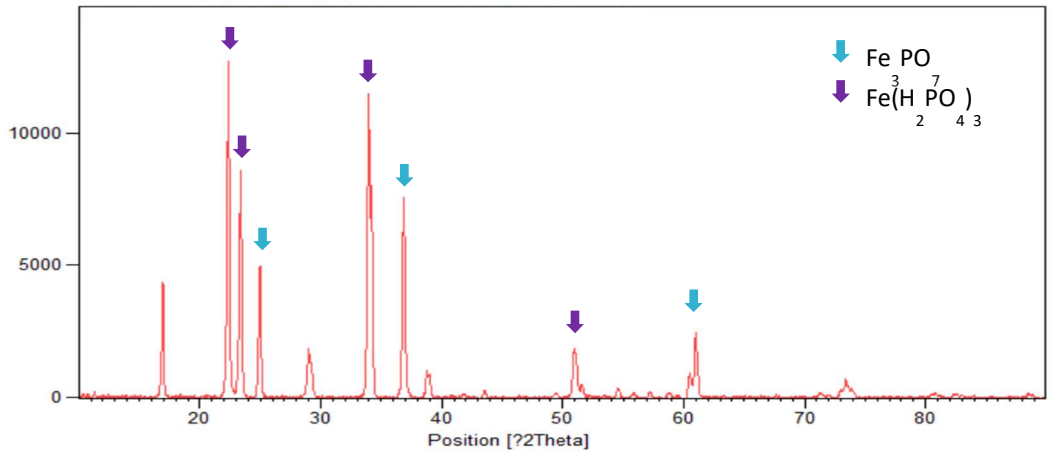


Figure 6-6 XRD spectrum of the recovered powders obtained from citric acid leaching at pH 2 after thermal treatment at 700°C

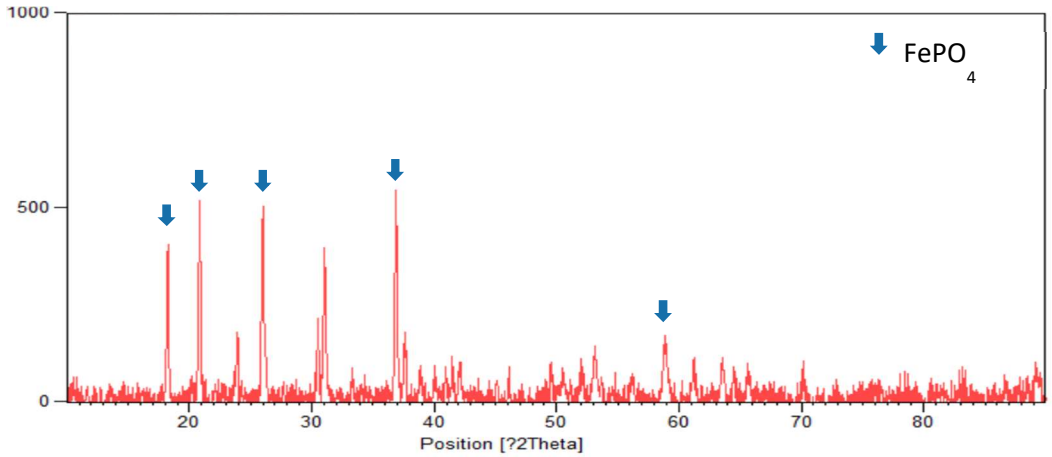


Figure 6-7 XRD spectrum of the recovered powders obtained from citric acid leaching at pH 5.5

On the other hand, selective leaching allows the recovery of iron (Fe) and phosphorus (P) in solid residues after leaching as $FePO_4$. The leachate obtained from this process requires only one precipitation and centrifugation step to remove Fe impurities, which make up approximately 2±1% of the total weight. The efficiency of Fe and P recovery from selective leaching is: 92±1% for Fe and 88±5% for P using citric acid 1 M and 6%vv hydrogen peroxide, 92±1% for Fe and 91±4% for P using citric acid 0.5 M and 6%vv hydrogen peroxide, and 92±1% for Fe and 93±4% for P using citric acid 0.25 M and 6%vv hydrogen peroxide. Thus, selective leaching presented higher efficiency in the overall amount of Fe and P recovered, requiring less process steps and no additional reagent to adjust the pH level. Besides, the leaching residues maintain the morphological structure required to precursors for cathode materials, without the need of further calcination processes.

Moreover, the concentration of impurities in the Fe- and P-rich powders was determined through XRF spectroscopy. It was found that the concentration of copper, nickel and silicon was below the detectable limit of XRF spectroscopy in all the precipitates. The predominant impurity found in the Fe- and P-rich powders precipitated from sulfuric acid leachate was sulfur (S), which exhibited a concentration of 8798±3061 mg/kg in the Iron Phosphate precipitate obtained at pH 2, and 8468±1925 mg/kg in the Vivianite precipitate obtained at pH 5.5. In addition to sulfur, the same powders also contained cobalt, which was primarily leached at pH 2, resulting in a concentration of 153±37 mg/kg of precipitate. The Vivianite precipitate exhibited contamination from aluminium at a concentration of 3287±1777 mg/kg, vanadium at a concentration of 520±155 mg/kg, and chlorine at a concentration of 181±31 mg/kg. On the other hand, the precipitated fraction obtained through conventional leaching with sulfuric acid demonstrated the presence of aluminum at a concentration of 1681±1063 mg/kg, chlorine at a concentration of 149±31 mg/kg, cobalt at a concentration of 128±51 mg/kg, sulfur at a concentration of 8104±2403 mg/kg, and vanadium at a concentration of 270±71 mg/kg.

The powders obtained via conventional leaching with citric acid exhibited contamination from aluminum at a concentration of 2010±62 mg/kg, vanadium at a concentration of 219±15 mg/kg, and chlorine at a concentration of 160±7 mg/kg at pH 2. At pH 5.5, the contamination levels were measured to be aluminum (1016±881 mg/kg), vanadium (158±13 mg/kg), and chlorine (136±5 mg/kg). The total contamination in the precipitates obtained through conventional leaching with citric acid were aluminum (1602±381 mg/kg), chlorine (149±7 mg/kg), cobalt (155±24 mg/kg), sulfur (193±7 mg/kg), and vanadium (234±14 mg/kg).

The residues obtained from selective leaching displayed lower concentrations of aluminum, sulfur, zinc, and chlorine compared to the precipitates obtained through conventional leaching. Specifically, the contamination levels in the leaching residues after

selective leaching were measured to be aluminum (736±97 mg/kg), chlorine (80±4 mg/kg), cobalt (202±176 mg/kg), sulfur (354±7 mg/kg), and vanadium (339±12 mg/kg) with the usage of citric acid 1M and hydrogen peroxide. With citric acid 0.5M and hydrogen peroxide, the contamination levels were aluminum (383±663 mg/kg), chlorine (91±5 mg/kg), cobalt (146±75 mg/kg), sulfur (331±19 mg/kg), and vanadium (328±2 mg/kg). Lastly, with citric acid 0.25M and hydrogen peroxide, the contamination levels were aluminum (665±557 mg/kg), chlorine (101±6 mg/kg), cobalt (277±69 mg/kg), sulfur (499±10 mg/kg), and vanadium (357±9 mg/kg).

6.3.4 Lithium recovery

To recover lithium after both conventional and selective leaching, two precipitation steps were carried out. The first step involved increasing the pH to 12, while the second step involved adding Sodium carbonate at 95°C. Additionally, two centrifugation steps were performed to separate the precipitates and facilitate the recovery of lithium. The total recovery of lithium was found to be 21±2% for the sulfuric acid route (98±12% as Li_2SO_4 and 2±0.7% as Li_2CO_3) and 29±5% for the citric acid and hydrogen peroxide route (66±7% as Li3PO4 and 34±5% as Li_2CO_3).

Lithium recovered from conventional leaching with sulfuric acid has been identified as lithium sulfate (98±12%wt. of recovered Lithium), see Figure 6-8, whereas lithium recovered from selective leaching was in the form of lithium phosphate (66±7%wt. of recovered Lithium), see Figure 6-9. The presence of lithium in form of phosphate alongside lithium carbonate is due to the lower solubility constant of lithium phosphate ($2.37 \cdot 10^{-11}$) compared with lithium carbonate ($8.15 \cdot 10^{-4}$) (Lide, 2004).

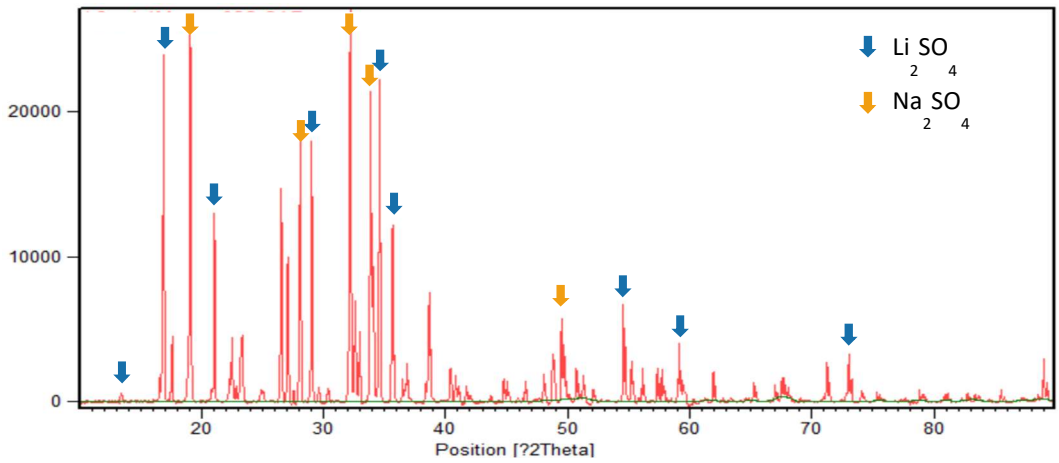


Figure 6-8 XRD spectra of precipitates obtained at pH 12 from conventional sulfuric acid leachates

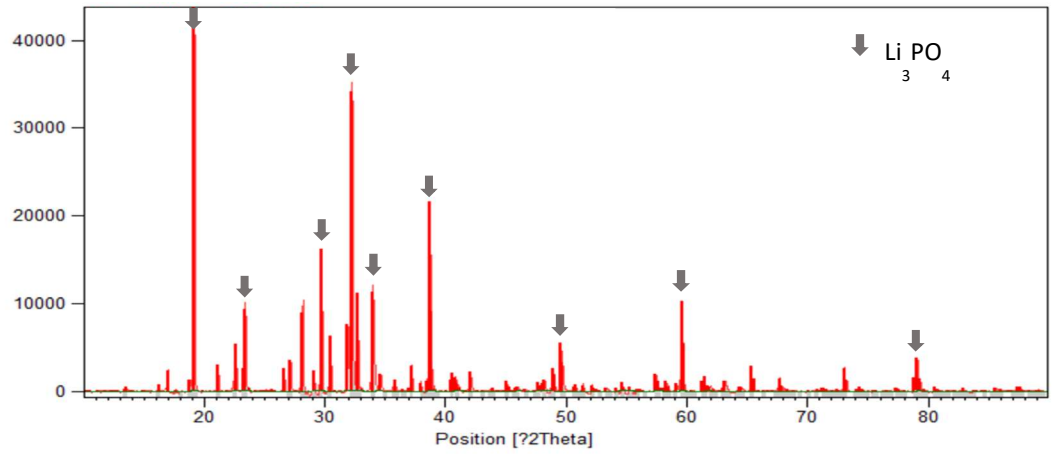


Figure 6-9 XRD spectra of precipitates obtained at pH 12 from selective 0.25M citric acid and hydrogen peroxide leachates

6.3.5 Regeneration through carbothermal reduction

The powders obtained from the conventional leaching with sulfuric acid, as well as the 0.25 M citric acid routes, experienced carbothermal reduction in order to obtain precursors for recycled LFP cathodes. The precipitates of iron, phosphorous and lithium from conventional leaching have been arranged in the desired stoichiometric ratio of Li:Fe:P=1:1:1 and mixed with glucose prior to calcination. The same procedure has been followed with the leaching residues and lithium precipitate from selective leaching. The recovered LFP material presented olivine structure both from conventional and selective leaching. In the XRD spectra of both materials, the presence of Lithium Iron Phosphate, see Figure 6-10 and Figure 6-11. Olivine crystalline structure was detected with the LFP powders obtained from the sulfuric acid route containing impurities in the form of iron oxides.

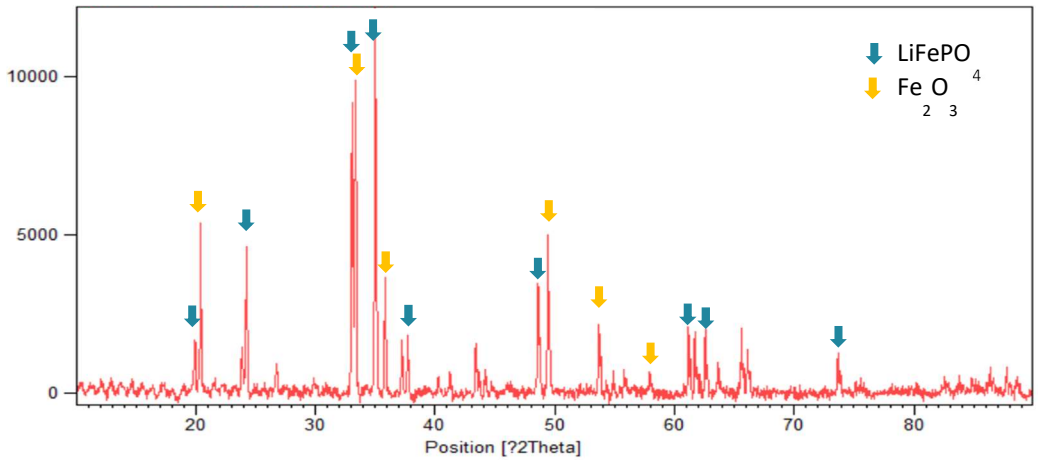


Figure 6-10 XRD spectra of recycled LFP powders deriving from conventional leaching with sulfuric acid

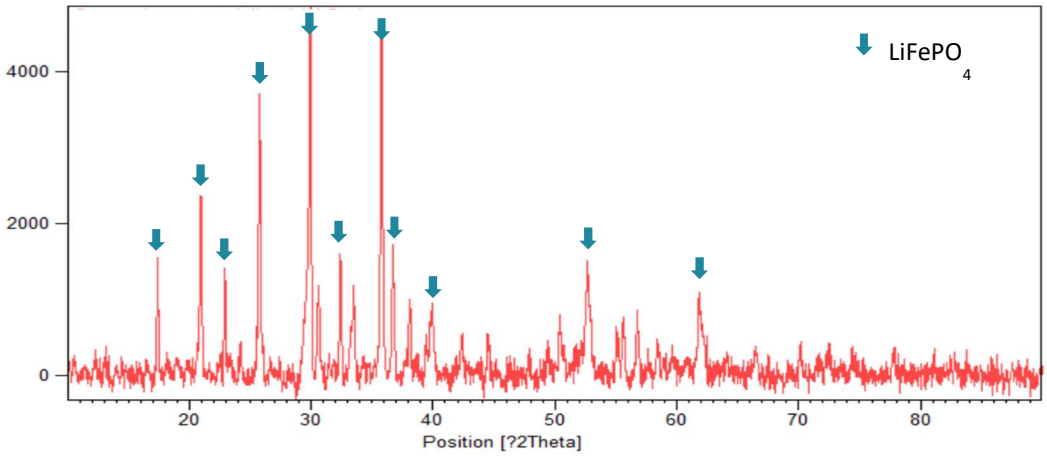


Figure 6-11 XRD spectra of recycled LFP powders deriving from selective leaching with citric acid and hydrogen peroxide

6.4 Discussions

This Chapter presented a comparison between conventional and selective leaching for hydrometallurgical recycling of LFP cathodes. Selective leaching offers several advantages over conventional hydrometallurgy, including shorter processing times and lower concentrations of leaching agents, limiting waste generation and reducing both the environmental impact and economic costs associated with the recycling process (Kumar et al., 2022; K. Liu et al., 2023). The environmental benefits of selective leaching can be further enhanced by the use of organic acids, which are considered less persistent than inorganic acids, (Golmohammadzadeh et al., 2018; Zhou et al., 2023b) and can avoid the release of harmful gases, such as Cl_2, NO_x, and SO_3 (Golmohammadzadeh et al., 2017; Meng et al., 2020). Besides, citric acid, in particular, is easily soluble and naturally biodegradable and has been proposed as a "green chemical" for the hydrometallurgical recycling of LIBs (Li et al., 2010b).

The results of conventional leaching with sulfuric acid align closely with previous studies (Zheng et al., 2016), where a higher concentration of sulfuric acid, longer contact time, and a lower solid-to-liquid ratio led to the leaching of 97% of Li and 98% of Fe. The relatively lower performance of citric acid, in comparison to sulfuric acid, can be attributed to the milder leaching conditions employed (25°C for 1 hour as opposed to 40°C for 2 hours

The chemical reactions taking place during leaching of leaching in LFP cathodes using sulfuric acid, citric acid, and hydrogen peroxide are delineated in equations 1, 2, and 3.

(Eq. 1) $2\ LiFePO_4 + H_2SO_4 \rightarrow 2\ FeSO_4 + Li_2SO_4 + 2\ H_3PO_4$

(Eq. 2) $3\ H_3cit + 3\ LiFePO_4 \rightarrow Fe_3\ (cit)_2 + Li_3cit + 3\ H_3PO_4$

(Eq. 3) $2\ H_3cit + 3\ H_2O_2 + 6\ LiFePO_4 \rightarrow 6\ FePO_4 + 2\ Li_3cit + 6\ H_2O$

The selective leaching process relies on hydrogen peroxide as an oxidant to enhance the olivine structure of $FePO_4$ by oxidizing Fe^{2+} to Fe^{3+}. Previous studies have supported similar conclusions (Niu et al., 2023). Another study confirmed these results by using a limited amount of sulfuric acid without hydrogen peroxide, displaying selectivity towards Fe while still leaching 20% of P (Tao et al., 2019). In contrast to previous research indicating increased Li leaching efficiency with hydrogen peroxide presence (Mahandra and Ghahreman, 2021), this study found no significant impact of hydrogen peroxide concentration on lithium leaching efficiency. Specifically, leaching with 1M citric acid and 6% v.v. hydrogen peroxide yielded 92±2% of Li leached without hydrogen peroxide. However, the presence of hydrogen peroxide limited Fe and P leaching efficiencies, ensuring the selectivity of lithium leaching. Notably, the lithium recovery efficiency in this study was lower than in previous literature reports for both selective and conventional leaching, which typically reported values between 70 and 85%wt (Dolotko et al., 2020; Kumar et al., 2020). This lower recovery efficiency could be attributed to the relatively low masses used (4 g of EoL LFP cathodic powders producing 0.86 g of Lithium-rich precipitates from conventional leaching with sulfuric acid and 1.16 g from selective leaching with citric acid and hydrogen peroxide), potentially affected by material losses during leaching and recovery processes.

6.5 Conclusions

Despite the fact that hydrometallurgical recycling of LIBs is currently being widely implemented on a full-scale and extensively researched, current full-scale technologies are not economically viable for Lithium Iron Phosphate (LFP) batteries. This Chapter presented a comparison between conventional hydrometallurgical methods and selective leaching to shorten the loop of LFP cathodes' recycling.

Conventional leaching with sulfuric acid has proven to be effective in recovering lithium (Li), iron (Fe), and phosphorus (P) through multiple steps of chemical precipitation. On the other hand, selective leaching with citric acid and hydrogen peroxide has successfully recovered Fe and P as residual material subsequent to leaching. Chemical precipitation is used solely for the recovery of Li in this particular pathway, thereby reducing the number of steps required for material recovery.

In terms of the conventional leaching process with sulfuric acid, this method was followed by a chemical precipitation step, which resulted in the recovery of 69±15% of Fe and 70±18% of P. However, it is important to note that this process also led to the presence of certain contaminations, including Al (1681±1063 mg/kg), Cl (149±31 mg/kg), Co (128±51 mg/kg), S (8104±2403 mg/kg), and V (270±71 mg/kg). On the other hand, the selective leaching process with 0.25M citric acid and 6%vv. hydrogen peroxide proved to be more efficient, allowing for the recovery of 92±1% of Fe and 93±4% of P in the leaching residues, while also resulting in lower levels of contaminations: 665±557 mg/kg of Al, 101±6 mg/kg of Cl, 277±69 mg/kg of Co, 499±10 mg/kg of S, and 357±9 mg/kg of V.

In conclusion, selective leaching with citric acid and hydrogen peroxide, as opposed to conventional hydrometallurgical recycling, represents a promising strategy to shorten the recycling process and a viable alternative for the recycling of EoL LFP cathodic powders.

Chapter 7

Hydrometallurgical recycling of lithium iron phosphate cathodes production scraps

This chapter regards hydrometallurgical recycling of LFP cathodes production scraps through selective leaching. According to the results of conventional and selective leaching on end-of-life LFP cathodes (Chapter 6), leaching parameters have been adjusted to target selective recovery of lithium from LFP production scraps. The content of this chapter will be presented in the research paper "*Selective leaching for the recycling of lithium, iron and phosphorous from lithium-ion battery cathodes' production scraps*" authored by **Martina Bruno**, Professor Julia Amici and Professor Silvia Fiore (under review).

7.1 Introduction

The growing demand of LIBs, due to their application in the automotive sector, increased from 330GWh in 2021 to 550 GWh (+65%) in 2022 (International Energy Agency, 2023). The increase in LIBs manufacturing to supply the demands set by the market, especially in the transport sector, poses concerns on the security of the supply chains for primary raw materials, as addressed in Chapter 2. However, the rise of LIBs production rate generates an increasing amount of production scraps (Gaines et al., 2021).

Production scraps are generated in the greatest quantity during cells manufacturing and at lower scale during the Research and Development (R&D) of new batteries technologies (Yu et al., 2024). They consist of electrodes trimmings and elements which failed the quality checks along the production process. Production scraps are generated with a rate between 5% and 10% of batteries production (Gaines et al., 2021). Economic profitability of LIBs manufacturing is ensured when the generation of production scraps is below the threshold of 8% of batteries production (Yu et al., 2024). However, considering the steep increase of current LIBs manufacturing rate, recycled production scraps represent a feedstock for LIBs supply chain more significant than end-of-life batteries, which quantity is depended on LIBs manufacturing rate of the past 10 years (Gaines et al., 2021; Gaines and Wang, 2021).

Recycling of LIBs production scraps can be advantageous to recover materials to supply LIBs manufacturing compared with end-of-life batteries: production scraps do not require dismantling and sorting, since their composition is known, and their management is considered safer since they have not been in contact with electrolytes solutions, and they do not hold residual voltage. However the potential for recovering critical raw materials from production scraps generated during battery manufacturing has been largely overlooked by research, which mainly focused on optimizing the recycling of end-of-life cathodes (Ahuis et al., 2024).

LIBs recycling is more economical favourable throughout hydrometallurgical processes, as discussed in Chapter 3. Moreover, in order to mitigate the environmental and economic impacts of hydrometallurgical recycling and reach economic viability for recycling of LFP cathodes, selective leaching has emerged as a viable solution, according to the results presented in Chapter 6. Selective leaching involves selectively extracting lithium while leaving iron and phosphorous in the solid residue. This approach offers several advantages over conventional hydrometallurgy, including shorter process times, lower acid concentrations, reduced energy requirements, and minimized waste generation (Kumar et al., 2020). Furthermore, the iron phosphate remaining in the leaching residues

retains its original olivine structure and can be directly reused as a precursor for cathode production, thereby reducing costs (X. J. Wang et al., 2022).

Previous literature on selective leaching of LFP cathodes has primarily focused on sulfuric acid combined with oxidizing agents such as hydrogen peroxide (Ku and Chen, 2022; Li et al., 2017) or sodium hypochlorite (Tang et al., 2020), which have demonstrated the ability to recover over 96% of lithium while limiting iron leaching to between 0.027% (Li et al., 2017) and 5% (Ku and Chen, 2022). Organic acids, such as formic acid combined with hydrogen peroxide (Mahandra and Ghahreman, 2021), as well as acetic acid and hydrogen peroxide (Yang et al., 2018), have also shown promising results, achieving high selectivity and leaching efficiencies for lithium. Additionally, mechanochemical leaching with citric acid and hydrogen peroxide has proven effective, with leaching efficiencies of 99.35% for lithium and limited iron leaching of 3.86% (Li et al., 2019). An alternative approach utilizing CO_2 gas in the presence of an oxidizing solution has enabled the selective recovery of 90% of lithium as bicarbonate (Larouche et al., 2022).

Nonetheless, previous research focused on recycling of end-of-life LFP cathodes, which behave differently than production scraps during recycling, as observed in Chapter 5. This Chapter focus on the hydrometallurgical recycling of LFP production scraps throughout selective leaching processes, based on the use of sulfuric and citric acid combined with hydrogen peroxide, as a reducing agent.

7.2 Methodology

Production scraps from LFP cathodes manufacturing were provided by National Research and Development Institute for Cryogenic and Isotopic Technologies – ICSI Rm. Valcea, in Romania. The active material from the cathodes production scraps has been detached from current collectors, as described in Chapter 5. The LFP production scraps were thermally treated at 200°C for 30 minutes in a muffle furnace and ball milled for 5 minutes at 840 rpm. Finally, the powders were manually sieved in order to eliminate any particles exceeding the dimensions of 1 mm.

Selective leaching has been tested comparing sulfuric and citric acid, as leaching agents, combined with hydrogen peroxide as a reducing agent. Afterwards, the leaching residues have been separated by centrifugation and rinsed with deionized water before characterization. Whereas the leached lithium has been recovered by chemical precipitation.

Operative conditions (acid concentration, hydrogen peroxide concentration, temperature, time and solid/liquid ratio) applied during leaching have been reported in Table 7-1.

Table 7-1 Leaching conditions (concentration of leaching agents and hydrogen peroxide, temperature, contact time, S/L: solid to liquid ratio)

Acid	Concentration	Concentration H_2O_2	Temperature	Time	S/L ratio
Sulfuric acid	0.5 M	6 %vv.	25°C	1 h	50 g/L
Sulfuric acid	0.5 M	3 %vv.	25°C	1 h	50 g/L
Sulfuric acid	0.25 M	6 %vv.	25°C	1 h	50 g/L
Sulfuric acid	0.25 M	3 %vv.	25°C	1 h	50 g/L
Citric acid	0.5 M	6 %vv.	25°C	1 h	70 g/L
Citric acid	0.5 M	3 %vv.	25°C	1 h	70 g/L
Citric acid	0.25 M	6 %vv.	25°C	1 h	70 g/L
Citric acid	0.25 M	3 %vv.	25°C	1 h	70 g/L

Leaching tests were conducted for a duration of 1 hour at 25°C, utilizing sulfuric acid (0.25-0.5 M) in combination with hydrogen peroxide (3-6%vv.), as well as citric acid (0.25-0.5 M) in combination with hydrogen peroxide (3-6%vv.). The solid/liquid ratio employed during the leaching process was 50 g/l for the sulfuric acid and hydrogen peroxide combination, and 70 g/l for the citric acid and hydrogen peroxide combination. Leaching residues have been separated through centrifugation and rinsed with deionized water, before characterization. Afterwards, lithium has been recovered through chemical precipitation as Li_2CO_3, by adding 10 M NaOH and a stoichiometric amount of Na_2CO_3. The experimental activity described in this Chapter is shown in Figure 7-1

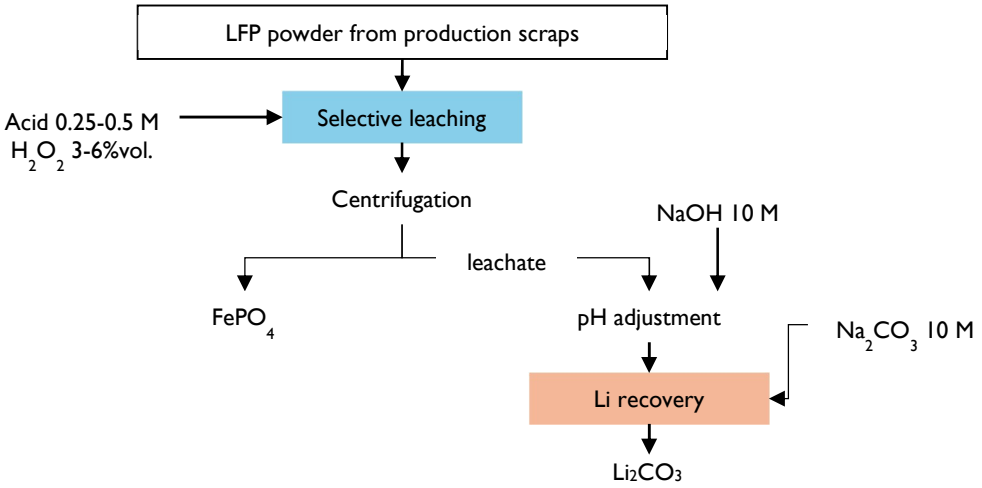


Figure 7-1 Outline of the experimental approach for selective leaching of production scraps cathodes

The following reagents were used: sulfuric acid (CAS: 7664-93-9, >96% purity, Carlo Erba Reagents); citric acid (CAS: 77-92-9, >99.5% purity, Sigma Aldrich); hydrogen peroxide (CAS: 7722-84-1, 30%v.v., Carlo Erba Reagents); sodium hydroxide (CAS: 1310-73-2, >98% purity, Honeywell/Fluka) and sodium carbonate (CAS: 497-19-8, >99.8% purity, Sharlab). Additionally, the equipment used were: AREX-6DIGITAL PRO heating magnetic stirrer and VTF EVO digital thermoregulatory, both from VELP Scientifica, for leaching and precipitation processes, a Hermle Labor Technik Z 206 A centrifuge for separation of the liquid solution, an ARGO LAB TCN 30 oven to dry the sample before characterization. Eventually, the samples were characterized with a Rigaku, NEX-DE XRF spectrometer, a PANanalytical X'Pert X-ray Diffraction (XRD) spectrometer and a GFA-EX7 FAA spectrometer. Besides the structure of leaching residues has been characterized by Field Emission Scanning Electron Microscopy (FESEM) with a Zeiss SUPRA TM 40 with Gemini column and Schottky field emission tip.

7.3 Results

7.3.1 Initial sample characterization

The X-ray diffraction (XRD) spectra of the LFP samples clearly indicated the presence of Li-Fe Phosphate, see Figure 7-2.

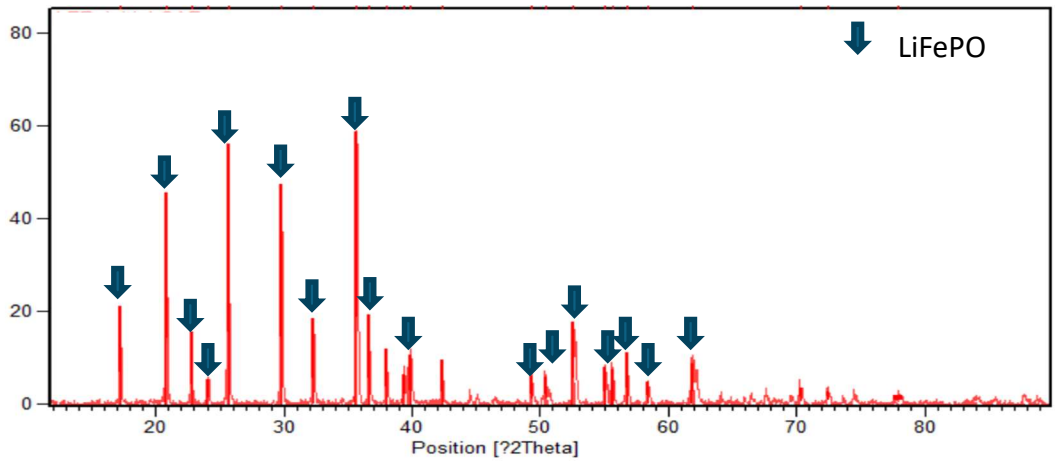


Figure 7-2 XRD spectrum of LFP cathodes' production scraps

The composition of the LFP production scraps used in this study was found to be approximately 2.1 ±0.1%wt. of Li, 29.5±4.5%wt. of Fe, and 16.4±2.5%wt. of P. Analysis of the samples also revealed the presence of impurities, with Al being present at a level of 610±157 mg/kg, Ca at 179±98 mg/kg, Cl at 346±19 mg/kg, Cr at 61±17 mg/kg, Co at 92±70 mg/kg, Ni at 20±4 mg/kg, S at 588±28 mg/kg, and V at 1766±124 mg/kg. Notably, Si, Cu, and Zn were not detected in the samples. It is worth mentioning that the composition

range of End-of-Life (EoL) LFP cathodes, as reported in the literature, fell within the following ranges: 1.6-4.4%wt. of Li, 26.43-35.4%wt. of Fe, and 14.1-19.63%wt. of P (Gaines et al., 2018; Yagci et al., 2021; L. Zhang et al., 2022).

7.3.2 Leaching process

Selective leaching results are shown in Figure 7-3 for leaching with sulfuric acid and hydrogen peroxide and Figure 7-4 for leaching with citric acid and hydrogen peroxide.

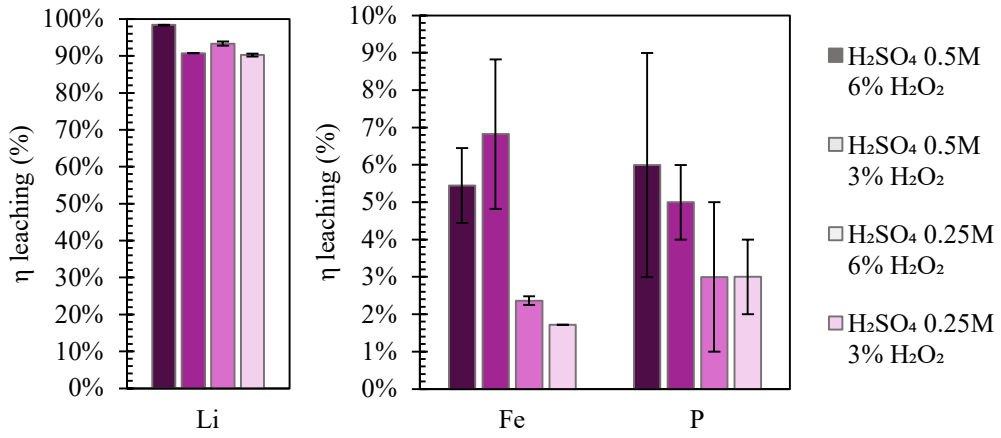


Figure 7-3 Leaching efficiency (%) of lithium, iron and phosphorous via selective leaching with sulfuric acid and hydrogen peroxide

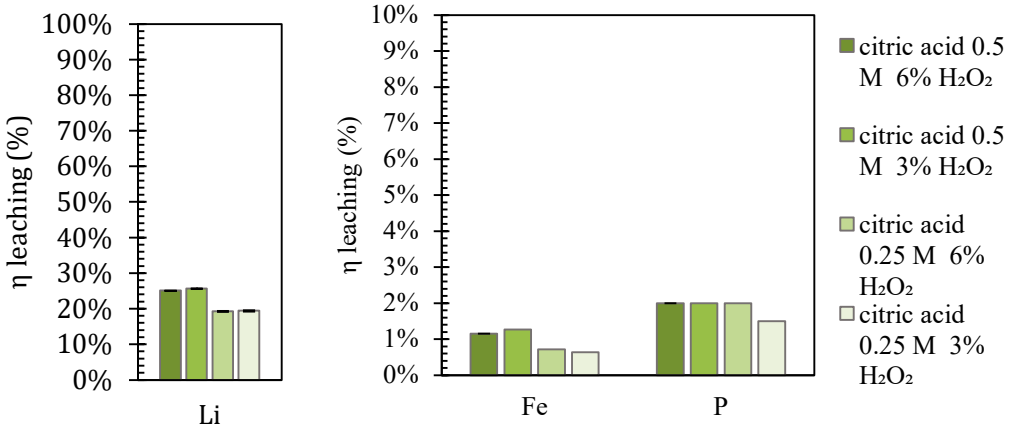


Figure 7-4 Leaching efficiency (%) of lithium, iron and phosphorous via selective leaching with citric acid and hydrogen peroxide

Results of selective leaching confirmed that the addition of hydrogen peroxide effectively hindered the solubilization of Fe and P in both leaching routes. However, it was observed that the leaching efficiency for Li was higher when sulfuric acid was employed compared to citric acid. Specifically, leaching with 0.5 M sulfuric acid and 6%vv. hydrogen peroxide

resulted in the solubilization of 98±1% of Li, 5±1% of Fe, and 6±3% of P. Similar results were obtained with varied concentrations of sulfuric acid and hydrogen peroxide, wherein 0.5 M sulfuric acid and 3%vv. hydrogen peroxide leached 91±2% of Li, 5±2% of Fe, and 7±2% of P. Additionally, 0.25 M sulfuric acid and 6%vv. hydrogen peroxide leached 93±1% of Li, 2±0.4% of Fe, and 3±2% of P, while 0.25 M sulfuric acid and 3%vv. hydrogen peroxide leached 90±3% of Li, 2±1% of Fe, and 3±1% of P. Lower leaching efficiency has been attained during the leaching process when employing citric acid and hydrogen peroxide as leaching agents. This can be observed from the following results. A 0.5 M citric acid solution and 6%vv. hydrogen peroxide resulted in the leaching of approximately 25±1% of Li, 1±0.4% of Fe, and 2±1% of P. Similarly, a 0.5 M citric acid solution and 3%vv. hydrogen peroxide resulted in the leaching of approximately 26±2% of Li, 1±0.6% of Fe, and 2±1% of P. However, it is important to note that a lower concentration of citric acid further reduced the leaching efficiency of Li. For instance, when a 0.25 M citric acid solution was used in conjunction with 6%vv. hydrogen peroxide, approximately 18±3% of Li, 1±0.4% of Fe, and 2±1% of P were leached. Similarly, when a 0.25 M citric acid solution was used in conjunction with 3%vv. hydrogen peroxide, approximately 19±2% of Li, 1±0.6% of Fe, and 2±1% of P were leached.

Fe and P leaching rate during the selective leaching tests increased with the concentration of sulfuric or citric acid, with a greater extent using sulfuric acid. Specifically, approximately 95±6% of Fe and 94±7% of P were recovered in the solid residues obtained from selective leaching with 0.5 M sulfuric acid and 6% hydrogen peroxide. Similarly, approximately 95±7% of Fe and 93±4% of P were recovered in the solid residues obtained from selective leaching with 0.5 M sulfuric acid and 3% hydrogen peroxide. However, when the concentration of sulfuric acid was reduced to 0.25 M, a higher recovery rate of approximately 98±3% of Fe and 96±4% of P was achieved in the solid residues obtained from selective leaching with 6%vv. hydrogen peroxide, and 97±2% of Fe and 98±5% of P with 3%vv. hydrogen peroxide.

Analysing the composition of the solid residues after leaching with citric acid and hydrogen peroxide, it was found that they consisted predominantly of Fe and P. Specifically, after leaching with 0.5 M citric acid and 6%vv. hydrogen peroxide, approximately 98±2% of Fe and 97±4% of P were present in the solid residues. Similarly, after leaching with 0.5 M citric acid and 3%vv. hydrogen peroxide, approximately 98±3% of Fe and 98±3% of P were present. Moreover, after leaching with 0.25 M citric acid and 6%vv. hydrogen peroxide, approximately 97±2% of Fe and 96±3% of P were found in the solid residues. Finally, after leaching with 0.25 M citric acid and 3%vv. hydrogen peroxide, approximately 98±6% of Fe and 95±2% of P were observed. To confirm the presence of Fe and P in the leaching residues, X-ray diffraction (XRD) analyses were conducted. The

results from these analyses validated that the Fe and P in the leaching residues were in the form of iron phosphate, see Figure 7-5 and Figure 7-6.

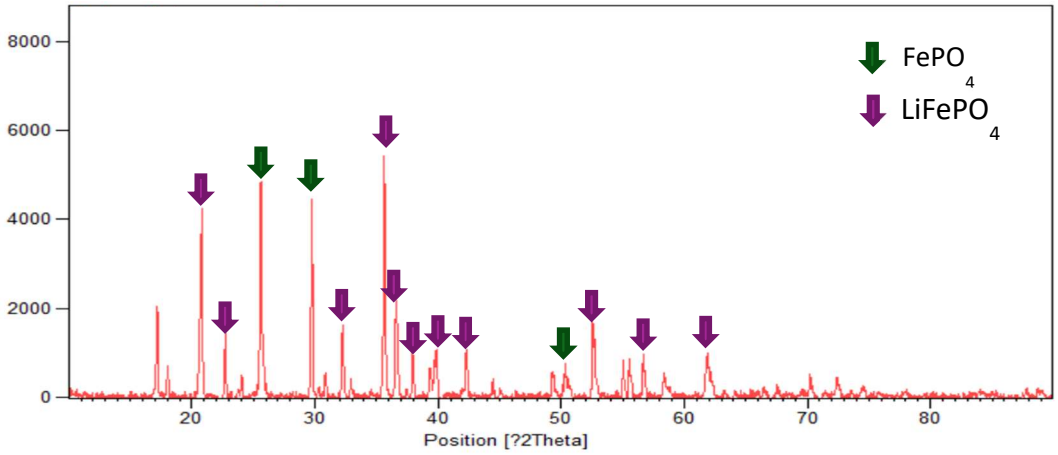


Figure 7-5 XRD spectra of solid residues after leaching with sulfuric acid and hydrogen peroxide

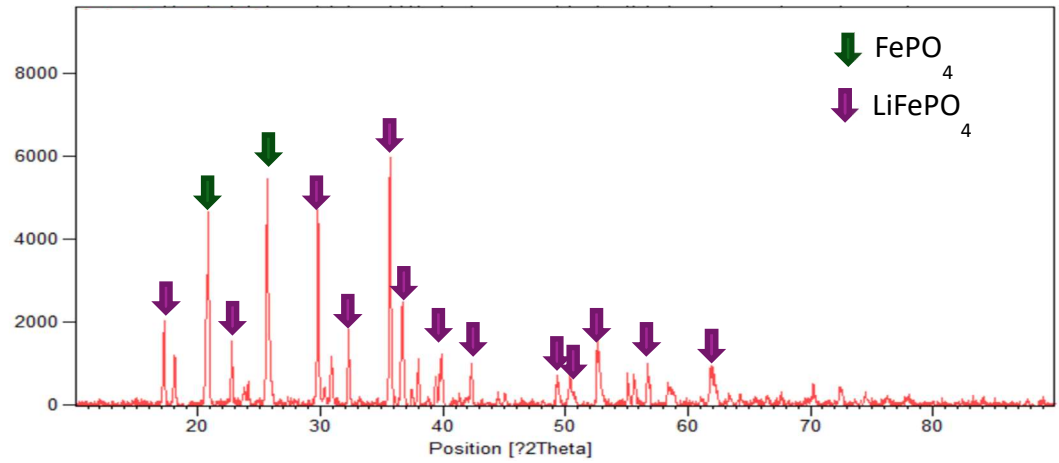


Figure 7-6 XRD spectra of solid residues after leaching with citric acid and hydrogen peroxide

Furthermore, the impurity contents in the leaching residues were examined. When sulfuric acid was used as the leaching agent, it was found that the main impurity present in the residues was sulfur. The concentration of sulfur in the residues varied depending on the leaching conditions. For instance, after leaching with 0.5 M sulfuric acid and 6%vv. hydrogen peroxide, the sulfur content was measured to be approximately 4363±581 mg/kg. Similarly, after leaching with 0.5 M sulfuric acid and 3%vv. hydrogen peroxide, the sulfur content increased to approximately 17,033±2,173 mg/kg. However, when the concentration of sulfuric acid was reduced to 0.25 M, the sulfur content in the residues decreased. Specifically, with 6%vv. hydrogen peroxide, the sulfur content was approximately

1363±835 mg/kg, and with 3%vv. hydrogen peroxide, the sulfur content was approximately 4586±966 mg/kg.

The concentration of sulfur was observed to be lower subsequent to the process of leaching with a sulfuric acid solution of 0.25 M. Specifically, the sulfur concentration was measured to be 1363±835 mg/kg when leached with 6%vv. hydrogen peroxide, and 4586±966 mg/kg when leached with 3%vv. hydrogen peroxide. Furthermore, when leached with citric acid, the sulfur concentration in the residues was found to be 537±29 mg/kg with a citric acid concentration of 0.5 M and 6%vv. hydrogen peroxide, 561±27 mg/kg with a citric acid concentration of 0.5 M and 3%vv. hydrogen peroxide, 640±38 mg/kg with a citric acid concentration of 0.25 M and 6%vv. hydrogen peroxide, and 545±37 mg/kg with a citric acid concentration of 0.25 M and 3%vv. hydrogen peroxide. It is worth noting that the concentrations of other impurities, including Al, Ca, Cl, Cr, Co, Ni, and V, were all found to be within the reported range for the LFP sample, as mentioned in section 3.1.

In order to gain further insights into the morphology of the leaching residues, a comparison was made with the original LFP sample using FESEM characterization, see Figure 7-7. The residues recovered subsequent to sulfuric acid leaching exhibited a wider particle size distribution compared to the initial sample and the residues obtained after citric acid leaching. Moreover, larger crystals were found to be dispersed throughout the finer grains. On the other hand, the $FePO_4$ powders recovered after leaching with citric acid displayed particles of inhomogeneous sizes, typically on the order of hundreds of nanometers. However, it is worth mentioning that this particle size distribution is consistent with that of the initial sample. Furthermore, the morphology of the leaching residues appeared to maintain the same level of crystallinity observed in the initial sample.

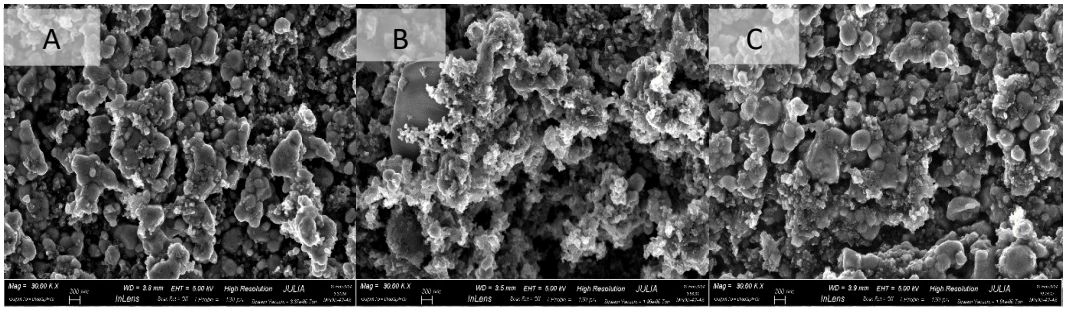


Figure 7-7 FESEM images of (A) initial LFP powder, (B) residues after sulfuric acid leaching and (C) after citric acid leaching

7.3.3 Lithium recovery

The recovery of lithium was achieved through a chemical precipitation process conducted at a temperature of 95°C and a pH of 12. This precipitation process involved the addition of a stoichiometric amount of Sodium carbonate. The overall efficiency of lithium recovery

was determined to be 28.6±4% when leached with a sulfuric acid concentration of 0.5 M and 6%vv. hydrogen peroxide, 25±2% when leached with a sulfuric acid concentration of 0.5 M and 3%vv. hydrogen peroxide, 26±1% when leached with a sulfuric acid concentration of 0.25 M and 6%vv. hydrogen peroxide, and 25±6% when leached with a sulfuric acid concentration of 0.5 M and 6%vv. hydrogen peroxide. Regrettably, the chemical precipitation process following citric acid leaching did not yield sufficient lithium recovery to proceed with the subsequent characterization of the samples. Similar to the leaching residues, the precipitates obtained from sulfuric acid leaching contained a higher concentration of impurities. Specifically, the concentration of sulfur in these precipitates was measured to be 1770±233 mg/kg when leached with a sulfuric acid concentration of 0.5 M and 6%vv. hydrogen peroxide, 5250±41 mg/kg when leached with a sulfuric acid concentration of 0.5 M and 3%vv. hydrogen peroxide, 3380±163 mg/kg when leached with a sulfuric acid concentration of 0.25 M and 6%vv. hydrogen peroxide, and 9393±775 mg/kg when leached with a sulfuric acid concentration of 0.25 M and 3%vv. hydrogen peroxide. Further XRD analyses revealed the presence of sodium sulfate and lithium sodium sulfate in these precipitates, see Figure 7-8.

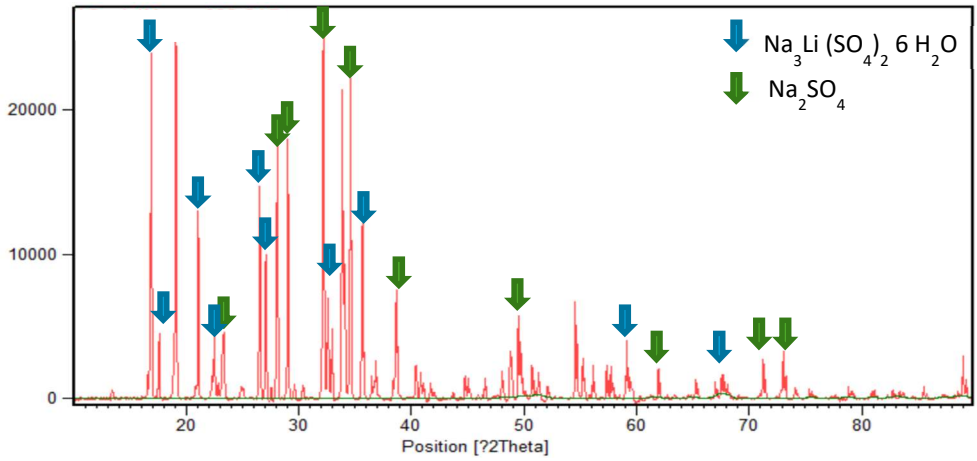


Figure 7-8 XRD spectra of precipitates obtained at pH 12 from selective leaching with sulfuric acid and hydrogen peroxide

7.4 Discussion

The production rates of batteries continue to increase; hence the generation of production scraps is expected to grow accordingly. Recovering materials from production scraps offers several advantages. Firstly, the pre-treatment processes are much simpler compared to end-of-life cathodes, as there is no need for discharge and dismantling, and the scraps are already sorted according to specific chemistries. Secondly, the morphological and chemical structures of production scraps closely resemble those of pristine batteries. However, the

presence of binders makes the recycling of production scraps more challenging compared to end-of-life electrodes. Thus, further research is needed to address the unique issues associated with recycling production scraps and fully harness their potential for sustainable materials recovery.

The results presented in this Chapter suggest that the combination sulfuric acid and hydrogen peroxide, at a mild concentration and at room temperature, can effectively and selectively extract lithium from LFP production scraps. Additionally, the results obtained from this study also confirmed the role of hydrogen peroxide in the process of selective leaching. It was observed that hydrogen peroxide acts as an oxidizing agent for iron, which is then oxidized to form Fe (III), subsequently resulting in the formation of phosphate salts that are not soluble at room temperature. The chemical reaction taking place during selective leaching with sulfuric acid and hydrogen peroxide is shown in equation 1.

(Eq. 1) $2\ LiFePO_4 + H_2SO_4 + H_2O_2 \rightarrow 2\ FePO_4 + Li_2SO_4 + 2H_2O$

In comparison to sulfuric acid, citric acid and hydrogen peroxide were found to be less effective in selectively leaching lithium from LFP production scraps. This apparent contradiction to the results presented in Chapter 6 on the selective leaching applied to end-of-life LFP cathodes, where 87±2% of lithium was leached by 0.25 M citric acid and 6%vv. hydrogen peroxide, can be attributed to the fact that pristine electrodes do not experience the same loss of structural and chemical integrity over time as end-of-life electrodes. Therefore, recycling pristine electrodes poses a greater challenge. In fact, citric acid was found to be ineffective in selectively leaching lithium from LFP production scraps. On the other hand, sulfuric acid was identified as a more viable alternative due to its higher leaching efficiency and lower cost when compared to citric acid. It is important to note that the products recovered through sulfuric acid leaching exhibited higher contamination of sulfur.

7.5 Conclusions

This Chapter presented the comparison of different selective leaching methods to recycle LFP production scraps. The combination of sulfuric acid and citric acid with hydrogen peroxide was compared at different concentrations. It was observed that sulfuric acid provided a higher leaching efficiency for lithium, ranging from 90±3% to 98±1%, whereas citric acid could not surpass a leaching efficiency of 26±2%. The optimal recycling process for LFP production scraps involved leaching with 0.25 M sulfuric acid and 3%vv. hydrogen peroxide at a temperature of 25°C for a duration of 1 hour. This particular condition allowed for the leaching of 90±3% of lithium and the recovery of 97±2% of iron and 98±5% of

phosphorus in the leaching residues. However, it should be noted that the selective leaching process with sulfuric acid had its drawbacks, including the limited recovery of lithium and the presence of sulfur impurities in the leaching residues and precipitates.

In conclusion, a novel method for the recovery of lithium, iron, and phosphorus from LFP production scraps, which can be considered as an untapped resource for the retrieval of materials for battery manufacturing. However, further research is required to optimize lithium recovery and minimize impurities in the recovered materials.

Chapter 8

Economic analysis of lithium iron phosphate cathodes recycling

This chapter regards the environmental and economic analysis of the recycling processes tested on end-of-life and production scraps LFP cathodes. The environmental and economic analysis are based on the results of the experimental activities described through Chapters 5 to 7. The content of this Chapter has been presented in three research papers: "*Low-cost and environmentally friendly physic-mechanical pre-treatments to recycle lithium iron phosphate cathodes*" authored by **Martina Bruno** and Professor Silvia Fiore and published in Journal of Environmental Chemical Engineering (Bruno and Fiore, 2024b); "*Closed-loop recycling of Lithium Iron Phosphate cathodic powders via citric acid leaching*" authored by **Martina Bruno**, Professor Carlotta Francia and Professor Silvia Fiore and published in Environmental Science and Pollution Research (Bruno et al., 2024) and "*Selective leaching for the recycling of lithium, iron and phosphorous from lithium-ion battery cathodes' production scraps*" authored by **Martina Bruno**, Professor Julia Amici and Professor Silvia Fiore (under review).

8.1 Introduction

The importance of LIBs technology to achieve the transition towards cleaner energy and the decarbonification of transport system, boosted their market prominence (T. Zhao et al., 2024). Global revenues for LIBs market are expected to reach 91.9 billion US dollars by 2026 (Statista, 2023a), subsequently the market size of LIBs recycling is foreseen to increased up to 11 billion US dollars in the same year (Statista, 2023b). LIBs recycling has been proven to play a crucial role both in providing raw materials for new LIBs manufacturing, see Chapter 2, and to reduce the environmental impacts associated by mining activities for primary raw materials supply, see Chapter 3.

The economic balance of LIBs recycling has traditionally been sustained by the potential of cobalt recovery (Wang et al., 2014). Cobalt is deemed a costly resource, prompting manufacturers to shift towards more cost-effective cathode materials in a bid to curtail battery production expenses (International Energy Agency, 2023). Thus, LIBs market is starting to transition towards more economical alternatives. LFP and LMO are anticipated to emerge as the forthcoming generation of LIB technologies (Ritchie and Howard, 2006). This transition from pricier cathode materials to more economical alternatives diminishes the financial motivation for recycling batteries at the end of their lifespan (T. Zhao et al., 2024).

The necessity of developing of novel recycle technologies aimed at reducing chemical reagents consume and energy demand has been severely addressed by previous research (D. Song et al., 2023; Woeste et al., 2024). Simplifying recycling processes and reducing their economic costs is particularly essential for LFP batteries, which do not contain economically valuable metals, such as cobalt, nickel and manganese, as stated in Chapter 3.

Nonetheless, the analysis of economic aspects entailed by LFP recycling has not yet been extensively researched. Previous studies based their models on secondary data from external sources and when primary data are collected during experimental activities there are numerous inconsistencies in the results, due to differences in functional units, currencies and costs parameters, e.g. reagents, energy, labour and general expenses (Hu et al., 2024; Yadav et al., 2020; T. Yang et al., 2023). Besides, the boundary of the considered recycling process is variable between different studies: most of them focused exclusively on leaching during hydrometallurgical recycling (Jha et al., 2013; Jin et al., 2023).

This Chapter presents the results of environmental and economic analysis associated with the recycling processes proposed for LFP production scraps and end-of-life cathodes, considering the results of pre-treatments and hydrometallurgical recycling from Chapters 5 to 7.

8.2 Methodology

The economic analysis presented in this Chapter were based on primary data collected during the experimental activity: they should be considered purely preliminary and aimed at comparing the recycling processes. The economic analysis presented in this Chapter relies on direct measurements of primary costs for the experimental processes presented in Chapters 5, 6 and 7. The costs due to reagents, water and energy have been considered by measuring the amount of reagents and water used with a precision scale and the amount of energy consumed with a PM10 Maxcio power meter.

To allow comparison among results, based on various equipment at lab scale, all experimental results were scaled up referring to a functional unit equal to 1 kg of LFP cathodes processed for pre-treatments and 1 kg of LFP cathodic powders for hydrometallurgical recycling. Besides, the scale-up of the processes consumption of energy and water considered the processing capacity of the equipment applied, which amounts to 1.8 kg of samples (corresponding to 18 l of water) for the ultrasound bath, 50 g of samples for the muffle furnace and 5 g for the ball mill.

The economic analysis was based on the specific energy demand, on the consumption of deionised water and reagents. The cost of energy has been considered as 0.1986 €/kWh, which is the average European price of electricity for non-households consumers (Eurostat, 2023), while the costs of reagents (deionized water, citric acid, sulfuric acid, hydrogen peroxide, sodium hydroxide and sodium carbonate have been retrieved from Ecoinvent database (Ecoinvent, 2023).

8.3 Results

8.3.1 Physical mechanical detachment

The economic analysis of physic-mechanical pre-treatments to detach cathodes active materials from current collectors was based on energy and water consumption, see Figure 8-1Figure 8-1.

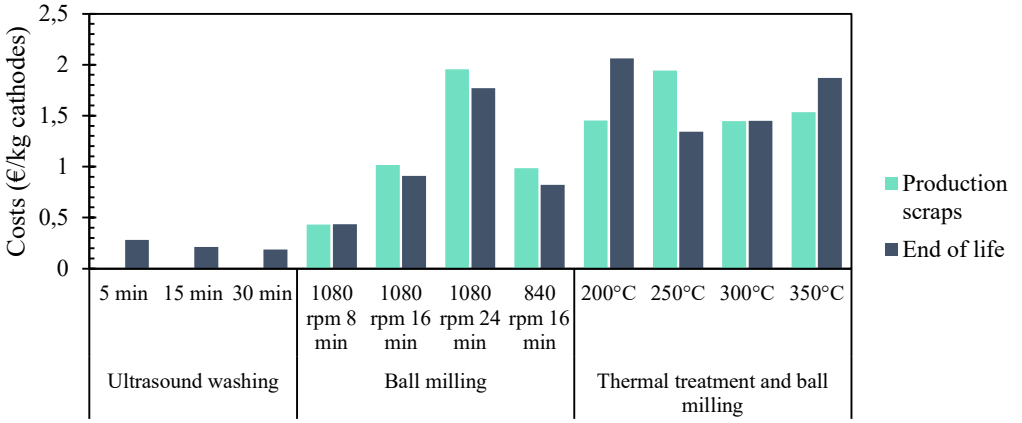


Figure 8-1 Operative costs of pre-treatments for 1 kg of LFP cathodes

The most economically convenient detachment method has been identified in ultrasound washing, which costed 0.28±0.02 €/kg of detached cathode material after 5 minutes, 0.21±0.02 €/kg of detached cathode material after 15 minutes, 0.19±0.02 €/kg of detached cathode material after 30 minutes for end-of-life cathodes. Higher costs are entailed by ball milling, ranging between 0.43±0.05 €/kg for production scraps and 0.44±0.06 €/kg for end-of-life cathodes after 8 minutes at 1080 rpm and1.95±0.18 €/kg for production scraps and 1.77±0.13 €/kg for end-of-life cathodes after 24 minutes at 1080 rpm.

The most expensive detachment method corresponds to thermal treatment followed by ball milling, due to its high energy demand, see Figure 5-11. The cost of this process was: 21.45±0.24 €/kg of detached cathode material at 200°C, 1.94±0.18 €/kg at 250°C, 1.45±0.18 €/kg at 300°C and 1.53±0.18 €/kg at 350°C for production scraps and 2.06±0.21 €/kg at 200°C, 1.34±0.11 €/kg at 250°C, 1.45±0.21 €/kg at 300°C and 1.87±0.10 €/kg at 350°C for end-of-life cathodes. Market value of LFP cathodes material is about 20 €/kg (Ecoinvent, 2023), thereby the cost associated water and energy consumption during the proposed pre-treatments range between 1% and 10% of the potential revenues from the recovery of cathodic materials.

8.3.2 Hydrometallurgical recycling of end-of-life cathodes

The hydrometallurgical recycling of end-of-life LFP cathodes have been performed comparing conventional and selective leaching. Conventional leaching required a single leaching step at 40°C, three precipitation and six centrifugation steps to retrieve the precipitates. On the other hand, selective leaching required a single leaching step at 25°C, one precipitation, and two centrifugations. Both conventional and selective leaching methods required two precipitation steps (one at pH 12 and room temperature, and the other

at 95°C) were necessary to recover the lithium-rich precipitates. The costs associated with hydrometallurgical recycling of end-of-life cathodes are shown in Figure 8-2.

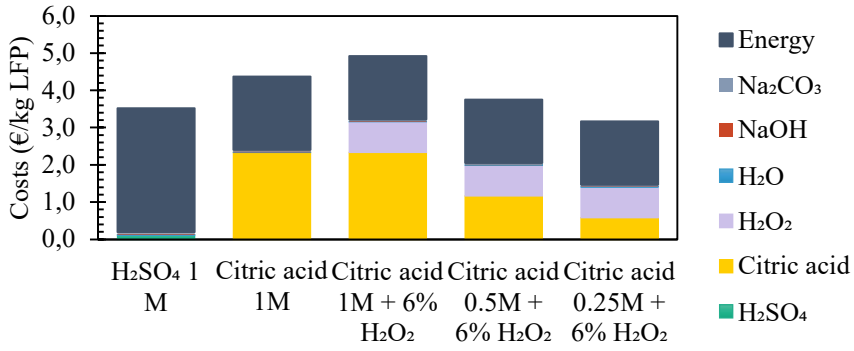


Figure 8-2 Operative costs of the considered routes applied to recycling of 1 kg of end-of-life LFP cathodic material

The total operational expenses associated with the comparison of recycling pathways, see Figure 8-2, amounted to 3.52 € per kilogram of recycled LFP for 1 M sulfuric acid leaching. In contrast, the cost was 4.37 € per kilogram for 1 M citric acid leaching without hydrogen peroxide. By decreasing the citric acid concentration and incorporating hydrogen peroxide, the expenses of selective leaching were reduced. For instance, the cost decreased from 4.93 € per kilogram of recycled LFP for 1 M, to 3.76 € for 0.5 M, and 3.17 € for 0.25 M. The costliest reagents were hydrogen peroxide (0.82 € per kilogram of recycled LFP) and citric acid (2.34 € per kilogram for 1 M, 1.17 € for 0.5 M, and 0.59 € for 0.25 M). The process of lithium recovery exhibited the highest energy demand due to the elevated temperatures required for precipitating Li_2CO_3, amounting to 1.59 € per kilogram. Overall, the expenses associated with the sulfuric acid route were primarily (94%) attributed to energy demand, while chemical reagents such as H_2SO_4, NaOH, and Na_2CO_3 accounted for 0.20 € per kilogram of recycled LFP. In the case of the 1 M Citric acid route, the costs were evenly split between chemicals (55%) and energy demand (45%). However, with the addition of hydrogen peroxide and a reduction in citric acid concentration to 0.25 M, there was a shift in the cost distribution, with 46% attributed to chemicals and 54% to energy demand.

8.3.3 Hydrometallurgical recycling of production scraps

Hydrometallurgical recycling of production scraps cathodes has been tested comparing different operative conditions for selective leaching of lithium from the cathodic powder. The economic evaluation of varying experimental conditions, see Figure 8-3, revealed that the operational expenses ranged from 2.24 €/kg (0.25 M citric acid and 3%vv. hydrogen peroxide) to 2.98 €/kg (0.5 M sulfuric acid and 6%vv. hydrogen peroxide).

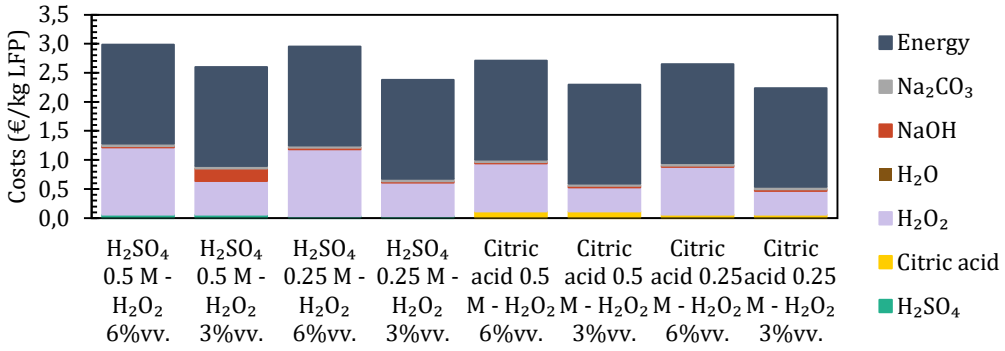


Figure 8-3 Operative costs of the considered routes applied to recycling of 1 kg of LFP cathodic material from production scraps

The economic boundaries of this analysis are primarily defined by the leaching and precipitation procedures involved. Energy consumption costs were found to be relatively similar across all pathways, with the priciest recycling phase being the Li chemical precipitation process demanding a temperature of 95°C. It is worth noting that the final step of Li precipitation has consistently emerged as the primary bottleneck within the recycling framework due to its substantial energy requirements. The primary factor distinguishing these processes lies in the reagent costs, particularly hydrogen peroxide, where the process cost stood at 2.24 €/kg for a hydrogen peroxide concentration of 3%vv. and ranged between 2.50 €/kg and 3.00 €/kg with 6%vv. hydrogen peroxide.

8.4 Discussion

Economic analysis of different pre-treatment strategies outlined how ultrasound washing displays the lowest costs, due to the limited energy demand. However, from a technical perspective, ultrasound washing had the lowest recovery efficiency among other proposed treatments. Thereby, more effort should be directed towards the optimization of this technology, which shows the greatest potential to reduce operative costs of pre-treatments for LFP recycling. On the other hand, the best performing processes costed 1.34 €/kg of cathodes for end-of-life cathodes and 1.45 €/kg of cathodes for production scraps.

Considering hydrometallurgical recycling, it is worth noting that the concentration of hydrogen peroxide plays a significant role in the overall cost of the leaching process. Previous research has proposed that a concentration of 6%vv. is optimal when organic acids are present. However, the results presented in Chapter 6 have demonstrated that reducing the concentration of hydrogen peroxide from 6%vv. to 3%vv. did not have any impact on the efficiency of leaching lithium, iron, and phosphorus. Therefore, it can be concluded that diminishing the concentration of sulfuric acid, citric acid, and hydrogen peroxide did not result in a decrease in leaching efficiency. The operational costs of the proposed recycling

processes ranged up to 3.00 €/kg, but these costs were reduced to 3.17 €/kg for end-of-life cathodes and to 2.24 €/kg for production scraps with the optimal leaching conditions.

Overall, the operative costs of recycling, considering pre-treatment for detachment of cathodic materials from current collectors and hydrometallurgical recycling, amounted to 4.24 €/kg for end-of-life cathodes and 3.40 €/kg for production scraps. The results obtained have been compared with the economic analysis reported by previous studies on different methods for LFP recycling, see Table 8-1.

Table 8-1 Results of economic analysis from literature overview on LFP recycling

Functional unit	Process	Considered costs									Costs	Income	Profit	Reference
		Raw materials	Reagents	Energy	Labour	Equipment	Waste management	Fixed charges	Plant overhead	General Expenses				
1 kg of LFP (input)	Selective leaching	x	x	x	x						15.98 $	17.79 $	1.82 $	(Zhou et al., 2023a)
	Selective leaching	x	x	x	x						8.27 $	9.98 $	1.71 $	(Zhou et al., 2023b)
	Mechanochemical with Na-citrate	x	x	x							32.8 $	44.7 $	11.9 $	(Q. Zhang et al., 2023b)
1 kg of cell (input)	Electrolysis		x	x									25.8 $	(J. Zhao et al., 2024)
1 kg of LFP battery (input)	Leaching		x					x	x	x	1.65 $	5.97 $	4.32 $	(Jin et al., 2023)
	Leaching with H_2SO_4 and H_2O_2		x	x	x	x		x	x	x	2.86 $	5.85 $	2.99 $	(C. Xu et al., 2023)
	Leaching with H_2SO_4 and H_2O_2	x	x	x							15.81 $	19.84 $	4.03 $	(Y. Yang et al., 2023)
	H_2O_2 method		x					x	x	x	1.25 $	8.98 $	7.73 $	(Jin et al., 2023)
	Leaching with CO_2 and H_2O_2		x	x	x	x		x	x	x	2.38 $	6.13 $	3.75 $	(C. Xu et al., 2023)
	Leaching with CO_2 and O_2		x	x	x	x		x	x	x	2.09 $	6.13 $	4.04 $	(C. Xu et al., 2023)
	Self-catalytic air pressure leaching		x					x	x	x	1.11 $	9.09 $	7.98 $	(Jin et al., 2023)
	Mechanochemical	x	x	x							1.85 $	6.62 $	4.768	(G. Liu et al., 2023)
1 t of LFP (input)	Leaching with H_2SO_4	x	x	x							1,418 $	2,716 $	1,297 $	(Song et al., 2021)
	Selective leaching	x	x								26,49 $	40,58 $	7,46 $	(Hu et al., 2022)

	Selective leaching	x	x							35,700 ¥	54,520 ¥	18,820 ¥	(S. Song et al., 2023)
	Selective leaching	x	x	x						1962.4 $	1242.4 $	719.6 $	(Hu et al., 2024)
	Selective air oxidation leaching	x	x	x	x	x				2,051 $	4,081 $	2,030 $	(Jin et al., 2022)
	Mechanochemical	x	x	x						1,580 $	6,539 $	4,959 $	(Wu et al., 2023)
	Electrolysis	x	x	x						2225 $	9148 $	6923 $	(Yang et al., 2024)
1 kg of recovered	Leaching		x	x						18.60 $			(Du et al., 2024)
	Leaching with citric acid and MSA		x	x						4.35 $			(Kim et al., 2023)
	Selective pressure leaching with H_2SO_4		x	x						17.36 $			(Du et al., 2024)
1 kg of $FePO_4$ leaching residues (input)	Ultrasonic centrifugation with H_3PO_4		x	x			x			1.25 $	1.80 $	0.55 $	(Han et al., 2023)
100 kWh	Leaching with methanesulfonic acid (MSA), p-toluenesulfonic acid (Ts OH)		x	x	x	x	x		x	970 $	1,129 $	159 $	(Yadav et al., 2020)

Previous research has examined the financial implications and potential profits associated with recycling LFP batteries, with findings being standardized into a common unit of measurement (€/kg LFP). The average cost of LFP recycling, as reported in the literature, is approximately 15.5±22.4 €/kg. The significant variance in these findings can be attributed to the diverse range of cost elements taken into account by each study, including raw materials, reagents, energy usage, labor, equipment expenses, overhead costs, and various process stages. Notably, all the studies considered the expenses related to reagents, while nearly 80% accounted for energy consumption costs, and 50% factored in the value of spent LFP batteries as raw materials for the recycling process. Furthermore, less than 30% of the studies included supplementary costs like labor expenses, equipment maintenance, plant overheads, and general operational costs, with only 8% focusing on waste management expenditures. Additionally, less than 38% of the research incorporated the expenses linked to pre-treatment or final regeneration of the recovered products, and merely 17% analyzed both of these stages.

The economic analysis presented in this Chapter focused exclusively on the process costs attributed to reagents and energy, which were directly quantified during experimental tests to enable a comparative analysis of different operational scenarios. However, determining the economic viability of the process necessitates a broader perspective incorporating additional cost elements such as labor expenses, management of waste streams, plant upkeep, and the amortization of initial capital investments. Thereby the results presented should not be considered as an evaluation of economic viability of the processes as much as comparison of different recycling strategies from an economic point of view, beyond technical performances of the processes.

8.5 Conclusions

This Chapter reported the results of the economic analysis applied to the recycling processes presented in the previous Chapters (5-7). Economic costs associated with physic-mechanical pre-treatments are strongly affected by the necessity of thermal treatments, which is highly energy intensive.

Furthermore, comparing conventional and selective leaching, the main drivers behind increase of economic costs were reagents costs for selective leaching and energy consumption for conventional leaching. Selective leaching requires citric acid and hydrogen peroxide which are more expensive, however the limited energy demand, especially since leaching is performed at room temperature, the reduced number of steps to precipitate the desired precursors, lower down process costs. As a results, selective leaching

was found to be an efficient method for LFP recycling, increasing pureness of recycling products and limiting operative costs.

On the other hand, sulfuric acid could be effectively applied for selective leaching of lithium from production scraps, according to the results presented in Chapter 7. This way the economic cost associated with hydrometallurgical recycling could be further reduced. Eventually, the recycling processes evaluated in this Thesis require operative costs below the average of results (15.5 €/kg) from previous studies on LFP recycling, both for production scraps and end-of-life cathodes.

Conclusions

This Thesis regards the recycling of LIBs, an emerging technology utilized for energy storage that has a wide range of applications, including electric vehicles and portable electronic devices such as laptops, smartphones, and tablets. LIBs play a crucial role in the transition to clean energy and the decarbonization of transportation and energy systems. However, Li-ion batteries are composed of several economically valuable elements and critical raw materials, which often imply mining activities associated with elevated costs and environmental impacts. The demand of raw materials for LIBs production is expected to increase dramatically in the near future, and recycling processes for the recovery of secondary raw materials are essential to ensure the LIBs supply chain and limit the environmental impacts and costs associated with the extraction of raw materials.

LIBs recycling requires in a series of treatments involving discharge of residual voltage present in end-of-life batteries, dismantling of batteries and cells casing, and thermo-chemical processes to remove residual electrolyte solutions and organic binders from the electrodes; thermo-mechanical processes to concentrate the active materials for further pyrometallurgical or hydrometallurgical recycling processes. Pyrometallurgy is a well-established technology to recover valuable metals, e.g. cobalt, manganese, and nickel, as alloys. Despite its effectiveness, this technology is faced with challenges such as high energy requirements, the release of gaseous pollutants, and the unsatisfactory efficiency in lithium recovery. Conversely, hydrometallurgy is a technology to recover target metals, including lithium, through acid leaching and consequent separation processes.

This Thesis analysed the circular economy perspectives for LIBs applied in electric vehicles in Europe. The materials flow associated with these LIBs identified the inadequacy of the European recycling infrastructure, both in collecting the expected waste stream of end-of-life LIBs and in providing the required secondary raw materials to supply the manufacturing of future LIBs, hence closing the circularity loop. The inventory of the European LIBs recycling plants performed in this Thesis resulted in an overall capacity around 55 kt/y, with the majority of recycling facilities performing pyrometallurgical processes (55% of recycling capacity) or a combination of pyrometallurgical and hydrometallurgical processes (21% of recycling capacity). Nonetheless, the current size of European LIBs recycling infrastructure will be defective in processing the foreseen waste stream coming by end-of-life LIBs by 2030, leaving untreated an 80% surplus.

The importance of improving the European LIBs recycling infrastructure has been highlighted also by the results of the environmental analysis of full-scale recycling processes performed in this Thesis. Avoiding the mining of primary minerals for metals

extraction will pose an environmental benefit on GHGs emissions associated with LIBs recycling processes. The foreseen materials requirements for LIBs supply chain to meet electric vehicles demand in 2030 will amount to almost 100 kt, and the recycled metals provided by the European LIBs recycling facilities could provide only 2%-wt of the demand. Nonetheless, this limited replacement rate of secondary raw materials could reduce the net Carbon footprint of LIBs recycling processes by 28%. Further improvements could be sustained reducing the environmental impacts of currently applied recycling processes, consistently with the trends emerged in the literature review.

Moreover, considering the economic analysis of LIBs recycling, hydrometallurgy will entail the best trade-off and will pose a strategic recycling route for the design of future recycling facilities. The combination of pyrometallurgical and hydrometallurgical technologies yields the highest revenues, nonetheless the elevated operative costs entailed by conventional pyrometallurgy hinder the economic balance, and hydrometallurgy emerged as the optimal solution for battery recycling in terms of cost-benefit analysis. Thus, given the acknowledged insufficiency of the current recycling infrastructure in Europe, hydrometallurgy will establish itself as a strategic solution for the design of future LIBs recycling facilities.

The experimental activities addressed the recycling of lithium batteries to tackle the bottlenecks of currently applied technologies and reduce their prices and environmental impacts. The first aspect studied was the electrochemical discharge of LIBs cells adopting non-corrosive solutions made of carbonates, as corrosion and hazardous gaseous emissions are the key issues in actual discharge operations. Gaseous emissions and the pH of the saline solutions have been monitored to better understand the LIBs discharge mechanism. The pH trend followed the curve of H_2 emissions rate during discharge and then slowly decreased matching the discharge rate of the battery. The obtained results confirmed the efficiency of the proposed discharging solutions and proved that pH could be monitored continuously, providing a back-up system for emissions control and avoiding the need of removing the batteries from the discharge solutions to measure the residual voltage.

Afterwards, different recycling processes have been studied to recover LFP cathodic powders from end-of-life cathodes and production scraps. Physic-mechanical pre-treatments have been explored and optimized to detach LFP active materials from the current collectors. Mechanical pre-treatments performed better on end-of-life samples than on production scraps samples, both in terms of separation rate and material loss. Ultrasound washing was unsuccessful for the detachment of cathode material from production scraps samples. The highest separation efficiencies were obtained by low intensity ball milling for a short time preceded by thermal treatment. These results provide a simple and “chemicals free” detachment process, able to decrease the environmental impacts associated with pre-

treatments by one order of magnitude. Nonetheless, the application of ultrasound washing merits additional research to further reduce the energy demand required by pre-treatments and subsequently the associated environmental impacts.

Then, the recycling of end-of-life LFP cathodes has been studied comparing conventional hydrometallurgy with a novel selective leaching method. Hydrometallurgy was performed comparing one inorganic acid, sulfuric acid, with an organic acid, citric acid, and they provided comparable recycling efficiency. On the other hand, selective leaching was found to be a promising alternative to recover all components of LFP active material, in form of iron phosphate and lithium phosphate and carbonate with higher efficiency and lower energy demand compared to hydrometallurgy based on sulfuric acid.

Thereby, the application of selective leaching for the recycling of LFP cathodes production scraps was analysed, comparing inorganic and organic acids combined with hydrogen peroxide. Similarly to the remarks made after exploring physic-mechanical pre-treatments, the recycling of LFP production scraps was less efficient compared to end-of-life cathodes. Indeed, citric acid proved ineffective for selective leaching of LFP cathodes production scraps, and future research should focus on tuning the operative parameters to improve this process based on the use of a more environmentally friendly organic acid.

Finally, comparing the operational economic costs associated with the proposed recycling methods for LFP cathodes (end-of-life and production scraps), they are three times lower than the average costs reported by previous studies on the recycling of LFP cathodes. This result is justified by the shorter processing times and lower concentrations of leaching agents, required by selective leaching. These aspects limit waste generation and reduce the overall environmental impacts of hydrometallurgical recycling. Besides, they have been proved to play a key role in reducing the operative costs of LIBs recycling, which is essential for LFP cathodes, as their economic value does not sustain the cost of recycling processes currently applied at industrial scale.

In conclusion, this Thesis provides an extensive circularity analysis of LIBs management by examining the full-scale infrastructure of materials supply chain and recycling in the European context, considering both environmental and economic aspects related to the associated material flows. Then, the experimental activity focused on waste LFP cathodes (production scraps and end-of-life), as their recycling is not economically profitable according to state-of-the-art recycling technologies. The experimental activity delivered novel “green” processes to limit the environmental and economic impacts of LIBs recycling, considering a wide approach starting from electrochemical discharge, and also involving pre-treatments and hydrometallurgical recycling.

References

1. Abe, Y., Watanabe, R., Yodose, T., Kumagai, S., 2024. Cathode active materials using rare metals recovered from waste lithium-ion batteries: A review. Heliyon. https://doi.org/10.1016/j.heliyon.2024.e28145
2. Aboulaich, A., Yaden, A., Elhalya, N., Tayoury, M., Aqil, M., Hdidou, L., Dahbi, M., Alami, J., 2022. Synthesis and Recyclability of Sheet-like Cobalt Carbonate Recovered from Spent Li-Ion Batteries Using a Simple Hydrometallurgy Process. Sustain. 14. https://doi.org/10.3390/su14052552
3. Agusdinata, D.B., Liu, W., Eakin, H., Romero, H., 2018. Socio-environmental impacts of lithium mineral extraction: Towards a research agenda. Environ. Res. Lett. 13. https://doi.org/10.1088/1748-9326/aae9b1
4. Ahmadi, L., Young, S.B., Fowler, M., Fraser, R.A., Achachlouei, M.A., 2017. A cascaded life cycle: reuse of electric vehicle lithium-ion battery packs in energy storage systems. Int. J. Life Cycle Assess. 22, 111–124. https://doi.org/10.1007/s11367-015-0959-7
5. Ahuis, M., Aluzoun, A., Keppeler, M., Melzig, S., Kwade, A., 2024. Direct recycling of lithium-ion battery production scrap – Solvent-based recovery and reuse of anode and cathode coating materials. J. Power Sources 593, 233995. https://doi.org/10.1016/j.jpowsour.2023.233995
6. Aichberger, C., Jungmeier, G., 2020. Environmental Life Cycle Impacts of Automotive Batteries Based on a Literature Review. Energies 13, 6345. https://doi.org/10.3390/en13236345
7. Alfaro-Algaba, M., Ramirez, F.J., 2020. Techno-economic and environmental disassembly planning of lithium-ion electric vehicle battery packs for remanufacturing. Resour. Conserv. Recycl. 154, 104461. https://doi.org/10.1016/j.resconrec.2019.104461
8. Amici, J., Asinari, P., Ayerbe, E., Barboux, P., Bayle-Guillemaud, P., Behm, R.J., Berecibar, M., Berg, E., Bhowmik, A., Bodoardo, S., Castelli, I.E., Cekic-Laskovic, I., Christensen, R., Clark, S., Diehm, R., Dominko, R., Fichtner, M., Franco, A.A., Grimaud, A., Guillet, N., Hahlin, M., Hartmann, S., Heiries, V., Hermansson, K., Heuer, A., Jana, S., Jabbour, L., Kallo, J., Latz, A., Lorrmann, H., Løvvik, O.M., Lyonnard, S., Meeus, M., Paillard, E., Perraud, S., Placke, T., Punckt, C., Raccurt, O., Ruhland, J., Sheridan, E., Stein, H., Tarascon, J.M., Trapp, V., Vegge, T., Weil, M., Wenzel, W., Winter, M., Wolf, A., Edström, K., 2022. A Roadmap for Transforming Research to Invent the Batteries of the Future Designed

within the European Large Scale Research Initiative BATTERY 2030+. Adv. Energy Mater. https://doi.org/10.1002/aenm.202102785

9. Apalkova, V., Tsyganov, S., Chernytska, T., Meshko, N., Tsyganova, N., 2021. Evaluating the economic and ecological effects of investment projects: A new model and its application to smartphone manufacturing in Europe. Invest. Manag. Financ. Innov. 18, 252–265. https://doi.org/10.21511/IMFI.18(4).2021.22
10. Arain, A.L., Neitzel, R.L., Nambunmee, K., Hischier, R., Jindaphong, S., Austin-Breneman, J., Jolliet, O., 2022. Material flow, economic and environmental life cycle performances of informal electronic waste recycling in a Thai community. Resour. Conserv. Recycl. 180. https://doi.org/10.1016/j.resconrec.2021.106129
11. Asadi Dalini, E., Karimi, G., Zandevakili, S., Goodarzi, M., 2020. A Review on Environmental, Economic and Hydrometallurgical Processes of Recycling Spent Lithium-ion Batteries. Miner. Process. Extr. Metall. Rev. https://doi.org/10.1080/08827508.2020.1781628
12. Assefi, M., Maroufi, S., Yamauchi, Y., Sahajwalla, V., 2020. Pyrometallurgical recycling of Li-ion, Ni–Cd and Ni–MH batteries: A minireview. Curr. Opin. Green Sustain. Chem. 24, 26–31. https://doi.org/10.1016/j.cogsc.2020.01.005
13. Azadi, M., Northey, S.A., Ali, S.H., Edraki, M., 2020. Transparency on greenhouse gas emissions from mining to enable climate change mitigation. Nat. Geosci. 13, 100–104. https://doi.org/10.1038/s41561-020-0531-3
14. Baars, J., Domenech, T., Bleischwitz, R., Melin, H.E., Heidrich, O., 2021. Circular economy strategies for electric vehicle batteries reduce reliance on raw materials. Nat. Sustain. 4, 71–79. https://doi.org/10.1038/s41893-020-00607-0
15. Balakrishnan, N.T.M., Paul, A., Krishnan, M.A., Das, A., Raphaez, L.R., Ahn, J.-H., Jabeen Fatima, M.J., Prasanth, R., 2021. Lithium Iron Phosphate (LiFePO4) as High-Performance Cathode Material for Lithium-ion Batteries. Springer, Cham, pp. 35–73. https://doi.org/10.1007/978-3-030-63791-0_2
16. Beak, M., Park, S., Kim, S., Park, J., Jeong, S., Thirumalraj, B., Jeong, G., Kim, T., Kwon, K., 2021. Effect of Na from the leachate of spent Li-ion batteries on the properties of resynthesized Li-ion battery cathodes. J. Alloys Compd. 873, 159808. https://doi.org/10.1016/j.jallcom.2021.159808
17. Bella, F., De Luca, S., Fagiolari, L., Versaci, D., Amici, J., Francia, C., Bodoardo, S., 2021. An overview on anodes for magnesium batteries: Challenges towards a promising storage solution for renewables. Nanomaterials. https://doi.org/10.3390/nano11030810

18. Bertrand, N., Desgranges, C., Poquillon, D., Lafont, M.C., Monceau, D., 2010. Iron oxidation at low temperature (260-500 °C) in air and the effect of water vapor. Oxid. Met. 73, 139–162. https://doi.org/10.1007/s11085-009-9171-0
19. Bi, H., Zhu, H., Zu, L., Gao, Y., Gao, S., Bai, Y., 2020. Environment-friendly technology for recovering cathode materials from spent lithium iron phosphate batteries. Waste Manag. Res. 38, 911–920. https://doi.org/10.1177/0734242X20931933
20. Bi, H., Zhu, H., Zu, L., Gao, Y., Gao, S., Wu, Z., 2019. Eddy current separation for recovering aluminium and lithium-iron phosphate components of spent lithium-iron phosphate batteries. Waste Manag. Res. 37, 1217–1228. https://doi.org/10.1177/0734242X19871610
21. Biswas, J., Ulmala, S., Wan, X., Partinen, J., Lundström, M., Jokilaakso, A., 2023. Selective Sulfation Roasting for Cobalt and Lithium Extraction from Industrial LCO-Rich Spent Black Mass. Metals (Basel). 13. https://doi.org/10.3390/met13020358
22. Bizot, C., Blin, M.A., Guichard, P., Hamon, J., Fernandez, V., Soudan, P., Gaubicher, J., Poizot, P., 2021. Aluminum current collector for high voltage Li-ion battery. Part I: A benchmark study with statistical analysis. Electrochem. commun. 126. https://doi.org/10.1016/j.elecom.2021.107013
23. Bruno, M., Fiore, S., 2024a. Review of lithium-ion batteries' supply-chain in Europe: Material flow analysis and environmental assessment. J. Environ. Manage. 358, 120758. https://doi.org/https://doi.org/10.1016/j.jenvman.2024.120758
24. Bruno, M., Fiore, S., 2024b. Low-cost and environmentally friendly physic-mechanical pre-treatments to recycle lithium iron phosphate cathodes. J. Environ. Chem. Eng. 12, 112106. https://doi.org/10.1016/j.jece.2024.112106
25. Bruno, M., Fiore, S., 2023. Material Flow Analysis of Lithium-Ion Battery Recycling in Europe: Environmental and Economic Implications †. Batteries 9. https://doi.org/10.3390/batteries9040231
26. Bruno, M., Francia, C., Fiore, S., 2024. Closed - loop recycling of lithium iron phosphate cathodic powders via citric acid leaching. Environ. Sci. Pollut. Res. 2030. https://doi.org/10.1007/s11356-024-32837-6
27. Buken, O., Mancini, K., Sarkar, A., 2021. A sustainable approach to cathode delamination using a green solvent. RSC Adv. 11, 27356–27368. https://doi.org/10.1039/d1ra04922d
28. Burchart-Korol, D., Jursova, S., Folęga, P., Pustejovska, P., 2020. Life cycle impact assessment of electric vehicle battery charging in European Union countries. J. Clean. Prod. 257. https://doi.org/10.1016/j.jclepro.2020.120476

29. Cai, L., Lin, J., Fan, E., Wu, F., Chen, R., Li, L., 2022. Eco-Friendly Organic Acid-Assisted Mechanochemical Process for Metal Extraction from Spent Lithium-Ion Batteries. ACS Sustain. Chem. Eng. 10, 10649–10657. https://doi.org/10.1021/acssuschemeng.2c02553
30. Castro, F.D., Cutaia, L., Vaccari, M., 2021. End-of-life automotive lithium-ion batteries (LIBs) in Brazil: Prediction of flows and revenues by 2030. Resour. Conserv. Recycl. 169. https://doi.org/10.1016/j.resconrec.2021.105522
31. Chabhadiya, K., Srivastava, R.R., Pathak, P., 2021. Two-step leaching process and kinetics for an eco-friendly recycling of critical metals from spent Li-ion batteries. J. Environ. Chem. Eng. 9. https://doi.org/10.1016/j.jece.2021.105232
32. Chan, K.H., Anawati, J., Malik, M., Azimi, G., 2021. Closed-Loop Recycling of Lithium, Cobalt, Nickel, and Manganese from Waste Lithium-Ion Batteries of Electric Vehicles. ACS Sustain. Chem. Eng. 9, 4398–4410. https://doi.org/10.1021/acssuschemeng.0c06869
33. Chan, K.H., Malik, M., Anawati, J., Azimi, G., 2020. Recycling of end-of-life lithium-ion battery of electric vehicles, Minerals, Metals and Materials Series. https://doi.org/10.1007/978-3-030-36758-9_3
34. Chan, K.H., Malik, M., Azimi, G., 2023. Direct recycling of degraded lithium-ion batteries of an electric vehicle using hydrothermal relithiation. Mater. Today Energy 37, 101374. https://doi.org/10.1016/j.mtener.2023.101374
35. Chang, C., Sun, K., Liu, Y., Wang, H., Li, F., 2022. Regeneration of graphite and manganese carbonate from spent lithium-ion batteries for electric vehicles. Ionics (Kiel). 28, 2239–2246. https://doi.org/10.1007/s11581-022-04501-x
36. Charles, R.G., Davies, M.L., Douglas, P., Hallin, I.L., Mabbett, I., 2019. Sustainable energy storage for solar home systems in rural Sub- Saharan Africa e A comparative examination of lifecycle aspects of battery technologies for circular economy, with emphasis on the South African context. Energy 166, 1207–1215. https://doi.org/10.1016/j.energy.2018.10.053
37. Chen, L., Chao, Y., Li, X., Zhou, G., Lu, Q., Hua, M., Li, H., Ni, X., Wu, P., Zhu, W., 2021. Engineering a tandem leaching system for the highly selective recycling of valuable metals from spent Li-ion batteries. Green Chem. 23, 2177–2184. https://doi.org/10.1039/d0gc03820b
38. Chen, L., Dong, X., Wang, Y., Xia, Y., 2016. Separating hydrogen and oxygen evolution in alkaline water electrolysis using nickel hydroxide. Nat. Commun. 7, 1–8. https://doi.org/10.1038/ncomms11741
39. Chen, X., Cao, L., Kang, D., Li, J., Zhou, T., Ma, H., 2018a. Recovery of valuable metals from mixed types of spent lithium-ion batteries. Part II: Selective extraction

of lithium. Waste Manag. 80, 198–210. https://doi.org/10.1016/j.wasman.2018.09.013

40. Chen, X., Guo, C., Ma, H., Li, J., Zhou, T., Cao, L., Kang, D., 2018b. Organic reductants based leaching: A sustainable process for the recovery of valuable metals from spent lithium-ion batteries. Waste Manag. 75, 459–468. https://doi.org/10.1016/j.wasman.2018.01.021
41. Chen, X., Li, S., Wu, X., Zhou, T., Ma, H., 2020. In-situ recycling of coating materials and Al foils from spent lithium-ion batteries by ultrasonic-assisted acid scrubbing. J. Clean. Prod. 258. https://doi.org/10.1016/j.jclepro.2020.120943
42. Chen, X., Ma, H., Luo, C., Zhou, T., 2017a. Recovery of valuable metals from waste cathode materials of spent lithium-ion batteries using mild phosphoric acid. J. Hazard. Mater. 326, 77–86. https://doi.org/10.1016/j.jhazmat.2016.12.021
43. Chen, X., Zhou, T., 2014. Hydrometallurgical process for the recovery of metal values from spent lithium-ion batteries in citric acid media. Waste Manag. Res. 32, 1083–1093. https://doi.org/10.1177/0734242X14557380
44. Chen, X., Zhu, Y., Peng, W., Li, Y., Zhang, G., Zhang, F., Fan, X., 2017b. Direct exfoliation of the anode graphite of used Li-ion batteries into few-layer graphene sheets: a green and high yield route to high-quality graphene preparation. J. Mater. Chem. A 5, 5880–5885. https://doi.org/10.1039/c7ta00459a
45. Cheng, Q., Chirdon, W.M., Lin, M., Mishra, K., Zhou, X., 2019. Characterization, modeling, and optimization of a single-step process for leaching metallic ions from $LiNi_{1/3}Co_{1/3}Mn_{1/3}O_2$ cathodes for the recycling of spent lithium-ion batteries. Hydrometallurgy 185, 1–11. https://doi.org/10.1016/j.hydromet.2019.01.003
46. Cheng, X., Guo, G., Cheng, Y., Liu, M., Ji, J., 2022. Effect of Hydrogen Peroxide on the Recovery of Valuable Metals from Spent $LiNi_{0.6}Co_{0.2}Mn_{0.2}O_2$ Batteries. Energy Technol. 10, 1–12. https://doi.org/10.1002/ente.202200039
47. Chiu, K.L., Chen, W.S., 2017. Recovery and separation of valuable metals from cathode materials of spent lithium-ion Batteries (LIBs) by ion exchange. Sci. Adv. Mater. 9, 2155–2160. https://doi.org/10.1166/sam.2017.3214
48. Choi, J.W., Kim, J., Kim, S.K., Yun, Y.S., 2022. Simple, green organic acid-based hydrometallurgy for waste-to-energy storage devices: Recovery of $NiMnCoC_2O_4$ as an electrode material for pseudo capacitor from spent $LiNiMnCoO_2$ batteries. J. Hazard. Mater. 424, 127481. https://doi.org/10.1016/j.jhazmat.2021.127481
49. Chu, W., Zhang, Y.L., Chen, X., Huang, Y.G., Cui, H.Y., Wang, M., Wang, J., 2020. Synthesis of $LiNi_{0.6}Co_{0.2}Mn_{0.2}O_2$ from mixed cathode materials of spent lithium-ion batteries. J. Power Sources 449, 227567. https://doi.org/10.1016/j.jpowsour.2019.227567

50. Da Costa, A.J., Matos, J.F., Bernardes, A.M., Müller, I.L., 2015. Beneficiation of cobalt, copper and aluminum from wasted lithium-ion batteries by mechanical processing. Int. J. Miner. Process. 145, 77–82. https://doi.org/10.1016/j.minpro.2015.06.015
51. Dagdougui, H., Sacile, R., Bersani, C., Ouammi, A., 2018. Hydrogen Logistics: Safety and Risks Issues, in: Hydrogen Infrastructure for Energy Applications. Elsevier, pp. 127–148. https://doi.org/10.1016/b978-0-12-812036-1.00007-x
52. Danino-Perraud, R., 2020. The Recycling of Lithium-Ion Batteries: A Strategic Pillar for the European Battery Alliance, Études de l'Ifri.
53. de Oliveira Demarco, J., Stefanello Cadore, J., da Silveira de Oliveira, F., Hiromitsu Tanabe, E., Assumpção Bertuol, D., 2019. Recovery of metals from spent lithium-ion batteries using organic acids. Hydrometallurgy 190, 105169. https://doi.org/10.1016/j.hydromet.2019.105169
54. Delgado, Usai, Ellingsen, Pan, Strømman, 2019. Correction: Salgado Delgado, M.A., et al. Comparative Life Cycle Assessment of a Novel Al-Ion and a Li-Ion Battery for Stationary Applications. Materials 2019, 12, 3270. Materials (Basel). 12, 3893. https://doi.org/10.3390/ma12233893
55. Dewulf, J., Vorst, G. Van Der, Denturck, K., Langenhove, H. Van, Ghyoot, W., Tytgat, J., Vandeputte, K., 2011. Recycling rechargeable lithium-ion batteries: Critical analysis of natural resource savings. Resour., Conserv. Recycl. 54, 229–234. https://doi.org/10.1016/j.resconrec.2009.08.004
56. Diaz, F., Wang, Y., Weyhe, R., Friedrich, B., 2019. Gas generation measurement and evaluation during mechanical processing and thermal treatment of spent Li-ion batteries. Waste Manag. 84, 102–111. https://doi.org/10.1016/j.wasman.2018.11.029
57. Diaz, L.A., Strauss, M.L., Adhikari, B., Klaehn, J.R., McNally, J.S., Lister, T.E., 2020. Electrochemical-assisted leaching of active materials from lithium-ion batteries. Resour. Conserv. Recycl. 161. https://doi.org/10.1016/j.resconrec.2020.104900
58. Diouf, B., Pode, R., 2015. Potential of lithium-ion batteries in renewable energy. Renew. Energy 76, 375–380. https://doi.org/10.1016/j.renene.2014.11.058
59. Djoudi, N., Le Page Mostefa, M., Muhr, H., 2021. Influence of Temperature on Cobalt Hydroxide Precipitation for Recovery from Battery Leachates. Chem. Eng. Technol. 44, 962–971. https://doi.org/10.1002/ceat.202000330
60. Dolotko, O., Hlova, I.Z., Mudryk, Y., Gupta, S., Balema, V.P., 2020. Mechanochemical recovery of Co and Li from LCO cathode of lithium-ion battery. J. Alloys Compd. 824. https://doi.org/10.1016/j.jallcom.2020.153876

61. Du, J., Qing, J., Fang, K., Zhang, G., Cao, Z., 2024. The priority leaching of lithium from spent $LiFePO_4$ cathode without the oxidization. Resour. Conserv. Recycl. 202, 107374. https://doi.org/10.1016/j.resconrec.2023.107374
62. Dunn, J., Slattery, M., Kendall, A., Ambrose, H., Shen, S., 2021. Circularity of Lithium-Ion Battery Materials in Electric Vehicles. Environ. Sci. Technol. 55, 5189–5198. https://doi.org/10.1021/acs.est.0c07030
63. Dutta, D., Kumari, A., Panda, R., Jha, S., Gupta, D., Goel, S., Jha, M.K., 2018. Close loop separation process for the recovery of Co, Cu, Mn, Fe and Li from spent lithium-ion batteries. Sep. Purif. Technol. 200, 327–334. https://doi.org/10.1016/j.seppur.2018.02.022
64. Ebin, B., Petranikova, M., Steenari, B.M., Ekberg, C., 2019. Recovery of industrial valuable metals from household battery waste. Waste Manag. Res. 37, 168–175. https://doi.org/10.1177/0734242X18815966
65. Ecoinvent, 2023. Ecoinvent 3.9.1 [WWW Document]. URL https://support.ecoinvent.org/ecoinvent-version-3.9.1 (accessed 4.4.24).
66. EEA, 2021. New registrations of electric vehicles in Europe [WWW Document].
67. Ellingsen, L.A.W., Singh, B., Strømman, A.H., 2016. The size and range effect: Lifecycle greenhouse gas emissions of electric vehicles. Environ. Res. Lett. 11. https://doi.org/10.1088/1748-9326/11/5/054010
68. Esmaeili, M., Rastegar, S.O., Beigzadeh, R., Gu, T., 2020. Ultrasound-assisted leaching of spent lithium-ion batteries by natural organic acids and H_2O_2. Chemosphere 254. https://doi.org/10.1016/j.chemosphere.2020.126670
69. European Commission, 2020a. Regulation of the European Parliament and of the Council concerning batteries and waste batteries, repealing. Directive 2006/66/EC and amending Regulation (EU) No 2019/1020 0353.
70. European Commission, 2020b. Study on the EU's list of critical raw materials (2020): executive summary. Publications Office. https://doi.org/doi/10.2873/24089
71. European Commission, 2020c. EU transport in Figures Statistical pocketbook. https://doi.org/10.2832/491038
72. European Commission, 2020d. Green Deal: Sustainable batteries for a circular and climate neutral economy. https://ec.europa.eu/commission/presscorner/detail/en/ip_20_2312 . (Accessed 8.10.23)
73. European Commission, 2019a. The European Green Deal. Eur. Comm. 53, 24. https://doi.org/10.1017/CBO9781107415324.004

74. European Commission, 2019b. Commission staff working document on the evaluation of the Directive 2006/66/EC on batteries and accumulators and waste batteries and accumulators and repealing Directive 91/157/EEC 1–87.
75. European Commission, 2018. Commission staff working document: Critical raw materials and the circular economy. EUR, Sci. Tech. Res. Ser. 28832, 100. https://commission.europa.eu/publications/report-critical-raw-materials-and-circular-economy_en
76. European Commission, 2015. Circular economy action plan [WWW Document]. URL https://environment.ec.europa.eu/strategy/circular-economy-action-plan_en#documents (accessed 4.10.24).
77. European Environment Agency, 2023. Greenhouse gas emissions from transport in Europe [WWW Document]. URL https://www.eea.europa.eu/en/analysis/indicators/greenhouse-gas-emissions-from-transport (accessed 4.15.24).
78. European Environmental Agency, 2021. Greenhouse gas emission intensity of electricity generation [WWW Document]. URL https://www.eea.europa.eu/data-and-maps/daviz/co2-emission-intensity-14#tab-chart_7 (accessed 4.4.24).
79. Eurostat, 2023. Electricity prices for non-household consumers - bi-annual data (from 2007 onwards) https://ec.europa.eu/eurostat/databrowser/view/nrg_pc_205/default/table?lang=en (accessed 24.10.2023)
80. Fan, E., Li, L., Wang, Z., Lin, J., Huang, Y., Yao, Y., Chen, R., Wu, F., 2020a. Sustainable Recycling Technology for Li-Ion Batteries and Beyond: Challenges and Future Prospects. Chem. Rev. 120, 7020–7063. https://doi.org/10.1021/acs.chemrev.9b00535
81. Fan, E., Li, L., Zhang, X., Bian, Y., Xue, Q., Wu, J., Wu, F., Chen, R., 2018. Selective Recovery of Li and Fe from Spent Lithium-Ion Batteries by an Environmentally Friendly Mechanochemical Approach. ACS Sustain. Chem. Eng. 6, 11029–11035. https://doi.org/10.1021/acssuschemeng.8b02503
82. Fan, E., Shi, P., Zhang, X., Lin, J., Wu, F., Li, L., Chen, R., 2020b. Glucose oxidase-based biocatalytic acid-leaching process for recovering valuable metals from spent lithium-ion batteries. Waste Manag. 114, 166–173. https://doi.org/10.1016/j.wasman.2020.06.047
83. Fan, X., Song, C., Lu, X., Shi, Y., Yang, S., Zheng, F., Huang, Y., Liu, K., Wang, H., Li, Q., 2021. Separation and recovery of valuable metals from spent lithium-ion batteries via concentrated sulfuric acid leaching and regeneration of

$LiNi_{1/3}Co_{1/3}Mn_{1/3}O_2$. J. Alloys Compd. 863, 158775. https://doi.org/10.1016/j.jallcom.2021.158775

84. Fang, Z., Duan, Q., Peng, Q., Wei, Z., Cao, H., Sun, J., Wang, Q., 2022. Comparative study of chemical discharge strategy to pretreat spent lithium-ion batteries for safe, efficient, and environmentally friendly recycling. J. Clean. Prod. 359, 132116. https://doi.org/10.1016/j.jclepro.2022.132116
85. Farjana, S.H., Huda, N., Parvez Mahmud, M.A., Saidur, R., 2019. A review on the impact of mining and mineral processing industries through life cycle assessment. J. Clean. Prod. 231, 1200–1217. https://doi.org/10.1016/j.jclepro.2019.05.264
86. Ferreira, H., Leite, M.G.P., 2015. A Life Cycle Assessment study of iron ore mining. J. Clean. Prod. 108, 1081–1091. https://doi.org/10.1016/j.jclepro.2015.05.140
87. Fraunhofer ISI. (2023). Europe expands recycling of lithium-ion batteries: Focus on capacity development, demand analysis and market players - Fraunhofer ISI. https://www.isi.fraunhofer.de/en/blog/themen/batterie-update/recycling-lithium-ionen-batterien-europa-kapazitaeten-bedarf-akteure-markt-analyse.html (accessed 4.6.24).
88. Free, M.L., 2022. Hydrometallurgy, The Minerals, Metals & Materials Series. Springer International Publishing, Cham. https://doi.org/10.1007/978-3-030-88087-3
89. Fu, X., Beatty, D.N., Gaustad, G.G., Ceder, G., Roth, R., Kirchain, R.E., Bustamante, M., Babbitt, C., Olivetti, E.A., 2020. Perspectives on Cobalt Supply through 2030 in the Face of Changing Demand. Environ. Sci. Technol. 54, 2985–2993. https://doi.org/10.1021/acs.est.9b04975
90. Fu, Y., He, Y., Qu, L., Feng, Y., Li, J., Liu, J., Zhang, G., Xie, W., 2019. Enhancement in leaching process of lithium and cobalt from spent lithium-ion batteries using benzenesulfonic acid system. Waste Manag. 88, 191–199. https://doi.org/10.1016/j.wasman.2019.03.044
91. Gaines, L., 2014. The future of automotive lithium-ion battery recycling: Charting a sustainable course. SUSMAT 1–2, 2–7. https://doi.org/10.1016/j.susmat.2014.10.001
92. Gaines, L., Dai, Q., Vaughey, J.T., Gillard, S., 2021. Direct recycling R&D at the recell center. Recycling 6, 1–18. https://doi.org/10.3390/recycling6020031
93. Gaines, L., Richa, K., Spangenberger, J., 2018. Key issues for Li-ion battery recycling. MRS Energy Sustain. 5. https://doi.org/10.1557/mre.2018.13

94. Gaines, L., Wang, Y., 2021. How to Maximize the Value Recovered from Li-Ion Batteries: Hydrometallurgical or Direct Recycling? Electrochem. Soc. Interface 30, 51–54. https://doi.org/10.1149/2.F07213F
95. Gao, G., He, X., Lou, X., Jiao, Z., Guo, Y., Chen, S., Luo, X., Sun, S., Guan, J., Yuan, H., 2019. A Citric Acid/$Na_2S_2O_3$ System for the Efficient Leaching of Valuable Metals from Spent Lithium-Ion Batteries. JOM 71, 3673–3681. https://doi.org/10.1007/s11837-019-03629-y
96. Gao, W., Zhang, X., Zheng, X., Lin, X., Cao, H., Zhang, Y., Sun, Z., 2017. Lithium Carbonate Recovery from Cathode Scrap of Spent Lithium-Ion Battery: A Closed-Loop Process. Environ. Sci. Technol. 51, 1662–1669. https://doi.org/10.1021/acs.est.6b03320
97. Garg, A., Wei, L., Goyal, A., Cui, X., Gao, L., 2019. Evaluation of batteries residual energy for battery pack recycling: Proposition of stack stress-coupled-AI approach. J. Energy Storage 26. https://doi.org/10.1016/j.est.2019.101001
98. Georgi-Maschler, T., Friedrich, B., Weyhe, R., Heegn, H., Rutz, M., 2012. Development of a recycling process for Li-ion batteries. J. Power Sources 207, 173–182. https://doi.org/10.1016/j.jpowsour.2012.01.152
99. Gerold, E., Lerchbammer, R., Strnad, C., Antrekowitsch, H., 2023. Towards a sustainable approach using mineral or carboxylic acid to recover lithium from lithium iron phosphate batteries. Hydrometallurgy 222, 106187. https://doi.org/10.1016/j.hydromet.2023.106187
100. Ghassa, S., Farzanegan, A., Gharabaghi, M., Abdollahi, H., 2020. The reductive leaching of waste lithium-ion batteries in presence of iron ions: Process optimization and kinetics modelling. J. Clean. Prod. 262, 121312. https://doi.org/10.1016/j.jclepro.2020.121312
101. Golmohammadzadeh, R., Faraji, F., Rashchi, F., 2018. Recovery of lithium and cobalt from spent lithium-ion batteries (LIBs) using organic acids as leaching reagents: A review. Resour. Conserv. Recycl. 136, 418–435. https://doi.org/10.1016/j.resconrec.2018.04.024
102. Golmohammadzadeh, R., Rashchi, F., Vahidi, E., 2017. Recovery of lithium and cobalt from spent lithium-ion batteries using organic acids: Process optimization and kinetic aspects. Waste Manag. 64, 244–254. https://doi.org/10.1016/j.wasman.2017.03.037
103. Golroudbary, S.R., Calisaya-Azpilcueta, D., Kraslawski, A., 2019. The life cycle of energy consumption and greenhouse gas emissions from critical minerals recycling: Case of lithium-ion batteries. Procedia CIRP 80, 316–321. https://doi.org/10.1016/j.procir.2019.01.003

104. Gong, R., Li, C., Meng, Q., Dong, P., Zhang, Y., Zhang, B., Yan, J., Li, Y., 2022. A sustainable closed-loop method of selective oxidation leaching and regeneration for lithium iron phosphate cathode materials from spent batteries. J. Environ. Manage. 319, 115740. https://doi.org/10.1016/j.jenvman.2022.115740

105. Granata, G., Pagnanelli, F., Moscardini, E., Takacova, Z., Havlik, T., Toro, L., 2012. Simultaneous recycling of nickel metal hydride, lithium-ion and primary lithium batteries: Accomplishment of European Guidelines by optimizing mechanical pre-treatment and solvent extraction operations. J. Power Sources 212, 205–211. https://doi.org/10.1016/j.jpowsour.2012.04.016

106. Greim, P., Solomon, A.A., Breyer, C., 2020. Assessment of lithium criticality in the global energy transition and addressing policy gaps in transportation. Nat. Commun. 11. https://doi.org/10.1038/s41467-020-18402-y

107. Guo, X., Cao, X., Huang, G., Tian, Q., Sun, H., 2017. Recovery of lithium from the effluent obtained in the process of spent lithium-ion batteries recycling. J. Environ. Manage. 198, 84–89. https://doi.org/10.1016/j.jenvman.2017.04.062

108. Guo, Y., Li, F., Zhu, H., Li, G., Huang, J., He, W., 2016. Leaching lithium from the anode electrode materials of spent lithium-ion batteries by hydrochloric acid (HCl). Waste Manag. 51, 227–233. https://doi.org/10.1016/j.wasman.2015.11.036

109. Haas, P., Pfeifer, S., Jannes, M., Bradtm, C., 2018. Recycling of Lithium-Ion Batteries Chapter 9 Separation of the Electrolyte—Solvent Extraction, Recycling of Lithium-Ion Batteries. https://doi.org/10.1007/978-3-319-70572-9_9

110. Habib, K., Hamelin, L., Wenzel, H., 2016. A dynamic perspective of the geopolitical supply risk of metals. J. Clean. Prod. 133, 850–858. https://doi.org/10.1016/j.jclepro.2016.05.118

111. Han, F., Fang, D., Feng, Y., Fan, Y., Wei, Y., Liu, Y., Qu, L., 2023. The recovery of high purity iron phosphate from the spent lithium extraction slag by a simple phosphoric acid pickling. Sep. Purif. Technol. 323, 124358. https://doi.org/10.1016/j.seppur.2023.124358

112. Hanisch, C., Haselrieder, W., Kwade, A., 2011. Recovery of active materials from spent lithium-ion electrodes and electrode production rejects, in: Localized Solutions for Sustainability in Manufacturing - Proceedings of the 18th CIRP International Conference on Life Cycle Engineering. Springer Science and Business Media, LLC, pp. 85–89. https://doi.org/10.1007/978-3-642-19692-8_15

113. Hanisch, C., Loellhoeffel, T., Diekmann, J., Markley, K.J., Haselrieder, W., Kwade, A., 2015. Recycling of lithium-ion batteries: A novel method to

separate coating and foil of electrodes. J. Clean. Prod. 108, 301–311. https://doi.org/10.1016/j.jclepro.2015.08.026

114. Hao, H., Mu, Z., Jiang, S., Liu, Z., Zhao, F., 2017a. GHG Emissions from the production of lithium-ion batteries for electric vehicles in China. Sustain. 9. https://doi.org/10.3390/su9040504

115. Hao, H., Qiao, Q., Liu, Z., Zhao, F., 2017b. Impact of recycling on energy consumption and greenhouse gas emissions from electric vehicle production: The China 2025 case. Resour. Conserv. Recycl. 122, 114–125. https://doi.org/10.1016/j.resconrec.2017.02.005

116. Harper, G., Sommerville, R., Kendrick, E., Driscoll, L., Slater, P., Stolkin, R., Walton, A., Christensen, P., Heidrich, O., Lambert, S., Abbott, A., Ryder, K., Gaines, L., Anderson, P., 2019. Recycling lithium-ion batteries from electric vehicles. Nature. https://doi.org/10.1038/s41586-019-1682-5

117. He, K., Zhang, Z.-Y., Alai, L., Zhang, F.-S., 2019. A green process for exfoliating electrode materials and simultaneously extracting electrolyte from spent lithium-ion batteries. J. Hazard. Mater. 375, 43–51. https://doi.org/10.1016/j.jhazmat.2019.03.120

118. He, K., Zhang, Z.Y., Zhang, F.S., 2020. Selectively peeling of spent LiFePO4 cathode by destruction of crystal structure and binder matrix for efficient recycling of spent battery materials. J. Hazard. Mater. 386, 121633. https://doi.org/10.1016/j.jhazmat.2019.121633

119. He, L.-P., Sun, S.-Y., Song, X.-F., Yu, J.-G., 2017. Leaching process for recovering valuable metals from the $LiNi_{1/3}Co_{1/3}Mn_{1/3}O_2$ cathode of lithium-ion batteries. Waste Manag. 64, 171–181. https://doi.org/10.1016/j.wasman.2017.02.011

120. He, L.P., Sun, S.Y., Mu, Y.Y., Song, X.F., Yu, J.G., 2017. Recovery of Lithium, Nickel, Cobalt, and Manganese from Spent Lithium-Ion Batteries Using l -Tartaric Acid as a Leachant. ACS Sustain. Chem. Eng. 5, 714–721. https://doi.org/10.1021/acssuschemeng.6b02056

121. He, M., Zhang, P., Duan, X., Teng, L., Li, H., Meng, F., Liu, Q., Liu, W., 2023. Selective recovery of lithium from spent lithium-ion battery by an emission-free sulfation roasting strategy. Process Saf. Environ. Prot. 177, 1035–1044. https://doi.org/10.1016/j.psep.2023.07.065

122. He, Y., Yuan, X., Zhang, G., Wang, H., Zhang, T., Xie, W., Li, L., 2021. A critical review of current technologies for the liberation of electrode materials from foils in the recycling process of spent lithium-ion batteries. Sci. Total Environ. 766, 142382. https://doi.org/10.1016/j.scitotenv.2020.142382

123. Heelan, J., Gratz, E., Zheng, Z., Wang, Q., Chen, M., Apelian, D., Wang, Y., 2016. Current and Prospective Li-Ion Battery Recycling and Recovery Processes. JOM 68, 2632–2638. https://doi.org/10.1007/s11837-016-1994-y

124. Holzer, A., Wiszniewski, L., Windisch-Kern, S., Raupenstrauch, H., 2022. Optimization of a Pyrometallurgical Process to Efficiently Recover Valuable Metals from Commercially Used Lithium-Ion Battery Cathode Materials LCO, NCA, NMC622, and LFP. Metals (Basel). 12. https://doi.org/10.3390/met12101642

125. Hu, G., Gong, Y., Peng, Z., Du, K., Huang, M., Wu, J., Guan, D., Zeng, J., Zhang, B., Cao, Y., 2022. Direct Recycling Strategy for Spent Lithium Iron Phosphate Powder: An Efficient and Wastewater-Free Process. ACS Sustain. Chem. Eng. https://doi.org/10.1021/acssuschemeng.2c03520

126. Hu, G., Huang, K., Du, K., Peng, Z., Cao, Y., 2024. Efficient recovery and regeneration of FePO 4 from lithium extraction slag: Towards sustainable $LiFePO_4$ battery recycling. J. Clean. Prod. 434, 140091. https://doi.org/10.1016/j.jclepro.2023.140091

127. Hu, X., Mousa, E., Tian, Y., Ye, G., 2021a. Recovery of Co, Ni, Mn, and Li from Li-ion batteries by smelting reduction - Part I: A laboratory-scale study. J. Power Sources 483. https://doi.org/10.1016/j.jpowsour.2020.228936

128. Hu, X., Mousa, E., Ye, G., 2021b. Recovery of Co, Ni, Mn, and Li from Li-ion batteries by smelting reduction - Part II: A pilot-scale demonstration. J. Power Sources 483. https://doi.org/10.1016/j.jpowsour.2020.229089

129. Iclodean, C., Varga, B., Burnete, N., Cimerdean, D., Jurchiş, B., 2017. Comparison of Different Battery Types for Electric Vehicles. IOP Conf. Ser. Mater. Sci. Eng. 252. https://doi.org/10.1088/1757-899X/252/1/012058

130. Iglesias-Émbil, M., Valero, A., Ortego, A., Villacampa, M., Vilaró, J., Villalba, G., 2020. Raw material uses in a battery electric car – a thermodynamic rarity assessment. Resour. Conserv. Recycl. 158. https://doi.org/10.1016/j.resconrec.2020.104820

131. Ilyas, S., Srivastava, R.R., Kim, H., 2023. Cradle-to-cradle recycling of spent NMC batteries with emphasis on novel Co^{2+}/Ni^{2+} separation from HCl leached solution and synthesis of new ternary precursor. Process Saf. Environ. Prot. 170, 584–595. https://doi.org/10.1016/j.psep.2022.12.045

132. International Energy Agency, 2023. Global EV Outlook 2023 [WWW Document]. IEA. URL www.iea.org/reports/global-ev-outlook-2023

133. Jafari, M., Torabian, M.M., Bazargan, A., 2020. A Facile Chemical-Free Cathode Powder Separation Method for Lithium-ion Battery Resource Recovery. J. Energy Storage 31. https://doi.org/10.1016/j.est.2020.101564

134. Jafari, Milad, Torabian, M.M., Bazargan, A., 2020. A Facile Chemical-Free Cathode Powder Separation Method for Lithium-ion Battery Resource Recovery. J. Energy Storage 31, 101564. https://doi.org/10.1016/j.est.2020.101564

135. Jantunen, N., Virolainen, S., Sainio, T., 2022. Direct Production of Ni–Co–Mn Mixtures for Cathode Precursors from Cobalt-Rich Lithium-Ion Battery Leachates by Solvent Extraction. Metals (Basel). 12. https://doi.org/10.3390/met12091445

136. Jha, M.K., Kumari, A., Jha, A.K., Kumar, V., Hait, J., Pandey, B.D., 2013. Recovery of lithium and cobalt from waste lithium-ion batteries of mobile phone. Waste Manag. 33, 1890–1897. https://doi.org/10.1016/j.wasman.2013.05.008

137. Jian, Y., Yanqing, L., Fangyang, L., Ming, J., Liangxing, J., 2020. Countercurrent leaching of Ni, Co, Mn, and Li from spent lithium-ion batteries. Waste Manag. Res. 38, 1358–1366. https://doi.org/10.1177/0734242X20944498

138. Jian, Yang, Yanqing, L., Fangyang, L., Ming, J., Liangxing, J., 2020. Countercurrent leaching of Ni, Co, Mn, and Li from spent lithium-ion batteries. Waste Manag. Res. 38, 1358–1366. https://doi.org/10.1177/0734242X20944498

139. Jiang, F., Chen, Y., Ju, S., Zhu, Q., Zhang, L., Peng, J., Wang, X., Miller, J.D., 2018. Ultrasound-assisted leaching of cobalt and lithium from spent lithium-ion batteries. Ultrason. Sonochem. 48, 88–95. https://doi.org/10.1016/j.ultsonch.2018.05.019

140. Jiang, G., Zhang, Yannan, Meng, Q., Zhang, Yingjie, Dong, P., Zhang, M., Yang, X., 2020. Direct Regeneration of $LiNi_{0.5}Co_{0.2}Mn_{0.3}O_2$ Cathode from Spent Lithium-Ion Batteries by the Molten Salts Method. ACS Sustain. Chem. Eng. 8, 18138–18147. https://doi.org/10.1021/acssuschemeng.0c06514

141. Jiang, S., Zhang, L., Li, F., Hua, H., Liu, X., Yuan, Z., Wu, H., 2020. Environmental impacts of lithium production showing the importance of primary data of upstream process in life-cycle assessment. J. Environ. Manage. 262, 110253. https://doi.org/10.1016/j.jenvman.2020.110253

142. Jiang, Y., Chen, X., Yan, S., Li, S., Zhou, T., 2021. Pursuing green and efficient process towards recycling of different metals from spent lithium-ion batteries through Ferro-chemistry. Chem. Eng. J. 426, 131637. https://doi.org/10.1016/j.cej.2021.131637

143. Jiang, Y., Chen, X., Yan, S., Ou, Y., Zhou, T., 2022. Mechanochemistry-induced recycling of spent lithium-ion batteries for synergistic treatment of mixed cathode powders. Green Chem. 24, 5987–5997. https://doi.org/10.1039/d2gc01929a

144. Jin, H., Zhang, J., Wang, D., Jing, Q., Chen, Y., Wang, C., 2022. Facile and efficient recovery of lithium from spent $LiFePO_4$ batteries via air oxidation–water leaching at room temperature. Green Chem. 24, 152–162. https://doi.org/10.1039/d1gc03333f

145. Jin, H., Zhang, J., Yang, C., Ma, L., Chen, Y., Wang, C., 2023. Selective recovery of lithium from spent $LiFePO_4$ battery via a self-catalytic air oxidation method. Chem. Eng. J. 460, 141805. https://doi.org/10.1016/j.cej.2023.141805

146. Jo, M., Ku, H., Park, S., Song, J., Kwon, K., 2018. Effects of Residual Lithium in the precursors of Li $[Ni_{1/3}Co_{1/3}Mn_{1/3}]O_2$ on their lithium-ion battery performance. J. Phys. Chem. Solids 118, 47–52. https://doi.org/10.1016/j.jpcs.2018.02.043

147. Kader, Z.A., Marshall, A., Kennedy, J., 2021. A review on sustainable recycling technologies for lithium-ion batteries. Emergent Mater. 4, 725–735. https://doi.org/10.1007/s42247-021-00201-w

148. Kamran, M., Raugei, M., Hutchinson, A., 2021. A dynamic material flow analysis of lithium-ion battery metals for electric vehicles and grid storage in the UK: Assessing the impact of shared mobility and end-of-life strategies. Resour. Conserv. Recycl. 167. https://doi.org/10.1016/j.resconrec.2021.105412

149. Kim, H., Jang, Y.-C., Hwang, Y., Ko, Y., Yun, H., 2018. End-of-life batteries management and material flow analysis in South Korea. Front. Environ. Sci. Eng. 12. https://doi.org/10.1007/s11783-018-1019-x

150. Kim, J.Y., Wu, J., Woo, E., Yoo, K., Kim, J., Jae, J., Jai, L., Byeon, W., Ahn, J., Lee, J., 2023. Recycling for Recovery of Critical Metals from - $LiCoO_2$ Cathode Material Through Methanesulfonic Acid - Citric Acid Organic Leaching System. Mining, Metall. Explor. 40, 1455–1467. https://doi.org/10.1007/s42461-023-00837-8

151. Kim, S., Bang, J., Yoo, J., Shin, Y., Bae, J., Jeong, J., Kim, K., Dong, P., Kwon, K., 2021. A comprehensive review on the pretreatment process in lithium-ion battery recycling. J. Clean. Prod. 294, 126329. https://doi.org/10.1016/j.jclepro.2021.126329

152. Kong, S., Zhang, Y., Liu, W., 2022. Parallel Disassembly Sequence Planning of Retired Lithium-ion-battery Pack based on Heuristic Algorithm, in:

Journal of Physics: Conference Series. Institute of Physics, p. 012010. https://doi.org/10.1088/1742-6596/2254/1/012010

153. Kordkheili, R.A., Mohammadi, M., 2017. Smart scheduling and economic analysis of electric vehicles for peak load shaving considering renewable energy resources. Smart Grid Conf. SGC 2015 115–121. https://doi.org/10.1109/SGC.2015.7857420

154. Ku, C.Y., Chen, J.H., 2022. The Recovery of Lithium Iron Phosphate from Lithium-ion Battery. Proc. 2022 8th Int. Conf. Appl. Syst. Innov. ICASI 2022 201–204. https://doi.org/10.1109/ICASI55125.2022.9774480

155. Kumar, J., Neiber, R.R., Park, J., Ali Soomro, R., Greene, G.W., Ali Mazari, S., Young Seo, H., Hong Lee, J., Shon, M., Wook Chang, D., Yong Cho, K., 2022. Recent progress in sustainable recycling of $LiFePO_4$-type lithium-ion batteries: Strategies for highly selective lithium recovery. Chem. Eng. J. 431, 133993. https://doi.org/10.1016/j.cej.2021.133993

156. Kumar, J., Shen, X., Li, B., Liu, H., Zhao, J., 2020. Selective recovery of Li and $FePO_4$ from spent $LiFePO_4$ cathode scraps by organic acids and the properties of the regenerated $LiFePO_4$. Waste Manag. 113, 32–40. https://doi.org/10.1016/j.wasman.2020.05.046

157. Kumawat, S., Singh, D., Saini, A., 2023. Recycling of spent lithium-iron phosphate batteries: toward closing the loop. Mater. Manuf. Process. 38, 135–150. https://doi.org/10.1080/10426914.2022.2136387

158. Kwade, A., Haselrieder, W., Leithoff, R., Modlinger, A., Dietrich, F., Droeder, K., 2018. Current status and challenges for automotive battery production technologies. Nat. Energy 3, 290–300. https://doi.org/10.1038/s41560-018-0130-3

159. Lähdesmäki, S., Hanski, J., Huttunen-saarivirta, E., 2023. Insights into Circular Economy Potential of Lithium by System Dynamic Modelling of Material Streams. Batter. Supercaps 202300231. https://doi.org/10.1002/batt.202300231

160. Langner, T., Sieber, T., Acker, J., 2021. Studies on the deposition of copper in lithium-ion batteries during the deep discharge process. Sci. Rep. 11, 1–9. https://doi.org/10.1038/s41598-021-85575-x

161. Larouche, F., Amouzegar, K., Houlachi, G., Bouchard, P., Demopoulos, G.P., 2022. Conversion of $LiFePO_4$ to $FePO_4$ via Selective Lithium Bicarbonation: A Direct Pathway Towards Battery Recycling. J. Electrochem. Soc. 169, 073509. https://doi.org/10.1149/1945-7111/ac801f

162. Larouche, F., Tedjar, F., Amouzegar, K., Houlachi, G., Bouchard, P., Demopoulos, G.P., Zaghib, K., 2020. Progress and Status of Hydrometallurgical

and Direct Recycling of Li-Ion Batteries and Beyond. Materials (Basel). https://doi.org/10.3390/ma13030801

163. Latini, D., Vaccari, M., Lagnoni, M., Orefice, M., Mathieux, F., Huisman, J., Tognotti, L., Bertei, A., 2022. A comprehensive review and classification of unit operations with assessment of outputs quality in lithium-ion battery recycling. J. Power Sources 546, 231979. https://doi.org/10.1016/j.jpowsour.2022.231979

164. Lebedeva, N., Di Persio, F., Boon-Brett, L., 2017. Lithium-ion battery value chain and related opportunities for Europe. Luxembourg. https://doi.org/10.2760/6060

165. Lee, H., Kim, Y.T., Lee, S.W., 2023. Optimization of the Electrochemical Discharge of Spent Li-Ion Batteries from Electric Vehicles for Direct Recycling. Energies 16, 1–12. https://doi.org/10.3390/en16062759

166. Lewandowski, D., Kozłowski, J., Potempa, M., 2020. Recycling of Li-ion batteries with the application of mechanical and pyrometallurgical methods. World Metall. - ERZMETALL 73, 123–127.

167. Li, D., Zhang, B., Ou, X., Zhang, J., Meng, K., Ji, G., Li, P., Xu, J., 2021. Ammonia leaching mechanism and kinetics of $LiCoO_2$ material from spent lithium-ion batteries. Chinese Chem. Lett. 32, 2333–2337. https://doi.org/10.1016/j.cclet.2020.11.074

168. Li, H., Xing, S., Liu, Y., Li, F., Guo, H., Kuang, G., 2017. Recovery of Lithium, Iron, and Phosphorus from Spent $LiFePO_4$ Batteries Using Stoichiometric Sulfuric Acid Leaching System. ACS Sustain. Chem. Eng. 5, 8017–8024. https://doi.org/10.1021/acssuschemeng.7b01594

169. Li, J., Ma, Z.-F., 2019. Past and Present of $LiFePO_4$: From Fundamental Research to Industrial Applications. Chem 5, 3–6. https://doi.org/10.1016/j.chempr.2018.12.012

170. Li, J., Wang, G., Xu, Z., 2016. Environmentally friendly oxygen-free roasting/wet magnetic separation technology for in situ recycling cobalt, lithium carbonate and graphite from spent $LiCoO_2$/graphite lithium batteries. J. Hazard. Mater. 302, 97–104. https://doi.org/10.1016/j.jhazmat.2015.09.050

171. Li, Jia, Wang, G., Xu, Z., 2016. Generation and detection of metal ions and volatile organic compounds (VOCs) emissions from the pretreatment processes for recycling spent lithium-ion batteries. Waste Manag. 52, 221–227. https://doi.org/10.1016/j.wasman.2016.03.011

172. Li, L., Bian, Y., Zhang, X., Yao, Y., Xue, Q., Fan, E., Wu, F., Chen, R., 2019. A green and effective room-temperature recycling process of $LiFePO_4$

cathode materials for lithium-ion batteries. Waste Manag. 85, 437–444. https://doi.org/10.1016/j.wasman.2019.01.012

173. Li, L., Ge, J., Chen, R., Wu, F., Chen, S., Zhang, X., 2010a. Environmentally friendly leaching reagent for cobalt and lithium recovery from spent lithium-ion batteries. Waste Manag. 30, 2615–2621. https://doi.org/10.1016/j.wasman.2010.08.008

174. Li, L., Ge, J., Wu, F., Chen, R., Chen, S., Wu, B., 2010b. Recovery of cobalt and lithium from spent lithium-ion batteries using organic citric acid as leachant. J. Hazard. Mater. 176, 288–293. https://doi.org/10.1016/j.jhazmat.2009.11.026

175. Li, L., Lu, J., Ren, Y., Zhang, X.X., Chen, R.J., Wu, F., Amine, K., 2012. Ascorbic-acid-assisted recovery of cobalt and lithium from spent Li-ion batteries. J. Power Sources 218, 21–27. https://doi.org/10.1016/j.jpowsour.2012.06.068

176. Li, M., Zhang, B., Qu, X., Cai, M., Liu, D., Zhou, F., Xie, H., Gao, S., Yin, H., 2022. A SiCl4-Assisted Roasting Approach for Recovering Spent $LiCoO_2$ Cathode. ACS Sustain. Chem. Eng. 10, 8305–8313. https://doi.org/10.1021/acssuschemeng.2c00814

177. Li, P., Luo, S., Zhang, L., Wang, Y., Zhang, H., Wang, J., Yan, S., Hou, P., Wang, Q., Zhang, Y., Liu, X., Lei, X., Mu, W., 2022. Study on efficient and synergistic leaching of valuable metals from spent lithium iron phosphate using the phosphoric acid-oxalic acid system. Sep. Purif. Technol. 303, 122247. https://doi.org/10.1016/j.seppur.2022.122247

178. Li, Z., Zheng, Q., Nakajima, A., Zhang, Z., Watanabe, M., 2023. Organic Acid-Based Hydrothermal Leaching of $LiFePO_4$ Cathode Materials 2300421, 1–12. https://doi.org/10.1002/adsu.202300421

179. Liang, Q., Yue, H., Wang, S., Yang, S., Lam, K. ho, Hou, X., 2020. Recycling and crystal regeneration of commercial used $LiFePO_4$ cathode materials. Electrochim. Acta 330, 135323. https://doi.org/10.1016/j.electacta.2019.135323

180. Lide, D.R., 2004. CRC Handbook of Chemistry and Physics, 84th Edition Edited by David R. Lide (National Institute of Standards and Technology). CRC Press LLC: Boca Raton. 2003. 2616 pp. ISBN 0-8493-0484-9., Journal of the American Chemical Society. American Chemical Society (ACS). https://doi.org/10.1021/ja0336372

181. Liu, C., Gao, J., 2021. Analysis on the hazard control technology of volatile organic compounds. IOP Conf. Ser. Earth Environ. Sci. 791, 8–13. https://doi.org/10.1088/1755-1315/791/1/012166

182. Liu, G., Liu, Z., Gu, J., Yuan, H., Wu, Y., Chen, Y., 2023. A facile new process for the efficient conversion of spent $LiFePO_4$ batteries via $(NH_4)_2S_2O_8$ - assisted mechanochemical activation coupled with water leaching. Chem. Eng. J. 471, 144265. https://doi.org/10.1016/j.cej.2023.144265

183. Liu, J., Bai, X., Hao, J., Wang, H., Zhang, T., Tang, X., Wang, S., He, Y., 2021. Efficient liberation of electrode materials in spent lithium-ion batteries using a cryogenic ball mill. J. Environ. Chem. Eng. 9, 106017. https://doi.org/10.1016/j.jece.2021.106017

184. Liu, K., Wang, M., Zhang, Q., Xu, Z., Labianca, C., Komárek, M., Gao, B., Tsang, D.C.W., 2023. A perspective on the recovery mechanisms of spent lithium iron phosphate cathode materials in different oxidation environments. J. Hazard. Mater. 445. https://doi.org/10.1016/j.jhazmat.2022.130502

185. Liu, W., Li, K., Wang, W., Hu, Y., Ren, Z., Zhou, Z., 2022. Selective leaching of lithium-ions from $LiFePO_4$ powders using hydrochloric acid and sodium hypochlorite system. Can. J. Chem. Eng. https://doi.org/10.1002/cjce.24617

186. Liu, W., Liu, W., Li, X., Liu, Y., Ogunmoroti, A.E., Li, M., Bi, M., Cui, Z., 2021. Dynamic material flow analysis of critical metals for lithium-ion battery system in China from 2000–2018. Resour. Conserv. Recycl. 164. https://doi.org/10.1016/j.resconrec.2020.105122

187. Lombardo, G., Ebin, B., Steenari, B.-M., Alemrajabi, M., Karlsson, I., Petranikova, M., 2021. Comparison of the effects of incineration, vacuum pyrolysis and dynamic pyrolysis on the composition of NMC-lithium battery cathode-material production scraps and separation of the current collector. Resour. Conserv. Recycl. 164. https://doi.org/10.1016/j.resconrec.2020.105142

188. Ma, C., Svärd, M., Forsberg, K., 2022. Recycling cathode material $LiCo_{1/3}Ni_{1/3}Mn_{1/3}O_2$ by leaching with a deep eutectic solvent and metal recovery with antisolvent crystallization. Resour. Conserv. Recycl. 186. https://doi.org/10.1016/j.resconrec.2022.106579

189. Mahandra, H., Ghahreman, A., 2021. A sustainable process for selective recovery of lithium as lithium phosphate from spent $LiFePO_4$ batteries. Resour. Conserv. Recycl. 175, 105883. https://doi.org/10.1016/j.resconrec.2021.105883

190. Makuza, B., Tian, Q., Guo, X., Chattopadhyay, K., Yu, D., 2021. Pyrometallurgical options for recycling spent lithium-ion batteries: A comprehensive review. J. Power Sources 491, 229622. https://doi.org/10.1016/j.jpowsour.2021.229622

191. Mansur, M.B., Guimarães, A.S., Petraniková, M., 2021. An Overview on the Recovery of Cobalt from End-of-life Lithium-ion Batteries. Miner. Process. Extr. Metall. Rev. https://doi.org/10.1080/08827508.2021.1883014

192. Marshall, J., Gastol, D., Sommerville, R., Middleton, B., Goodship, V., Kendrick, E., 2020. Disassembly of Li ion cells—characterization and safety considerations of a recycling scheme. Metals (Basel). 10, 1–22. https://doi.org/10.3390/met10060773

193. Matos, C.T., Mathieux, F., Ciacci, L., Lundhaug, M.C., León, M.F.G., Müller, D.B., Dewulf, J., Georgitzikis, K., Huisman, J., 2022. Material system analysis: A novel multilayer system approach to correlate EU flows and stocks of Li-ion batteries and their raw materials. J. Ind. Ecol. 26, 1261–1276. https://doi.org/10.1111/jiec.13244

194. Mayyas, A., Steward, D., Mann, M., 2019. The case for recycling: Overview and challenges in the material supply chain for automotive li-ion batteries. Sustain. Mater. Technol. 19, e00087. https://doi.org/10.1016/j.susmat.2018.e00087

195. Meng, F., Liu, Q., Kim, R., Wang, J., Liu, G., Ghahreman, A., 2020. Selective recovery of valuable metals from industrial waste lithium-ion batteries using citric acid under reductive conditions: Leaching optimization and kinetic analysis. Hydrometallurgy 191. https://doi.org/10.1016/j.hydromet.2019.105160

196. Meng, Q., Zhang, Y., Dong, P., 2017. Use of glucose as reductant to recover Co from spent lithium-ions batteries. Waste Manag. 64, 214–218. https://doi.org/10.1016/j.wasman.2017.03.017

197. Meshram, P., Mishra, A., Abhilash, Sahu, R., 2020. Environmental impact of spent lithium-ion batteries and green recycling perspectives by organic acids – A review. Chemosphere 242, 125291. https://doi.org/10.1016/j.chemosphere.2019.125291

198. Miao, Y., Liu, L., Xu, K., Li, J., 2023. High concentration from resources to market heightens risk for power lithium - ion battery supply chains globally. Environ. Sci. Pollut. Res. 30, 65558–65571. https://doi.org/10.1007/s11356-023-27035-9

199. Miatto, A., Reck, B.K., West, J., Graedel, T.E., 2020. The rise and fall of American lithium. Resour. Conserv. Recycl. 162. https://doi.org/10.1016/j.resconrec.2020.105034

200. Mishra, G., Jha, R., Meshram, A., Singh, K.K., 2022. A review on recycling of lithium-ion batteries to recover critical metals. J. Environ. Chem. Eng. 10, 108534. https://doi.org/10.1016/j.jece.2022.108534

201. Modaresi, R., Pauliuk, S., Løvik, A.N., Müller, D.B., 2014. Global carbon benefits of material substitution in passenger cars until 2050 and the impact on the steel and aluminum industries. Environ. Sci. Technol. 48, 10776–10784. https://doi.org/10.1021/es502930w

202. Mossali, E., Picone, N., Gentilini, L., Rodrìguez, O., Pérez, J.M., Colledani, M., 2020. Lithium-ion batteries towards circular economy: A literature review of opportunities and issues of recycling treatments. J. Environ. Manage. 264. https://doi.org/10.1016/j.jenvman.2020.110500

203. Musariri, B., Akdogan, G., Dorfling, C., Bradshaw, S., 2019. Evaluating organic acids as alternative leaching reagents for metal recovery from lithium-ion batteries. Miner. Eng. 137, 108–117. https://doi.org/10.1016/j.mineng.2019.03.027

204. Nadimi, H., Karazmoudeh, N.J., 2021. Selective Separation and Purification of Mn from Co and Ni in Waste Mobile Phone Lithium-Ion Batteries Using D_2EHAP via Solvent Extraction Method. J. Sustain. Metall. 7, 653–663. https://doi.org/10.1007/s40831-021-00371-1

205. Nakajima, A., Zheng, Q., Ogawa, T., Hirama, S., Watanabe, M., 2022. Metal Recovery of $LiCoO_2$/$LiNiO_2$ Cathode Materials by Hydrothermal Leaching and Precipitation Separation. ACS Sustain. Chem. Eng. 10, 12852–12863. https://doi.org/10.1021/acssuschemeng.2c04259

206. Nancharaiah, Y. V., Mohan, S.V., Lens, P.N.L., 2016. Biological and Bioelectrochemical Recovery of Critical and Scarce Metals. Trends Biotechnol. 34, 137–155. https://doi.org/10.1016/j.tibtech.2015.11.003

207. Natarajan, S., Boricha, A.B., Bajaj, H.C., 2018. Recovery of value-added products from cathode and anode material of spent lithium-ion batteries. Waste Manag. 77, 455–465. https://doi.org/10.1016/j.wasman.2018.04.032

208. National Academies of Sciences Engineering and Medicine, 2021. Accelerating Decarbonization of the U.S. Energy System, Accelerating Decarbonization of the U.S. Energy System. National Academies Press. https://doi.org/10.17226/25932

209. Nayaka, G.P., Zhang, Y., Dong, P., Wang, D., Pai, K. V., Manjanna, J., Santhosh, G., Duan, J., Zhou, Z., Xiao, J., 2018. Effective and environmentally friendly recycling process designed for $LiCoO_2$ cathode powders of spent Li-ion batteries using mixture of mild organic acids. Waste Manag. 78, 51–57. https://doi.org/10.1016/j.wasman.2018.05.030

210. Nealer, R., Reichmuth, D., Anair, D., 2015. Cleaner Cars from Cradle to Grave: How Electric Cars Beat Gasoline Cars on Lifetime Global Warming

Emissions. Union Concerned Sci. 1–54. https://www.jstor.org/stable/resrep17225.1

211. Neidhardt, M., Mas-Peiro, J., Schulz-Moenninghoff, M., Pou, J.O., Gonzalez-Olmos, R., Kwade, A., Schmuelling, B., 2022. Forecasting the Global Battery Material Flow: Analyzing the Break-Even Points at Which Secondary Battery Raw Materials Can Substitute Primary Materials in the Battery Production. Appl. Sci. 12. https://doi.org/10.3390/app12094790

212. Nguyen, V.N.H., Lee, M.S., 2021. Separation of Co (II), Ni(II), Mn(II) and Li(I) from synthetic sulfuric acid leaching solution of spent lithium-ion batteries by solvent extraction. J. Chem. Technol. Biotechnol. 96, 1205–1217. https://doi.org/10.1002/jctb.6632

213. Nigl, T., Schwarz, T.E., Walch, C., Baldauf, M., Rutrecht, B., Pomberger, R., 2020. Characterisation and material flow analysis of end-of-life portable batteries and lithium-based batteries in different waste streams in Austria. Waste Manag. Res. 38, 649–659. https://doi.org/10.1177/0734242X20914717

214. Ning, P., Meng, Q., Dong, P., Duan, J., Xu, M., Lin, Y., Zhang, Y., 2020. Recycling of cathode material from spent lithium-ion batteries using an ultrasound-assisted DL-malic acid leaching system. Waste Manag. 103, 52–60. https://doi.org/10.1016/j.wasman.2019.12.002

215. Niu, Y., Peng, X., Li, J., Zhang, Y., Song, F., Shi, D., Li, L., 2023. Recovery of Li 2 CO 3 and FePO 4 from spent LiFePO 4 by coupling technics of isomorphic substitution leaching and solvent extraction. Chinese J. Chem. Eng. 54, 306–315. https://doi.org/10.1016/j.cjche.2022.04.005

216. Norgate, T.E., Jahanshahi, S., Rankin, W.J., 2007. Assessing the environmental impact of metal production processes. J. Clean. Prod. 15, 838–848. https://doi.org/10.1016/j.jclepro.2006.06.018

217. Ojanen, S., Lundström, M., Santasalo-Aarnio, A., Serna-Guerrero, R., 2018. Challenging the concept of electrochemical discharge using salt solutions for lithium-ion batteries recycling. Waste Manag. 76, 242–249. https://doi.org/10.1016/j.wasman.2018.03.045

218. Oliveira, L., Messagie, M., Rangaraju, S., Sanfelix, J., Hernandez Rivas, M., Van Mierlo, J., 2015. Key issues of lithium-ion batteries - From resource depletion to environmental performance indicators. J. Clean. Prod. 108, 354–362. https://doi.org/10.1016/j.jclepro.2015.06.021

219. Pagnanelli, F., Moscardini, E., Altimari, P., Abo Atia, T., Toro, L., 2017. Leaching of electrodic powders from lithium-ion batteries: Optimization of operating conditions and effect of physical pretreatment for waste fraction

retrieval. Waste Manag. 60, 706–715. https://doi.org/10.1016/j.wasman.2016.11.037

220. Partinen, J., Halli, P., Helin, S., Wilson, B.P., Lundström, M., 2022. Utilizing Cu+ as catalyst in reductive leaching of lithium-ion battery cathode materials in H_2SO_4–NaCl solutions. Hydrometallurgy 208. https://doi.org/10.1016/j.hydromet.2021.105808

221. Patil, D., Chikkamath, S., Keny, S., Tripathi, V., Manjanna, J., 2020. Rapid dissolution and recovery of Li and Co from spent $LiCoO_2$ using mild organic acids under microwave irradiation. J. Environ. Manage. 256. https://doi.org/10.1016/j.jenvman.2019.109935

222. Pehlken, A., Albach, S., Vogt, T., 2017. Is there a resource constraint related to lithium-ion batteries in cars? Int. J. Life Cycle Assess. 22, 40–53. https://doi.org/10.1007/s11367-015-0925-4

223. Peng, C., Hamuyuni, J., Wilson, B.P., Lundström, M., 2018. Selective reductive leaching of cobalt and lithium from industrially crushed waste Li-ion batteries in sulfuric acid system. Waste Manag. 76, 582–590. https://doi.org/10.1016/j.wasman.2018.02.052

224. Peng, F., Mu, D., Li, R., Liu, Y., Ji, Y., Dai, C., Ding, F., 2019. Impurity removal with highly selective and efficient methods and the recycling of transition metals from spent lithium-ion batteries. RSC Adv. 9, 21922–21930. https://doi.org/10.1039/c9ra02331c

225. Permatasari, N.V., Hadiyanto, H., Kawigraha, A., Warsito, B., Christwardana, M., 2023. Response surface methodology of nickel and cobalt recovery from battery using acid as leaching agent. Int. J. Energy Environ. Eng. 14, 309–320. https://doi.org/10.1007/s40095-022-00527-z

226. Peters, J.F., Baumann, M., Zimmermann, B., Braun, J., Weil, M., 2017. The environmental impact of Li-Ion batteries and the role of key parameters – A review. Renew. Sustain. Energy Rev. 67, 491–506. https://doi.org/10.1016/j.rser.2016.08.039

227. Picatoste, A., Justel, D., Mendoza, J.M.F., 2022. Circularity and life cycle environmental impact assessment of batteries for electric vehicles: Industrial challenges, best practices and research guidelines. Renew. Sustain. Energy Rev. 169, 112941. https://doi.org/10.1016/j.rser.2022.112941

228. Pindar, S., Dhawan, N., 2020a. Kinetics and thermodynamical evaluation of electrode material of discarded lithium-ion batteries and its impact on recycling. J. Therm. Anal. Calorim. https://doi.org/10.1007/s10973-020-10139-6.

229. Pindar, S., Dhawan, N., 2020b. Evaluation of carbothermic processing for mixed discarded lithium-ion batteries. Metall. Res. Technol. 117 https://doi.org/10.1051/ metal/2020025.

230. Pinegar, https://doi.org/10.1007/s42461-020-00230-9

231. Prasetyo, E., Muryanta, W.A., Anggraini, A.G., Sudibyo, S., Amin, M., Al Muttaqii, M., 2022. Tannic acid as a novel and green leaching reagent for cobalt and lithium recycling from spent lithium-ion batteries. J. Mater. Cycles Waste Manag. 24, 927–938. https://doi.org/10.1007/s10163-022-01368-y

232. Punt, T., Bradshaw, S.M., van Wyk, P., Akdogan, G., 2022. The Efficiency of Black Mass Preparation by Discharge and Alkaline Leaching for LIB Recycling. Minerals 12, 753. https://doi.org/10.3390/min12060753

233. Qiao, Q., Zhao, F., Liu, Z., Jiang, S., Hao, H., 2017. Comparative Study on Life Cycle CO_2 Emissions from the Production of Electric and Conventional Vehicles in China. Energy Procedia 105, 3584–3595. https://doi.org/10.1016/j.egypro.2017.03.827

234. Qin, X., Yang, G., Cai, F., Wang, B., Jiang, B., Chen, H., Tan, C., 2019. Recovery and Reuse of Spent $LiFePO_4$ Batteries. J. New Mater. Electrochem. Syst. 22, 119–124. https://doi.org/10.14447/jnmes.v22i3.a01

235. Rajaeifar, M.A., Ghadimi, P., Raugei, M., Wu, Y., Heidrich, O., 2022. Challenges and recent developments in supply and value chains of electric vehicle batteries: A sustainability perspective. Resour. Conserv. Recycl. https://doi.org/10.1016/j.resconrec.2021.106144

236. Rallo, H., Benveniste, G., Gestoso, I., Amante, B., 2020. Economic analysis of the disassembling activities to the reuse of electric vehicles Li-ion batteries. Resour. Conserv. Recycl. 159, 104785. https://doi.org/10.1016/j.resconrec.2020.104785

237. Raugei, M., Winfield, P., 2019. Prospective LCA of the production and EoL recycling of a novel type of Li-ion battery for electric vehicles. J. Clean. Prod. 213, 926–932. https://doi.org/10.1016/j.jclepro.2018.12.237

238. Reznikova, N., Zvarych, R., Zvarych, I., Shnyrkov, O., 2019. Global circular e-chain in overcoming the global waste. Procedia Environ. Sci. Eng. Manag. 6, 641–647. https://shorturl.at/aINQ3

239. Ritchie, A., Howard, W., 2006. Recent developments and likely advances in lithium-ion batteries. J. Power Sources 162, 809–812. https://doi.org/10.1016/j.jpowsour.2005.07.014

240. Romare, M., Dahllöf, L., 2017. The Life Cycle Energy Consumption and Greenhouse Gas Emissions from Lithium-Ion Batteries A study with focus on

Current Technology and batteries for ligh-duty vehicles., IVL Swedish Environmental Research Institute. https://shorturl.at/fhCX5

241. Ross, B.J., Leresche, M., Liu, D., Durham, J.L., Dahl, E.U., Lipson, A.L., 2020. Mitigating the Impact of Thermal Binder Removal for Direct Li-Ion Battery Recycling. ACS Sustain. Chem. Eng. 8, 12511–12515. https://doi.org/10.1021/acssuschemeng.0c03424

242. Rothermel, S., Evertz, M., Kasnatscheew, J., Qi, X., Grützke, M., Winter, M., Nowak, S., 2016. Graphite Recycling from Spent Lithium-Ion Batteries. ChemSusChem 9, 3473–3484. https://doi.org/10.1002/cssc.201601062

243. Rouhi, H., Karola, E., Serna-Guerrero, R., Santasalo-Aarnio, A., 2021. Voltage behavior in lithium-ion batteries after electrochemical discharge and its implications on the safety of recycling processes. J. Energy Storage 35. https://doi.org/10.1016/j.est.2021.102323

244. Rouhi, H., Serna-Guerrero, R., Santasalo-Aarnio, A., 2022. Electrochemical discharge of Li-ion batteries - A methodology to evaluate the potential of discharge electrolytes without corrosion. J. Energy Storage 55. https://doi.org/10.1016/j.est.2022.105734

245. Rouquette, L.M.J., Petranikova, M., Vieceli, N., 2023. Complete and selective recovery of lithium from EV lithium-ion batteries: Modeling and optimization using oxalic acid as a leaching agent. Sep. Purif. Technol. 320. https://doi.org/10.1016/j.seppur.2023.124143

246. Roy, J.J., Cao, B., Madhavi, S., 2021. A review on the recycling of spent lithium-ion batteries (LIBs) by the bioleaching approach. Chemosphere 282, 130944. https://doi.org/10.1016/j.chemosphere.2021.130944

247. Roy, J.J., Zaiden, N., Do, M.P., Cao, B., Srinivasan, M., 2023. Microbial recycling of lithium-ion batteries: Challenges and outlook. Joule 7, 450–456. https://doi.org/10.1016/j.joule.2023.01.004

248. Rui, X., Geng, Y., Sun, X., Hao, H., Xiao, S., 2021. Dynamic material flow analysis of natural graphite in China for 2001-2018. Resour. Conserv. Recycl. 173. https://doi.org/10.1016/j.resconrec.2021.105732

249. Ruismäki, R., Rinne, T., Da´nczak, A., Taskinen, P., Serna-guerrero, R., Jokilaakso, A., 2020. Integrating Flotation and Pyrometallurgy for Recovering Graphite and Valuable Metals from Battery Scrap. Metals (Basel).. https://doi.org/10.3390/met10050680

250. Saju, D., Ebenezer, J., Chandran, N., Chandrasekaran, N., 2023. Recycling of Lithium Iron Phosphate Cathode Materials from Spent Lithium-Ion Batteries: A

Mini-Review. Ind. Eng. Chem. Res. 62, 11768−11783. https://doi.org/10.1021/acs.iecr.3c01208

251. Salces, A.M., Bremerstein, I., Rudolph, M., Vanderbruggen, A., 2022. Joint recovery of graphite and lithium metal oxides from spent lithium-ion batteries using froth flotation and investigation on process water re-use. Miner. Eng. 184, 107670. https://doi.org/10.1016/j.mineng.2022.107670

252. Sattar, R., Ilyas, S., Bhatti, H.N., Ghaffar, A., 2019. Resource recovery of critically rare metals by hydrometallurgical recycling of spent lithium-ion batteries. Sep. Purif. Technol. 209, 725–733. https://doi.org/10.1016/j.seppur.2018.09.019

253. Schaeffer, N., Passos, H., Gras, M., Rodriguez Vargas, S.J., Neves, M.C., Svecova, L., Papaiconomou, N., Coutinho, J.A.P., 2020. Selective separation of manganese, cobalt, and nickel in a fully aqueous system. ACS Sustain. Chem. Eng. 8, 12260–12269. https://doi.org/10.1021/acssuschemeng.0c04043

254. Schiavi, P.G., Altimari, P., Branchi, M., Zanoni, R., Simonetti, G., Navarra, M.A., Pagnanelli, F., 2021. Selective recovery of cobalt from mixed lithium-ion battery wastes using deep eutectic solvent. Chem. Eng. J. 417. https://doi.org/10.1016/j.cej.2021.129249

255. Shafique, M., Akbar, A., Rafiq, M., Azam, A., Luo, X., 2023. Global material flow analysis of end-of-life of lithium nickel manganese cobalt oxide batteries from battery electric vehicles. https://doi.org/10.1177/0734242X221127175

256. Shafique, M., Rafiq, M., Azam, A., Luo, X., 2022. Material flow analysis for end-of-life lithium-ion batteries from battery electric vehicles in the USA and China. Resour. Conserv. Recycl. 178. https://doi.org/10.1016/j.resconrec.2021.106061

257. Shaw-Stewart, J., Alvarez-Reguera, A., Greszta, A., Marco, J., Masood, M., Sommerville, R., Kendrick, E., 2019. Aqueous solution discharge of cylindrical lithium-ion cells. Sustain. Mater. Technol. 22, e00110. https://doi.org/10.1016/j.susmat.2019.e00110

258. Shi, Y., Chen, G., Chen, Z., 2018. Effective regeneration of $LiCoO_2$ from spent lithium-ion batteries: A direct approach towards high-performance active particles. Green Chem. 20, 851–862. https://doi.org/10.1039/c7gc02831h

259. Shi, Y., Zhang, M., Meng, Y.S., Chen, Z., 2019. Ambient-Pressure Relithiation of Degraded $Li_xNi_{0.5}Co_{0.2}Mn_{0.3}O_2$ (0; x;1) via Eutectic Solutions for Direct Regeneration of Lithium-Ion Battery Cathodes. Adv. Energy Mater. 9, 1900454. https://doi.org/10.1002/aenm.201900454

260. Shin, D.J., Joo, S.-H., Oh, C.-H., Wang, J.-P., Park, J.-T., Min, D.J., Shin, S.M., 2019. A study on Zn recovery from other metals in the spent mixed batteries through a sequence of hydrometallurgical processes. Environ. Technol. (United Kingdom) 40, 3512–3522. https://doi.org/10.1080/09593330.2018.1480664

261. Shin, H., Zhan, R., Dhindsa, K.S., Pan, L., Han, T., 2020. Electrochemical Performance of Recycled Cathode Active Materials Using Froth Flotation-based Separation Process. J. Electrochem. Soc. 167. https://doi.org/10.1149/1945-7111/ab6280

262. Shin, Y., Kim, S., Park, S., Lee, J., Bae, J., Kim, D., Joo, H., Ban, S., Lee, H., Kim, Y., Kwon, K., 2023. A comprehensive review on the recovery of cathode active materials via direct recycling from spent Li-ion batteries. Renew. Sustain. Energy Rev. 187, 113693. https://doi.org/10.1016/j.rser.2023.113693

263. Sidiq, A.L., Floweri, O., Karunawan, J., Abdillah, O.B., Santosa, S.P., Iskandar, F., 2022. NCM cathode active materials reproduced from end-of-life Li-ion batteries using a simple and green hydrometallurgical recycling process. Mater. Res. Bull. 153, 111901. https://doi.org/10.1016/j.materresbull.2022.111901

264. Singh, M., Yuksel, T., Michalek, J.J., Azevedo, I.M.L., 2024. Ensuring greenhouse gas reductions from electric vehicles compared to hybrid gasoline vehicles requires a cleaner U.S. electricity grid. Sci. Rep. 14, 1–11. https://doi.org/10.1038/s41598-024-51697-1

265. Sobianowska-Turek, A., 2018. Hydrometallurgical recovery of metals: Ce, La, Co, Fe, Mn, Ni and Zn from the stream of used Ni-MH cells. Waste Manag. 77, 213–219. https://doi.org/10.1016/j.wasman.2018.03.046

266. Sohn, J., Kim, S., Yang, D., Kim, H., Lee, K., 2015. Recycling of spent lithium-ion batteries used in electric vehicles by physical treatment and acid leaching, in: EARTH 2015 - Proceedings of the 13th International Symposium on East Asian Resources Recycling Technology. International Symposium on East Asian Resources Recycling Technology, pp. 807–811.

267. Sommerville, R., Shaw-Stewart, J., Goodship, V., Rowson, N., Kendrick, E., 2020. A review of physical processes used in the safe recycling of lithium-ion batteries. Sustain. Mater. Technol. 25, e00197. https://doi.org/10.1016/j.susmat.2020.e00197

268. Song, D., Yu, J., Wang, M., Tan, Q., Liu, K., Li, J., 2023. Advancing recycling of spent lithium-ion batteries: From green chemistry to circular economy. Energy Storage Mater. https://doi.org/10.1016/j.ensm.2023.102870

269. Song, S., Liu, R., Sun, M., Zhen, A., 2023. Hydrometallurgical recovery of lithium carbonate and iron phosphate from blended cathode materials of spent lithium-ion battery. Rare Met. https://doi.org/10.1007/s12598-023-02493-9

270. Song, Y., Xie, B., Song, S., Lei, S., Sun, W., Xu, R., Yang, Y., 2021. Regeneration of $LiFePO_4$ from spent lithium-ion batteries: Via a facile process featuring acid leaching and hydrothermal synthesis. Green Chem. 23, 3963–3971. https://doi.org/10.1039/d1gc00483b

271. Statista, 2023a. Projected lithium-ion battery market size worldwide | Statista [WWW Document]. URL https://www.statista.com/statistics/1011187/projected-global-lithium-ion-battery-market-size/ (accessed 3.11.24).

272. Statista, 2023b. Global battery recycling market value 2021-2031 [WWW Document]. URL https://www-statista-com.ezproxy.biblio.polito.it/statistics/1103263/li-ion-battery-recycling-market-size/ (accessed 4.14.24).

273. Statista, 2021. Market share of different types of electric vehicles cathode chemistries in 2020 with a forecast for 2025 through 2050. https://www.statista.com/statistics/1248519/distribution-of-different-electric-vehicle-batteries-on-the- global-market/ (accessed 21.03. 2023).

274. Statista, 2017. Landfill tax in Europe https://www.cewep.eu/wp-content/uploads/2017/12/Landfill-taxes-and-bans-overview.pdf

275. Stehmann, F.M., Jahnke, S., Balmforth-Slater, C., Scholl, S., 2017. Adsorptive Exhaust Gas Cleaning for Recycling of Li-Ion-Batteries. ECS Trans. 75, 3–17. https://doi.org/10.1149/07520.0003ecst

276. Stief, P., Dantan, J., Etienne, A., Siadat, A., 2019. Concepts and Requirements for Flexible Disassembly Systems for Drive. https://doi.org/10.1016/j.procir.2021.01.154

277. Sullivan, J.L., Gaines, L., 2012. Status of life cycle inventories for batteries. Energy Convers. Manag. 58, 134–148. https://doi.org/10.1016/j.enconman.2012.01.001

278. Sultana, I., Chen, Y., Huang, S., Rahman, M.M., 2022. Recycled value-added circular energy materials for new battery application: Recycling strategies, challenges, and sustainability-a comprehensive review. J. Environ. Chem. Eng. 10, 108728. https://doi.org/10.1016/j.jece.2022.108728

279. Sun, C., Xu, L., Chen, X., Qiu, T., Zhou, T., 2018. Sustainable recovery of valuable metals from spent lithium-ion batteries using DL-malic acid: Leaching

and kinetics aspect. Waste Manag. Res. 36, 113–120. https://doi.org/10.1177/0734242X17744273

280. Sun, X., Hao, H., Hartmann, P., Liu, Z., Zhao, F., 2019. Supply risks of lithium-ion battery materials: An entire supply chain estimation. Mater. Today Energy 14, 100347. https://doi.org/10.1016/j.mtener.2019.100347

281. Swain, B., 2018. Cost effective recovery of lithium from lithium-ion battery by reverse osmosis and precipitation: a perspective. J. Chem. Technol. Biotechnol. 93, 311–319. https://doi.org/10.1002/jctb.5332

282. Swart, P., Dewulf, J., Biernaux, A., 2014. Resource demand for the production of different cathode materials for lithium-ion batteries. J. Clean. Prod. 84, 391–399. https://doi.org/10.1016/j.jclepro.2014.01.056

283. Takahashi, V.C.I., Botelho Junior, A.B., Espinosa, D.C.R., Tenório, J.A.S., 2020. Enhancing cobalt recovery from Li-ion batteries using grinding treatment prior to the leaching and solvent extraction process. J. Environ. Chem. Eng. 8, 103801. https://doi.org/10.1016/j.jece.2020.103801

284. Tan, W.J., Chin, C.M.M., Garg, A., Gao, L., 2021. A hybrid disassembly framework for disassembly of electric vehicle batteries. Int. J. Energy Res. 45, 8073–8082. https://doi.org/10.1002/er.6364

285. Tang, C., Sprecher, B., Tukker, A., Mogollón, J.M., 2021. The impact of climate policy implementation on lithium, cobalt and nickel demand: The case of the Dutch automotive sector up to 2040. Resour. Policy 74. https://doi.org/10.1016/j.resourpol.2021.102351

286. Tang, H., Dai, X.I., Li, Q., Qiao, Y., Tan, F., 2020. Selective Leaching of $LiFePO_4$ by H_2SO_4 in the Presence of $NaClO_3$ Rev. Chim. 71, 248–254. https://doi.org/10.37358/RC.20.7.8242

287. Tanong, K., Coudert, L., Chartier, M., Mercier, G., Blais, J.-F., 2017. Study of the factors influencing the metals solubilisation from a mixture of waste batteries by response surface methodology. Environ. Technol. 38, 3167-3179 https://doi.org/10.1080/09593330.2017.1291756

288. Tanong, K., Coudert, L., Mercier, G., Blais, J.F., 2016. Recovery of metals from a mixture of various spent batteries by a hydrometallurgical process. J. Environ. Manage. 181, 95–107. https://doi.org/10.1016/j.jenvman.2016.05.084

289. Tao, S., Li, J., Wang, L., Hu, L., Zhou, H., 2019. A method for recovering Li_3PO_4 from spent lithium iron phosphate cathode material through high-temperature activation. Ionics (Kiel). 25, 5643–5653. https://doi.org/10.1007/s11581-019-03070-w

290. Terlouw, T., Zhang, X., Bauer, C., Alskaif, T., 2019. Towards the determination of metal criticality in home-based battery systems using a Life Cycle Assessment approach. J. Clean. Prod. 221, 667–677. https://doi.org/10.1016/j.jclepro.2019.02.250

291. Torabian, M.M., Jafari, M., Bazargan, A., 2022. Discharge of lithium-ion batteries in salt solutions for safer storage, transport, and resource recovery. Waste Manag. Res. 40, 402–409. https://doi.org/10.1177/0734242X211022658

292. Tran, M.K., Rodrigues, M.T.F., Kato, K., Babu, G., Ajayan, P.M., 2019. Deep eutectic solvents for cathode recycling of Li-ion batteries. Nat. Energy 4, 339–345. https://doi.org/10.1038/s41560-019-0368-4

293. Urbańska, W., 2020. Recovery of Co, Li, and Ni from spent li-ion batteries by the inorganic and/or organic reducer assisted leaching method. Minerals 10, 1–13. https://doi.org/10.3390/min10060555

294. USGS, 2024. Mineral commodity summaries 2024, in: Mineral Commodity Summaries, U.S.G. Survey. https://pubs.usgs.gov/publication/mcs2024

295. Vandepaer, L., Cloutier, J., Bauer, C., Amor, B., 2019. Integrating Batteries in the Future Swiss Electricity Supply System: A Consequential Environmental Assessment. J. Ind. Ecol. 23, 709–725. https://doi.org/10.1111/jiec.12774

296. Vanderbruggen, A., Hayagan, N., Bachmann, K., Ferreira, A., Werner, D., Horn, D., Peuker, U., Serna-Guerrero, R., Rudolph, M., 2022. Lithium-Ion Battery Recycling─Influence of Recycling Processes on Component Liberation and Flotation Separation Efficiency. ACS ES T Eng. 2, 2130–2141. https://doi.org/10.1021/acsestengg.2c00177

297. Vieceli, N., Casasola, R., Lombardo, G., Ebin, B., Petranikova, M., 2021. Hydrometallurgical recycling of EV lithium-ion batteries: Effects of incineration on the leaching efficiency of metals using sulfuric acid. Waste Manag. 125, 192–203. https://doi.org/10.1016/j.wasman.2021.02.039

298. Virolainen, S., Wesselborg, T., Kaukinen, A., Sainio, T., 2021. Removal of iron, aluminium, manganese and copper from leach solutions of lithium-ion battery waste using ion exchange. Hydrometallurgy 202, 105602. https://doi.org/10.1016/j.hydromet.2021.105602

299. Vishvakarma, S., Dhawan, N., 2019. Recovery of Cobalt and Lithium Values from Discarded Li-Ion Batteries. J. Sustain. Metall. 5, 204–209. https://doi.org/10.1007/s40831-018-00208-4

300. Wang, F., Zhang, T., He, Y., Zhao, Y., Wang, S., Zhang, G., Zhang, Y., Feng, Y., 2018. Recovery of valuable materials from spent lithium-ion batteries by mechanical separation and thermal treatment. J. Clean. Prod. 185, 646–652. https://doi.org/10.1016/j.jclepro.2018.03.069

301. Wang, H., Burke, S., Yuan, R., Whitacre, J.F., 2023. Effective direct recycling of in homogeneously aged Li-ion battery cathode active materials. J. Energy Storage 60, 106616. https://doi.org/10.1016/j.est.2023.106616

302. Wang, H., Qu, G., Yang, J., Zhou, S., Li, B., Wei, Y., 2022. An effective and cleaner discharge method of spent lithium batteries. J. Energy Storage 54, 105383. https://doi.org/10.1016/j.est.2022.105383

303. Wang, J., Zhang, Q., Sheng, J., Liang, Z., Chen, Y., Zhou, G., Cheng, H., 2023. Direct and green repairing of degraded $LiCoO_2$ for reuse in lithium-ion batteries. Natl. Sci. Rev. 9. https://doi.org/10.1093/nsr/nwac097

304. Wang, K., Zhang, G., Luo, M., 2022. Recovery of Valuable Metals from Cathode—Anode Mixed Materials of Spent Lithium-Ion Batteries Using Organic Acids. Separations 9. https://doi.org/10.3390/separations9090259

305. Wang, M.-M., Zhang, C.-C., Zhang, F.-S., 2016. An environmental benign process for cobalt and lithium recovery from spent lithium-ion batteries by mechanochemical approach. Waste Manag. 51, 239–244. https://doi.org/10.1016/j.wasman.2016.03.006

306. Wang, M., Liu, K., Dutta, S., Alessi, D.S., Rinklebe, J., Ok, Y.S., Tsang, D.C.W., 2022. Recycling of lithium iron phosphate batteries: Status, technologies, challenges, and prospects. Renew. Sustain. Energy Rev. 163. https://doi.org/10.1016/j.rser.2022.112515

307. Wang, M., Tan, Q., Liu, L., Li, J., 2019. A low-toxicity and high-efficiency deep eutectic solvent for the separation of aluminum foil and cathode materials from spent lithium-ion batteries. J. Hazard. Mater. 380, 120846. https://doi.org/10.1016/j.jhazmat.2019.120846

308. Wang, S., Wang, C., Lai, F., Yan, F., Zhang, Z., 2020. Reduction-ammoniacal leaching to recycle lithium, cobalt, and nickel from spent lithium-ion batteries with a hydrothermal method: Effect of reductants and ammonium salts. Waste Manag. 102, 122–130. https://doi.org/10.1016/j.wasman.2019.10.017

309. Wang, X., Gaustad, G., Babbitt, C.W., Richa, K., 2014. Economies of scale for future lithium-ion battery recycling infrastructure. Resour. Conserv. Recycl. 83, 53–62. https://doi.org/10.1016/j.resconrec.2013.11.009

310. Wang, X.J., Zheng, S.L., Zhang, Ying, Zhang, Yang, Qiao, S., Long, Z. qi, Zhao, B., Li, Z. fei, 2022. Sulfuric acid leaching of ball-milling activated $FePO_4$

residue after lithium extraction from spent lithium iron phosphate cathode powder. Waste Manag. 153, 31–40. https://doi.org/10.1016/j.wasman.2022.08.009

311. Wang, Y., An, N., Wen, L., Wang, L., Jiang, X., Hou, F., Yin, Y., Liang, J., 2020. Recent progress on the recycling technology of Li-ion batteries. J. Energy Chem. 55, 391–419. https://doi.org/10.1016/j.jechem.2020.05.008

312. Wang, Y., Ge, J., 2020. Potential of urban cobalt mines in China: An estimation of dynamic material flow from 2007 to 2016. Resour. Conserv. Recycl. 161. https://doi.org/10.1016/j.resconrec.2020.104955

313. Wang, Y.H., Wu, J.J., Hu, G.C., Ma, W.H., 2023. Recovery of Li, Mn, and Fe from $LiFePO_4$/$LiMn_2O_4$ mixed waste lithium-ion battery cathode materials. J. Min. Metall. Sect. B Metall. 59, 17–26. https://doi.org/10.2298/JMMB220918002W

314. Wang, Z., Huang, Y., Wang, X., Wu, D., Wu, X., 2022. Advanced Solid-State Electrolysis for Green and Efficient Spent $LiFePO_4$ Cathode Material Recycling: Prototype Reactor Tests. Ind. Eng. Chem. Res. 61, 12318–12328. https://doi.org/10.1021/acs.iecr.2c02266

315. Wegener, K., Andrew, S., Raatz, A., Dröder, K., Herrmann, C., 2014. Disassembly of electric vehicle batteries using the example of the Audi Q5 hybrid system. Procedia CIRP 23, 155–160. https://doi.org/10.1016/j.procir.2014.10.098

316. Widijatmoko, S., Fu, G., Wang, Z., Hall, P., 2020a. Recovering lithium cobalt oxide, aluminium, and copper from spent lithium-ion battery via attrition scrubbing. J. Clean. Prod. 260. https://doi.org/10.1016/j.jclepro.2020.120869

317. Widijatmoko, S., Gu, F., Wang, Z., Hall, P., 2020b. Selective liberation in dry milled spent lithium-ion batteries. Sustain. Mater. Technol. 23. https://doi.org/10.1016/j.susmat.2019.e00134

318. Widijatmoko, S.D., Gu, F., Wang, Z., Hall, P., 2020. Selective liberation in dry milled spent lithium-ion batteries. Sustain. Mater. Technol. 23. https://doi.org/10.1016/j.susmat.2019.e00134

319. Winslow, K.M., Laux, S.J., Townsend, T.G., 2018. A review on the growing concern and potential management strategies of waste lithium-ion batteries. Resour. Conserv. Recycl. https://doi.org/10.1016/j.resconrec.2017.11.001

320. Woeste, R., Drude, E.S., Vrucak, D., Klöckner, K., Rombach, E., Letmathe, P., Friedrich, B., 2024. A techno-economic assessment of two recycling processes for black mass from end-of-life lithium-ion batteries. Appl. Energy 361, 122921. https://doi.org/10.1016/j.apenergy.2024.122921

321. Wu, L., Zhang, F.S., Zhang, Z.Y., Zhang, C.C., 2023. An environmentally friendly process for selective recovery of lithium and simultaneous synthesis of $LiFe_5O_8$ from spent $LiFePO_4$ battery by mechanochemical. J. Clean. Prod. 396, 136504. https://doi.org/10.1016/j.jclepro.2023.136504

322. Wu, Z., Soh, T., Chan, J.J., Meng, S., Meyer, D., Srinivasan, M., Tay, C.Y., 2020. Repurposing of Fruit Peel Waste as a Green Reductant for Recycling of Spent Lithium-Ion Batteries. Environ. Sci. Technol. 54, 9681–9692. https://doi.org/10.1021/acs.est.0c02873

323. Wuschke, L., Jäckel, H.-G., Leißner, T., Peuker, U.A., 2019. Crushing of large Li-ion battery cells. Waste Manag. 85, 317–326. https://doi.org/10.1016/j.wasman.2018.12.042

324. Wuschke, L., Jäckel, H.G., Peuker, U.A., Gellner, M., 2016. Separation of electrode foils from Li-ion traction batteries, in: IMPC 2016 - 28th International Mineral Processing Congress. Canadian Institute of Mining, Metallurgy and Petroleum.

325. Xiao, J., Guo, J., Zhan, L., Xu, Z., 2020. A cleaner approach to the discharge process of spent lithium-ion batteries in different solutions. J. Clean. Prod. 255. https://doi.org/10.1016/j.jclepro.2020.120064

326. Xie, J., Huang, K., Nie, Z., Yuan, W., Wang, X., Song, Q., Zhang, X., Zhang, C., Wang, J., Crittenden, J.C., 2021. An effective process for the recovery of valuable metals from cathode material of lithium-ion batteries by mechanochemical reduction. Resour. Conserv. Recycl. 168, 105261. https://doi.org/10.1016/j.resconrec.2020.105261

327. Xie, J., Lu, Y.C., 2020. A retrospective on lithium-ion batteries. Nat. Commun. 11, 9–12. https://doi.org/10.1038/s41467-020-16259-9

328. Xing, L., Bao, J., Zhou, S., Qiu, Y., Sun, H., Gu, S., Yu, J., 2021. Ultra-fast leaching of critical metals from spent lithium-ion batteries cathode materials achieved by the synergy-coordination mechanism. Chem. Eng. J. 420. https://doi.org/10.1016/j.cej.2021.129593

329. Xu, C., Hu, X., Yang, Y., Jian, Z., Chen, W., Yang, L., 2023. Integrated process of CO_2 sequestration and recycling spent $LiFePO_4$ batteries. Energy Storage Mater. 60, 102819. https://doi.org/10.1016/j.ensm.2023.102819

330. Xu, L., Chen, C., Fu, M.-L., 2020. Separation of cobalt and lithium from spent lithium-ion battery leach liquors by ionic liquid extraction using Cyphos IL-101. Hydrometallurgy 197. https://doi.org/10.1016/j.hydromet.2020.105439

331. Xu, P., Tan, D.H.S., Jiao, B., Gao, H., Yu, X., Chen, Z., 2023. A Materials Perspective on Direct Recycling of Lithium-Ion Batteries: Principles, Challenges and Opportunities. Adv. Funct. Mater. https://doi.org/10.1002/adfm.202213168

332. Yadav, P., Jie, C.J., Tan, S., Srinivasan, M., 2020. Recycling of cathode from spent lithium iron phosphate batteries. J. Hazard. Mater. 399, 123068. https://doi.org/10.1016/j.jhazmat.2020.123068

333. Yagci, M.C., Behmann, R., Daubert, V., Braun, J.A., Velten, D., Bessler, W.G., 2021. Electrical and Structural Characterization of Large-Format Lithium Iron Phosphate Cells Used in Home-Storage Systems. Energy Technol. 9. https://doi.org/10.1002/ente.202000911

334. Yang, H., Song, X., Zhang, X., Lu, B., Yang, D., Li, B., 2021. Uncovering the in-use metal stocks and implied recycling potential in electric vehicle batteries considering cascaded use: a case study of China. Environ. Sci. Pollut. Res. 28, 45867–45878. https://doi.org/10.1007/s11356-021-13430-7

335. Yang, T., Luo, D., Yu, A., Chen, Z., 2023. Enabling Future Closed-Loop Recycling of Spent Lithium-Ion Batteries: Direct Cathode Regeneration. Adv. Mater. 35, 1–13. https://doi.org/10.1002/adma.202203218

336. Yang, X., Zhang, Y., Meng, Q., Dong, P., Ning, P., Li, Q., 2020. Recovery of valuable metals from mixed spent lithium-ion batteries by multi-step directional precipitation. RSC Adv. 11, 268–277. https://doi.org/10.1039/d0ra09297e

337. Yang, Y., Meng, X., Cao, H., Lin, X., Liu, C., Sun, Y., Zhang, Y., Sun, Z., 2018. Selective recovery of lithium from spent lithium iron phosphate batteries: A sustainable process. Green Chem. 20, 3121–3133. https://doi.org/10.1039/c7gc03376a

338. Yang, Y., Sun, M., Yu, W., Ma, X., Lei, S., Sun, W., 2023. Recovering Fe, Mn and Li from $LiMn_{1-x}Fe_xPO_4$ cathode material of spent lithium-ion battery by gradient precipitation. Sustain. Mater. Technol. 36, e00625. https://doi.org/10.1016/j.susmat.2023.e00625

339. Yang, Y., Zhang, J., Zhang, H., Wang, Y., Chen, Y., 2024. Simultaneous anodic de-lithiation / cathodic lithium-embedded regeneration method for recycling of spent $LiFePO_4$ battery. Energy Storage Mater. 65, 103081. https://doi.org/10.1016/j.ensm.2023.103081

340. Yao, L.P., Zeng, Q., Qi, T., Li, J., 2020. An environmentally friendly discharge technology to pretreat spent lithium-ion batteries. J. Clean. Prod. 245, 118820. https://doi.org/10.1016/j.jclepro.2019.118820

341. Yu, J., He, Y., Qu, L., Yang, J., Xie, W., Zhu, X., 2020. Exploring the critical role of grinding modification on the flotation recovery of electrode

materials from spent lithium-ion batteries. J. Clean. Prod. 274, 123066. https://doi.org/10.1016/j.jclepro.2020.123066

342. Yu, L., Bai, Y., Polzin, B., Belharouak, I., 2024. Unlocking the value of recycling scrap from Li-ion battery manufacturing.: Challenges and outlook*. J. Power Sources 593. https://doi.org/10.1016/j.jpowsour.2023.233955

343. Yu, Y., Mao, J., Chen, X., 2020. Comparative analysis of internal and external characteristics of lead-acid battery and lithium-ion battery systems based on composite flow analysis. Sci. Total Environ. 746. https://doi.org/10.1016/j.scitotenv.2020.140763

344. Yue, Y., Wei, S., Yongjie, B., Chenyang, Z., Shaole, S., Yuehua, H., 2018. Recovering Valuable Metals from Spent Lithium-ion Battery via a Combination of Reduction Thermal Treatment and Facile Acid Leaching. ACS Sustain. Chem. Eng. 6, 10445–10453. https://doi.org/10.1021/acssuschemeng.8b01805

345. Zante, G., Braun, A., Masmoudi, A., Barillon, R., Trébouet, D., Boltoeva, M., 2020. Solvent extraction fractionation of manganese, cobalt, nickel and lithium using ionic liquids and deep eutectic solvents. Miner. Eng. 156, 106512. https://doi.org/10.1016/j.mineng.2020.106512

346. Zeng, X., Li, J., Shen, B., 2015. Novel approach to recover cobalt and lithium from spent lithium-ion battery using oxalic acid. J. Hazard. Mater. 295, 112–118. https://doi.org/10.1016/j.jhazmat.2015.02.064

347. Zhan, R., Payne, T., Leftwich, T., Perrine, K., Pan, L., 2020. De-agglomeration of cathode composites for direct recycling of Li-ion batteries. Waste Manag. 105, 39–48. https://doi.org/10.1016/j.wasman.2020.01.035

348. Zhan, R., Yang, Z., Bloom, I., Pan, L., 2021. Significance of a Solid Electrolyte Interphase on Separation of Anode and Cathode Materials from Spent Li-Ion Batteries by Froth Flotation. ACS Sustain. Chem. Eng. 9, 531–540. https://doi.org/10.1021/acssuschemeng.0c07965

349. Zhang, C., Yan, J., You, F., 2023. Critical metal requirement for clean energy transition: A quantitative review on the case of transportation electrification. Adv. Appl. Energy 9, 100116. https://doi.org/10.1016/j.adapen.2022.100116

350. Zhang, G., Liu, Z., Yuan, X., He, Y., Wei, N., Wang, H., Zhang, B., 2022. Recycling of valuable metals from spent cathode material by organic pyrolysis combined with in-situ thermal reduction. J. Hazard. Mater. 430, 128374. https://doi.org/10.1016/j.jhazmat.2022.128374

351. Zhang, G., Yuan, X., He, Y., Wang, H., Xie, W., Zhang, T., 2020. Organics removal combined with in situ thermal-reduction for enhancing the liberation and

metallurgy efficiency of $LiCoO_2$ derived from spent lithium-ion batteries. Waste Manag. 115, 113–120. https://doi.org/10.1016/j.wasman.2020.05.030

352. Zhang, J., 2022. Pyrometallurgy-based applications in spent lithium-ion battery recycling, in: Nano Technology for Battery Recycling, Remanufacturing, and Reusing. Elsevier, pp. 171–182. https://doi.org/10.1016/b978-0-323-91134-4.00002-9

353. Zhang, L., Teng, T., Xiao, L., Shen, L., Ran, J., Zheng, J., Zhu, Y., Chen, H., 2022. Recovery of $LiFePO_4$ from used lithium-ion batteries by sodium-bisulphate-assisted roasting. J. Clean. Prod. 379, 134748. https://doi.org/10.1016/j.jclepro.2022.134748

354. Zhang, L., Xu, Z., He, Z., 2020. Electrochemical Relithiation for Direct Regeneration of $LiCoO_2$ Materials from Spent Lithium-Ion Battery Electrodes. ACS Sustain. Chem. Eng. 8, 11596–11605. https://doi.org/10.1021/acssuschemeng.0c02854

355. Zhang, N., Xu, Z., Deng, W., Wang, X., 2022. Recycling and Upcycling Spent LIB Cathodes: A Comprehensive Review, Electrochemical Energy Reviews. Springer Nature Singapore. https://doi.org/10.1007/s41918-022-00154-6

356. Zhang, Q., Fan, E., Lin, J., Sun, S., Zhang, X., Chen, R., 2023a. Acid-free mechanochemical process to enhance the selective recycling of spent $LiFePO_4$ batteries. J. Hazard. Mater. 443, 130160. https://doi.org/10.1016/j.jhazmat.2022.130160

357. Zhang, Q., Fan, E., Lin, J., Sun, S., Zhang, X., Chen, R., 2023b. Acid-free mechanochemical process to enhance the selective recycling of spent $LiFePO_4$ batteries 443. https://doi.org/10.1016/j.jhazmat.2022.130160

358. Zhang, X., Cao, H., Xie, Y., Ning, P., An, H., You, H., Nawaz, F., 2015. A closed-loop process for recycling $LiNi_{1/3}Co_{1/3}Mn_{1/3}O_2$ from the cathode scraps of lithium-ion batteries: Process optimization and kinetics analysis. Sep. Purif. Technol. 150, 186–195. https://doi.org/10.1016/j.seppur.2015.07.003

359. Zhang, Y., Nguyen, R.T., Liaw, B., 2021. Status and Gap in Rechargeable Lithium Battery Supply Chain: Importance of Quantitative Failure Analysis. Proc. IEEE 109, 1029–1038. https://doi.org/10.1109/JPROC.2020.3047880

360. Zhao, J., Zhang, B., Xie, H., Qu, J., Qu, X., Xing, P., Yin, H., 2020. Hydrometallurgical recovery of spent cobalt-based lithium-ion battery cathodes using ethanol as the reducing agent. Environ. Res. 181. https://doi.org/10.1016/j.envres.2019.108803

361. Zhao, Jingjing, Zhang, B., Xie, H., Qu, J., Qu, X., Xing, P., Yin, H., 2020. Hydrometallurgical recovery of spent cobalt-based lithium-ion battery cathodes

using ethanol as the reducing agent. Environ. Res. 181, 108803. https://doi.org/10.1016/j.envres.2019.108803

362. Zhao, J., Zhou, F., Wang, H., Qu, X., Wang, Danfeng, Zheng, Z., Cai, Y., Gao, S., Wang, Dihua, Yin, H., 2024. Co-recovery of spent LiCoO2 and LiFePO4 by paired electrolysis. Green Chem. 26, 456–465. https://doi.org/10.1039/d3gc03322h

363. Zhao, S., Zhang, W., Li, G., Zhu, H., Huang, J., He, W., 2020. Ultrasonic renovating and coating modifying spent lithium cobalt oxide from the cathode for the recovery and sustainable utilization of lithium-ion battery. J. Clean. Prod. 257. https://doi.org/10.1016/j.jclepro.2020.120510

364. Zhao, T., Li, W., Traversy, M., Choi, Y., Ghahreman, A., Zhao, Z., Zhang, C., Zhao, W., Song, Y., 2024. A review on the recycling of spent lithium iron phosphate batteries. J. Environ. Manage. https://doi.org/10.1016/j.jenvman.2023.119670

365. Zhao, Y., Yuan, X., Jiang, L., Wen, J., Wang, H., Guan, R., Zhang, J., Zeng, G., 2020. Regeneration and reutilization of cathode materials from spent lithium-ion batteries. Chem. Eng. J. 383, 123089. https://doi.org/10.1016/j.cej.2019.123089

366. Zheng, R., Zhao, L., Wang, W., Liu, Y., Ma, Q., Mu, D., Li, R., Dai, C., 2016. Optimized Li and Fe recovery from spent lithium-ion batteries: Via a solution-precipitation method. RSC Adv. 6, 43613–43625. https://doi.org/10.1039/c6ra05477c

367. Zheng, X., Gao, W., Zhang, X., He, M., Lin, X., Cao, H., Zhang, Y., Sun, Z., 2017. Spent lithium-ion battery recycling – Reductive ammonia leaching of metals from cathode scrap by sodium sulphite. Waste Manag. 60, 680–688. https://doi.org/10.1016/j.wasman.2016.12.007

368. Zhong, X., Liu, W., Han, J., Jiao, F., Qin, W., Liu, T., Zhao, C., 2019. Pyrolysis and physical separation for the recovery of spent $LiFePO_4$ batteries. Waste Manag. 89, 83–93. https://doi.org/10.1016/j.wasman.2019.03.068

369. Zhou, H., Luo, Z., Wang, S., Ma, X., Cao, Z., 2023a. A mild closed-loop process for lithium – iron separation and cathode materials regeneration from spent $LiFePO_4$ batteries. Sep. Purif. Technol. 315, 123742. https://doi.org/10.1016/j.seppur.2023.123742

370. Zhou, H., Zhang, Y., Li, L., Cao, Z., 2023b. Integrated recycling of valuable elements from spent $LiFePO_4$ batteries: a green closed-loop process 7696–7706. https://doi.org/10.1039/d3gc02180g

371. Zhou, S., Zhang, Y., Meng, Q., Dong, P., Fei, Z., Li, Q., 2021. Recycling of $LiCoO_2$ cathode material from spent lithium-ion batteries by ultrasonic enhanced leaching and one-step regeneration. J. Environ. Manage. 277. https://doi.org/10.1016/j.jenvman.2020.111426

372. Zhu, X., Zhang, C., Feng, P., Yang, Xizu, Yang, Xiaojuan, 2021. A novel pulsated pneumatic separation with variable-diameter structure and its application in the recycling spent lithium-ion batteries. Waste Manag. 131, 20–30. https://doi.org/10.1016/j.wasman.2021.05.027

373. Zhuang, L., Sun, C., Zhou, T., Li, H., Dai, A., 2019. Recovery of valuable metals from $LiNi_{0.5}Co_{0.2}Mn_{0.3}O_2$ cathode materials of spent Li-ion batteries using mild mixed acid as leachant. Waste Manag. 85, 175–185. https://doi.org/10.1016/j.wasman.2018.12.034

374. Ziemann, S., Müller, D.B., Schebek, L., Weil, M., 2018. Modeling the potential impact of lithium recycling from EV batteries on lithium demand: A dynamic MFA approach. Resour. Conserv. Recycl. 133, 76–85. https://doi.org/10.1016/j.resconrec.2018.01.031

Appendix A

Academic dissemination

The results presented in this Thesis have been presented at international conferences and in open-access publications on scientific journals. The lists of per-reviewed open-access publications and conferences' oral presentation and related to circular economy of lithium-ion batteries are provided below. The full texts of the available publications cited in this Thesis are provided at the end of this Thesis.

Publications on circular economy and recycling of lithium-ion batteries

- Review of lithium-ion batteries' supply-chain in Europe: Material flow analysis and environmental assessment. **Bruno, M.,** Fiore, S. (2024). J. Environ. Manage. 358, 120758. https://doi.org/10.1016/j.jenvman.2024.120758
- Closed - loop recycling of lithium iron phosphate cathodic powders via citric acid leaching. **Bruno, M.,** Francia, C., Fiore, S. (2024). Environ. Sci. Pollut. Res. 2030. https://doi.org/10.1007/s11356-024-32837-6
- Low-cost and environmentally friendly physic-mechanical pre-treatments to recycle lithium iron phosphate cathodes. **Bruno, M.,** Fiore, S. (2024). J. Environ. Chem. Eng. 12, 112106. https://doi.org/10.1016/j.jece.2024.112106
- Material Flow Analysis of Lithium-Ion Battery Recycling in Europe: Environmental and Economic Implications †. **Bruno, M.,** Fiore, S. (2023). Batteries 9. https://doi.org/10.3390/batteries9040231
- Review of up-stream processes for Li-ion batteries recycling: safety and economic concerns. **Bruno, M.**, Fiore, S. (under review)
- Gas products detection and accurate pH monitoring for electrochemical discharge of Lithium-ion batteries. **Bruno, M.**, Santasalo-Aarnio, A., Fiore, S. (under review)
- Selective leaching for the recycling of lithium, iron and phosphorous from lithium-ion battery cathodes' production scraps. **Bruno, M.**, Amici, J., Fiore, S. (under review)

Conferences presentations on circular economy and recycling of lithium-ion batteries

- Physic-mechanical pre-treatments to recycle lithium iron phosphate cathodes. **Bruno, M.**, Fiore, S. (2024) presented at Waste Management Europe at Bergamo, Italy.

- Preliminary tests aimed at the recycling of Lithium Iron Phosphate (LFP) cathodes. **Bruno M.**, Francia, C., Fiore, S. (2023) presented at CHANIA2023 10th International Conference on Sustainable Waste Management at Chania, Greece.
- Material flow and economic analyses of Lithium-ion batteries recycling processes in Europe. **Bruno, M.**, Fiore, S. (2022) presented at CORFU2022 9th International Conference on Sustainable Solid Waste Management Corfu, Greece.
- Pre-treatments of lithium iron phosphate cathodes for lithium-ion batteries recycling. **Bruno, M.**, Fiore, S. (2022) presented at SUM2022 6th Symposium on Circular Economy and Urban Mining at Capri, Italy.

Additionally, during my PhD I took part in other research activities related to circular economy of other waste materials, in particular bottom ash from the thermovalorization of municipal solid waste and waste from electric and electronic equipment. The lists of per-reviewed open-access publications and conferences' oral presentation and related to these topics are provided below.

Publications on circular economy of waste from electric and electronic equipment

- Analysis of the influence of mobile phones' material composition on the economic profitability of their manual dismantling. **Bruno, M.**, Sotera, L., Fiore, S. (2022) J. Environ. Manage. 309, 114677. https://doi.org/10.1016/j.jenvman.2022.114677
- E-plastics in a circular economy: A comprehensive regulatory review. Barouta, D., Alassali, A., Picuno, C., **Bruno, M.**, Syranidou, E., Fiore, S., Kuchta, K. (2022) J. Clean. Prod. 355, 131711 https://doi.org/10.1016/j.jclepro.2022.131711

Conferences presentations on circular economy of waste from electric and electronic equipment

- Analysis of waste LCD dismantling operations. **Bruno M.**, Biosa, F., Fiore, S. (2022) presented at SUM2022 6th Symposium on Circular Economy and Urban Mining at Capri, Italy

Publications on circular economy and recycling of bottom ash from the thermovalorization of municipal solid waste

- Heavy metal recovery from the fine fraction of solid waste incineration bottom ash by wet density separation. Pienkoß, F., Abis, M., **Bruno, M.**, Grönholm, R., Hoppe, M., Kuchta, K., Fiore, S., Simon, F.G. (2022) J Mater Cycles Waste Manag 24, 364–377. https://doi.org/10.1007/s10163-021-01325-1

- Material flow, economic and environmental assessment of municipal solid waste incineration bottom ash recycling potential in Europe. **Bruno, M.**, Abis, M. Kuchta, K., Simon, F.G., Grönholm, R., Hoppe, M., Fiore, S. (2021). J. Clean. Prod. 317, 128511. https://doi.org/10.1016/j.jclepro.2021.128511
- A Novel Dry Treatment for Municipal Solid Waste Incineration Bottom Ash for the Reduction of Salts and Potential Toxic Elements. Abis, M.; **Bruno, M.**; Simon, F.-G.; Grönholm, R.; Hoppe, M.; Kuchta, K.; Fiore, S. (2021) Materials 14, 3133. https://doi.org/10.3390/ma14113133
- Assessment of the Synergy between Recycling and Thermal Treatments in Municipal Solid Waste Management in Europe. Abis, M.; **Bruno, M.**; Kuchta, K.; Simon, F.-G.; Grönholm, R.; Hoppe, M.; Fiore, S. (2020) Energies 13, 6412. https://doi.org/10.3390/en13236412

Appendix B

Relevant seminars and doctoral schools attended

During my PhD, I had the opportunity to take part in several international courses on circular economy and metallurgical processing of metals. The list of the seminars and doctoral school which I attended is provided below:

- Prometia 9th scientific seminar on mineral processing and extractive metallurgy for mining and recycling innovation, organized by PROMETIA between the 30th of November and the 2nd of December in Barcelona, Spain
- CIRCuIT Summer School, organized by Hamburg University of Technology between the 18th and the 22nd of July 2022 in Hamburg, Germany
- doc-ECE 6th Doctoral School on Entrepreneurship in the Circular Economy, organized by EIT Raw Materials and hold between the 4th and the 8th of July 2022 in Krakow, Poland
- Prometia 8th scientific seminar on mineral processing and extractive metallurgy for mining and recycling innovation, organized by PROMETIA between the 1st and the 3rd of December 2021 in Seville, Spain
- PROMETIA 2021 Tech Tour organized by PROMETIA between the 28th of November and the 1st of December 2021 in Seville and Huelva, Spain